DIELECTRIC RELAXATION OF DILUTE POLYSTYRENE LATICES

M.M. Springer

DIELECTRIC RELAXATION OF DILUTE POLYSTYRENE LATICES

Proefschrift
ter verkrijging van de graad van
doctor in de landbouwwetenschappen,
op gezag van de rector magnificus,
dr. H.C. van der Plas,
hoogleraar in de organische scheikunde,
in het openbaar te verdedigen
op vrijdag 2 november 1979
des namiddags te drie uur in de aula
van de Landbouwhogeschool te Wageningen.

778

STELLINGEN

I

De theorie van Ballario, Bonincontro en Cametti over dielectrische
eigenschappen van dispersies is geen wezenlijke verbetering van de
theorie van Schurr.

> C. Ballario, A. Bonincontro, C. Cametti, J. Colloid
> Interface Sci. 54 (1976), 415.
> J.M. Schurr, J. Phys. Chem. 68 (1964), 2407.
> Dit proefschrift, hoofdstuk 5.

II

Dielectrische relaxatie van latices is ionspecifiek.

> Dit proefschrift, hoofdstuk 4.

III

In tegenstelling tot wat door de meetresultaten van Engel wordt
gesuggereerd, blijkt uit elektrodecapaciteitsmetingen dat de
ruwheidsfactor van zilverjodide elektrode-oppervlakken afneemt
tijdens het verouderen.

> D.J.C. Engel, proefschrift Utrecht (1968), pag.32.
> K.J. Peverelli, proefschrift Wageningen (1979),
> pag.38.

IV

Bij elektrochemisch onderzoek van de binding van zware metaalionen
aan polyelektrolyten dient, zolang de metaalionconcentratie dit
toelaat, de voorkeur te worden gegeven aan normale pulspolarografie
boven differentiële pulspolarografie.

> W.T. Bresnahan, C.L. Grant, J.H. Weber,
> Anal. Chem. 50 (1978), 1675.
> H.P. van Leeuwen, Anal. Chem. 51 (1979), 1322.

V

Het niet tijdig onderkennen van het aspect tijdschaal leidt bij
het reologisch onderzoek van levensmiddelen nog te vaak tot een
ontijdig einde van het wetenschappelijk aspect in dit onderzoek.

> J. Text. Studies, 1-10 (1969-1979).

VI

De door Rowland en Labun met behulp van evenwichtszwelling be-
paalde verknopingsgraden van rubbernetwerken zijn slechts van
zeer beperkte kwalitatieve waarde.

> T.J. Rowland, L.C. Labun, Macromolecules, 11
> (1978), 466.

VII

Door de wijze waarop Taneya, Izutsu en Sone een geavanceerde
reologische theorie toepassen op resultaten van metingen aan
kaas, beïnvloeden zij het streven om reologische theorieën
ingang te doen vinden in het onderzoek van levensmiddelen op
negatieve wijze.

> S. Taneya, T. Izutsu, T. Sone in: "Food texture
> and rheology", editor P. Sherman, Acad. Press,
> London (1979), 369.

VIII

De pH-afhankelijkheid van de stabiliteitsconstanten zoals deze
voor verschillende cadmium-fulvinezuurcomplexen door Cheam en
Gamble zijn bepaald, wijst erop dat het gekozen complexerings-
model onjuist is. Bovendien zijn de gepresenteerde resultaten
veel onzekerder dan de auteurs aangeven.

> V. Cheam, D.S. Gamble, Can.J. Soil Sci. 54
> (1974), 413.

IX

Elementaire "wiskunde van het wachten" dient een verplicht
examenvak te worden voor opleidingen in de dienstverlenende
sector, zoals medicijnen en tandheelkunde.

> J. Sittig, Intermediair, 15 (1979), 9.

Proefschrift Marcus Marius Springer
"Dielectric relaxation of dilute polystyrene latices"
Wageningen, 2 november 1979.

Aan mijn ouders en schoonouders

Voor Gerardien, Jarl en Robert

Voorwoord

Bij het voltooien van dit proefschrift maak ik graag van de gelegenheid gebruik om allen, die hierin op enigerlei wijze een bijdrage geleverd hebben, mijn welgemeende dank te betuigen.

De basis voor dit proefschrift werd al gelegd tijdens het laatste gesprek over mijn aanstelling bij de vakgroep Fysische en Kolloidchemie van de Landbouwhogeschool. Mijn promotor, Prof. Dr. J. Lyklema, stelde tijdens dit gesprek voor om diëlectisch onderzoek aan latices te gaan verrichten. Hans, jouw belangstelling voor dit soort onderzoek, niet alleen als promotor, is met name in de periode waarin de verslaglegging plaats vond, stimulerend en van zeer veel waarde geweest. Voor de grote mate van vrijheid, die je mij niet alleen bij het onderzoek, maar ook bij mijn onderwijstaken liet, ben ik je zeer erkentelijk.

In het beginstadium van het onderzoek zijn de gesprekken met Joop Wisse, onder wiens leiding ik mijn na-kandidaatsstudie verricht heb, van veel nut geweest.

De vele proefmetingen zijn verricht samen met John Blom, die verder aan het ontwerp van de meetcel de belangrijkste bijdrage geleverd heeft. Het resultaat van deze samenwerking is de basis voor hoofdstuk twee geworden.

Ronald Wegh gaf adviezen op electronisch terrein en Simon Maasland construeerde de meetcel.

De veelzijdige bijdragen van Anton Korteweg in de realisatie van de meetopstelling, metingen en berekeningen is van essentieel belang geweest. Anton, jouw betrokkenheid bij het onderzoek bleek uit de accurate en inventieve inbreng gedurende de vele maanden waarin we op prettige wijze samengewerkt hebben. Met je vrouw, Ina, zorgde je er bovendien in eensgezinde samenwerking voor dat de meetresultaten via een terminal in het computergeheugen opgeslagen werden.

CONTENTS
1

LIST OF SYMBOLS

a	partiële radius
a_1	factor stemming from the theory of Dukhin and Shilov (see eq. 5-39)
a_2	factor stemming from the theory of Dukhin and Shilov (see eq. 5-39)
a_{10}	number average particle radius
a_{32}	parameter defined by equation (3-2)
A	area of a cross section of the cell, parallel to the electrode surfaces
A_1	factor stemming from the theory of Dukhin and Shilov (see eq. 5-37)
A_2	factor stemming from the theory of Dukhin and Shilov (see eq. 5-37)
c_b	concentration of electrolyte added to the latex sample
c_i	bulk concentration of ion species i.
C	capacitance
C_d	total capacitance of the phase sensitive detectors
C_e	electrode polarization capacitance
C_m	measured capacitance
C_p	parallel capacitance
C_r	residual capacitance
C_s	capacitance of the solution
C_x	unknown capacitance
d	distance between the electrodes of the measuring cell
D	diffusion coefficient
D_c	diffusion coefficient of the counter ion
D_e	parameter defined by equation (5-38)
D_+	diffusion coefficient of a positive ion
D_-	diffusion coefficient of a negative ion

5

e	elementary charge
E	applied electric field
F	Faraday constant
G	conductance
G_b	conductance of the conductance box
G_d	total conductance of the phase sensitive detectors
G_e	electrode polarization conductance
G_m	measured conductance
G_s	conductance of the solution
G_x	unknown conductance
H	high terminal
I	electric current
j	imaginarity unit
L	low terminal
L_b	lead inductance
L_c	inductance, due to the part of the cell not localized between the electrodes and due to the coaxial cables connecting the cell with the terminals of the bridge.
m	parameter defined by equation (5-16)
n	constant
n_i	number of particles
N	number of colloid particles per m^3
N_o	number of charges per m^3
r^2	correlation factor
R	gas constant
R_c	resistance, due to the part of the cell not localized between the electrodes and due to the coaxial cables connecting the cell with the terminals of the bridge.

6

t	time
T	absolute temperature
V	applied voltage
V_d	minimum detectable voltage
W	parameter defined by equation (5-33) or (5-36)
Y	admittance
Y_d	total admittance of the phase sensitive detectors
$Y_{e.s}$	external admittance standards
$Y_{i.s}$	internal admittance standards
Y_{st}	sum of external and internal admittance standards
Y_x	unknown admittance
z	charge number
z_i	valency of ion species i
z_+	charge number of a positive ion
z_-	charge number of a negative ion
Z	impedance
Z_e	electrode polarization impedance
Z_w	Warburg impedance
α	Cole–Cole distribution parameter
β	parameter defined by equation (5-34) or (5-37)
δ	phase angle, loss angle
δ_s	loss angle for a solution in the cell
ϵ	permittivity
ϵ_d	relative permittivity of the diffuse double layer
ϵ_r	relative permittivity
ϵ_s	permittivity at high frequencies
ϵ_w	relative permittivity of water
ϵ_o	absolute permittivity of free space
ϵ_1	relative permittivity of the dispersed medium
ϵ_∞	permittivity at high frequencies

ϵ' real part of ϵ

ϵ'' imaginary part of ϵ

$\Delta\epsilon_{st}$ static dielectric increment

ζ electrokinetic potential

η_w viscosity of water

κ^{-1} thickness of the diffuse double layer

κ_1^{σ} surface conductivity (section 5.2.1 only)

κ_1^{σ} surface conductivity due to a d.c. current

κ_2^{σ} surface conductivity due to a bound charge current

Λ molar conductivity of the electrolyte solution

Λ_+ molar conductivity of a positive ion

Λ_- molar conductivity of a negative ion

μ complex dipole moment

μ_o static dipole moment

ν frequency of the applied field

π ratio between circumference and diameter of a circle

σ conductivity

σ_b conductivity of the bulk electrolyte

σ_d conductivity of the diffuse double layer

σ_{dc} d.c. value of the conductivity

σ_w parameter defined by equation (5-31)

σ_o surface charge density

σ_1 conductivity of the dispersed medium

τ most probable relaxation time

ϕ volume fraction of the latex sample

ψ_d potential of the diffuse part of the double layer

ω angular frequency

ω_{cr} critical frequency

1. INTRODUCTION

1.1. Purpose of this study

The main aim of this investigation is to provide better experimental evidence which can be used to test theories of dielectric phenomena in colloid dispersions[*]. In particular, our results may be used to establish the limits of applicability of theories developed for dilute systems. It appeared possible to improve the calculation of the permittivity of suspended particles from the permittivity and the composition of the mixture by taking into account polarization at the charged phase boundary (O'Konski, 1955,1960; Lijklema, 1957).

Recent theoretical contributions, especially those of Dukhin and coworkers (e.g. 1969,1970,1971,1974) are very comprehensive. These authors gained insight into the mechanism by which concentration polarization of the double layer around colloid particles leads to the very strong low-frequency dielectric dispersion. Their analysis involves some of the principles of irreversible thermodynamics. Ion flux equations were used to calculate potentials in the perturbed double layers.

Dukhin et al. initially considered systems which, when subjected to a constant electric field, resulted in the formation of a stationary state of the charge distributions around the particles. Equations are obtained for the polarized diffuse double layer. These equations are used for the interpretation of electrokinetic measurements (Derjaguin and Dukhin, 1974).

As a next case, Dukhin et al. treated systems to which an alternating electric field was applied. In this case, the interfacial po-

---

[*] It is noted that the word "dispersion" is used with two distinct meanings, viz. in indicating the state of matter ("colloid dispersion") and in indicating frequency dependency ("dielectric dispersion"). We shall insert the words "colloid" or "dielectric" in those cases where confusion may arise.

larization created leads to an alternating polarization field, which is out of phase with the applied field. This corresponds to a relaxation effect of the conductance, from which the increase of the permittivity is calculated. Its value depends on some parameters characterizing the double layer under static conditions and on the diffusion coefficients of the ions. The theory enables calculation of ionic mobilities in the boundary layer to be made along with the ψ_d-potential in the double layer when the experimental data are obtained from dielectric measurements (Dukhin, 1970). Here, ψ_d is the potential of the diffuse part of the double layer. In both treatments the polarization of the double layer is the central theme. Reliable measurements are needed to test these theories.

The behaviour of the double layer under dynamic conditions is also crucial in developing a better understanding of electrokinetic phenomena, particularly as embodied in the retardation formulae relating mobilities to electrokinetic potentials in electrophoresis.

Our results may further be used to adapt the DLVO theory treating the stability of lyophobic colloids (Derjaguin and Landau, 1939; Verwey and Overbeek, 1948). In this theory, the repulsion between two colloid particles is attributed to the overlap of the diffuse part of the double layers around the colloid particles. An essential assumption of this theory is that during interaction the double layers are taken to be always in equilibrium. However, the possibility that the double layers, or part of them, relax on a time scale longer than the encounter time of two particles must be investigated. Hence it is not known to what extent the DLVO-theory applies under highly dynamic conditions. Our results may provide some insight into this matter.

The measurement of dielectric relaxation spectra is finding ever wider applications in research into both the processes of structure formation and to changes in structure under external influences. Consequently, this method of investigation is important for several as-

pects of colloid science. For instance, the size and shape of colloid particles are reflected in the dielectric dispersion.

These examples clearly illustrate the potential use of dielectric studies in colloid systems. However, in literature very few attempts to apply this method have been reported. The reason for this is that there are considerable difficulties involved. We shall now show what the main difficulties are and indicate some likely procedures to overcome them.

1.2. Outline of the experimental difficulties involved in connection with the theory

In order to apply the theories mentioned above, dilute colloid systems are required, in which the thickness of the double layer around the particles is very small compared with the linear dimension of the particles. This condition is expressed as (Dukhin and Shilov, 1974):

$$\kappa a \gg 1 \qquad\qquad (1-1)$$

As will be seen in section 1.3 only spherical particles will be used. In this case, a is the particle radius and κ^{-1} is the thickness of the diffuse double layer. κ is defined by the relation (e.g. Kruyt, 1952):

$$\kappa^2 = (\sum_i c_i z_i^2 F^2)/\varepsilon RT \qquad\qquad (1-2)$$

where c_i and z_i are the bulk concentrations and the valency, respectively, of ionic species i. F is the Faraday constant, ε the permittivity, R the gas constant and T the absolute temperature.

A second prerequisite, closely related to the first, is that κa is the same for all particles, i.e. the system should be homodisperse.

In practice it is difficult to meet condition (1-1), because both

an increase of a and an increase of κ give rise to experimental prob-
lems:

1) Increasing a leads to a shift of the relaxation spectrum to lower
   frequencies (Schwarz, 1962). However, measurement on aqueous solu-
   tions in the lower frequency range leads to an unacceptable influ-
   ence of electrode polarization (Oncley, 1942; Mandel, 1956,1965;
   Schwan, 1963). This effect is due to concentration gradients of
   ions present in the solution. The polarization can be described in
   terms of an impedance Z_e, localized at the electrodes and indepen-
   dent of the distance d between the electrodes of the measuring
   cell. Impedances containing the measured conductance G and capaci-
   tance C, can be plotted as a function of d. From the slopes of the
   straight lines obtained, the dielectric quantities can then be
   calculated. In doing so, Z_e is eliminated (Fricke and Curtis, 1937).
   As Z_e increases with decreasing frequency, it is necessary to mea-
   sure above a certain frequency to obtain sufficiently accurate
   measurements. In practice, the lowest frequency that may be ap-
   plied to attain a certain accuracy is dependent on:
   a) the quality of the measuring system;
   b) the dimensions of the measuring cell;
   c) the nature of the surface of the electrodes in the cell;
   d) the amount and nature of the electrolyte present in the solu-
      tion under investigation.
   Consequently, due to the experimental restrictions, there are se-
   rious restraints on the increase of a.

2) From equation (1-2) it follows that an increase in κ is obtained
   by increasing the amount of indifferent electrolyte in the solu-
   tion, also implying that the conductivity of the whole solution
   is increased. However, the very existence of a certain minimum
   resolution of all bridges, which are to be used for the measure-
   ments, imposes a restriction on the maximally tolerable value of

the conductance G. Difficulties arise when, at low frequencies,
the conductive currents through the solution become larger than
the capacitive ones. The relationship between G and C of the solu-
tion is given by the expression for the loss tangent δ:

$$\text{tg } \delta = G/\omega C \tag{1-3}$$

in which ω is the angular frequency of the applied electric field.
Therefore, the above condition can also be formulated such that
tg δ should remain below a certain limit. Fortunately, if κa in-
creases, the dielectric increment increases also, leading to a
decrease of tg δ.

In the above, it was mentioned that the minimum value of ω at
which measurements can be performed is determined by a. Therefore,
according to equation (1-3), the maximum amount of electrolyte in the
solution is also restricted by a.

Consequently κa >> 1 leads to the condition tg δ >> 1, so that
the two imposed restrictions are incompatible. In practice, some
compromise must be sought for.

Moreover, other problems also play a part, e.g.:
a) deviations from the ideal behaviour of the measuring cell, leading
   to stray capacitances;
b) non-ideality of the conductance standards used, leading to capaci-
   tance errors;
c) drift of the conductivity of the solution during the time required
   to perform the measurements at different frequencies.

In our study we used two transformer ratio arm bridges to be
able to cover the frequency range from about 100 Hz up to a few MHz.
By using this type of bridge in combination with a three-terminal
cell, shunt impedances from the terminals to earth are eliminated
(Calvert and Mildwater, 1963; Rosen, Bignall, Wisse and Van der Drift,
1969). The measuring cell was especially designed for the experiments

13

with the chosen colloid system (see section 1.3) with our bridges. Moreover, a conductance box was constructed to enlarge the conductance range of one of the bridges.

With the equipment used, up to about 1 mol/m^3 of a simple electrolyte (e.g. KCl) may be present in the dilute colloid systems used.

1.3. Choice of the subject to be investigated

This choice of the colloid system was limited by several restrictions:

1) In connection with the theoretical analysis it is very convenient to choose a system with spherical particles.
2) In order to find the most favourable radius of the particles (see section 1.2) it should be possible to vary the particle size.
3) A heterodisperse system leads to a very broad distribution of relaxation times. Therefore, the use of a monodisperse system is mandatory.
4) The system has to be stable in the colloid-chemical sense during the time of the measurements. The frequency spectrum has to be determined at several electrolyte concentrations. Considering the various extrapolations and standardizations which are necessary, this leads to a stability requirement of several weeks.
5) In order to check theoretical predictions, the surface should be non-porous and the surface charge or surface potential must be known.
6) It is desirable to be able to vary the surface charge density of the particles in connection with solving colloid-chemical problems.
7) Reasonable standard procedures should be available for characterizing the system (especially the particle size and the surface charge).

Monodisperse aqueous polystyrene latices, prepared according to a method described by Furusawa, Norde and Lyklema (1972), were found to be very suitable, because they meet all of the conditions mentioned

14

above. Such latices were used throughout our measurements.

Fortunately, much work has been performed during the last few years in characterizing these colloid systems (Furusawa, Norde and Lyklema, 1972; Goodwin, Hearn, Ho and Ottewill, 1973,1974; Small, 1974; Stone-Masui and Watillon, 1975; Norde, 1976; Takano, 1978; Bijsterbosch, 1978).

In summary, this thesis will describe progress in measuring the dielectric relaxation behaviour of colloids by simultaneously improving experimental techniques and using well-characterized model colloids.

2. EXPERIMENTAL EQUIPMENT AND MEASURING TECHNIQUE

2.1. Introduction

Several experimental set-ups have been developed to perform measurements on aqueous solutions. Cole and Gross (1949) designed a transformer bridge for measurements at frequencies up to 10 MHz. Schwan and Sittel (1953), Mandel and Jung (1952) and Van der Touw (1975a, 1975b) have built or modified Schering bridges for the frequency range 10 Hz up to a few hundred kHz. In the early sixties, bridges became commercially available.

Young and Grant (1968) used the less accurate Wayne Kerr B221 bridge, which covers the frequency range 10 Hz - 120 kHz. De Backer and Watillon (1966,1973) performed measurements with two Wayne Kerr bridges (B221 and B601). South and Grant (1970,1972) and Williams and James (1973,1976) have successfully employed a Wayne Kerr B201 bridge (0.1 - 5 MHz). Rosen, Bignall, Wisse and Van der Drift (1969) used a thoroughly calibrated Hatfield bridge, type LE/300A, for the frequency range 0.1 - 10 MHz. A part of the corresponding calibration work has been performed by the present author (Wisse et al., 1968).

The principles of four-terminal measurements are already known for many years (Ferris, 1963). Such measurements have been done with aqueous solutions by Berberian and Cole (1968,1969), Hayakawa, Kanda, Sakamoto and Wada (1975) and Zwolle (1978). Problems concerning the electronic part of the design are still difficult to overcome. Fortunately, a very suitable measuring system became commercially available recently from the General Radio Company, i.e. the GR1621 system.

2.2. Choice of the measurement equipment

For frequencies below 10 MHz the reliability obtained for the permittivity and dielectric loss of aqueous solutions is inevitably limited by technical difficulties in bridge measurements and cell design. We shall now describe the set-up in some detail.

2.2.1. *Bridge requirements*

Transformer ratio arm bridges were chosen because:

1) the potential across a transformer arm in series with the unknown is balanced in amplitude and phase with a similar potential from the standard admittance. The same standard components can be used for measurements over a wide range of admittances;

2) bridges with inductive ratio arms do not requite a Wagner earth arrangement. The associated inconvenience of double balancing is thereby avoided (Calvert, Cornelius, Griffiths and Stock, 1958);

3) transformer ratio arm bridges are particularly suitable for three-terminal measurements: residual impedance effects, due to resist-ances and shunt capacitances of the circuit elements and their leads, are minimized (Cole and Gross, 1949; Middelhoek, 1967; and Bordewijk, 1968). Only self-inductances play a part. However, as will be seen in section 2.7, the remaining self-inductances can be eliminated by performing measurements at different electrode separations.

A solution in the cell can be represented electrically by an ad-mittance:

$$Y = G + j\omega C \tag{2-1}$$

with $j = \sqrt{-1}$. The determination of Y involves the balancing of two currents in different parts of the circuits of the bridge, one of them flowing through the unknown admittance:

$$I = YV = (G + j\omega C) V \tag{2-2}$$

with I = electric current and V = applied voltage. In the mathematic-al representation this can be conceived as a current flowing through G in phase with V and a current flowing through C in quadrature with V (see fig. 2-1). The phase angle δ defined as the loss angle and the loss tangent is given by equation (1-3). For large values of tg δ, an

18
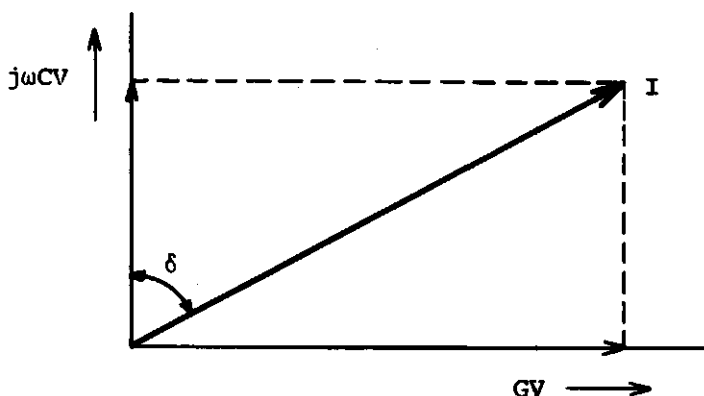
Figure (2-1): Argand diagram of the complex current.

accurate determination of both C and G demands extremely accurate
balancing of the current, especially at low ω values. Therefore, in
practice a limit of the highest value of tg δ will be met, depending
on the quality of the measuring system: special attention has to be
paid to the resolution when a choice is made for a measuring system.

2.2.2. *Problems involved in designing the cell*

In the case of dielectric measurements on aqueous solutions,
corrections must be made essentially for three possible errors, which
in part are characteristic for the aqueous solution case:

1) a contribution due to lead impedances;
2) deviations from ideality of the cell, resulting in a residual ca-
   pacitance;
3) a contribution by electrode polarization.

Ad 1): At high frequencies, deviations due to the occurrence of
inductances in the leads play a part. Attention must be paid to the
quality and length of the leads, connecting the cell with the bridge
and leads between the bridge and external standards, if any.

Ad 2): Residual capacitances arise if part of the electric field
lines pass out of the liquid (stray capacitances). Therefore, it is
important that such stray fields should be strictly controlled during
the experiment. In the cells used, field lines which did not pass

through the liquid to be tested were bound to travel through a layer of teflon (cell wall) either between the electrodes or from the electrodes into the third terminal.

Ad 3): Several methods are applicable to correct for the effects of electrode polarization:

a) Techniques to reduce the influence of electrode polarization on the measured quantities.

The enlargement of the electrode surfaces by applying platinum black electrodes or sandblasted electrodes especially has to be mentioned (Schwan, 1963,1966; Takashima, 1964). A disadvantage of platinum black electrodes is that they are easily damaged. The use of platinized electrodes is not sufficient to eliminate the polarization effect completely.

b) Frequency variation method.

Oncley (1942) plotted the measured capacitance C_x against $G_x^2 \nu^{-(2-n)}$ in which G_x is the measured conductance and n is assumed to be a constant over the entire frequency range used. A straight line is obtained, yielding the capacitance C_s of the solution as intercept. However, C_s has to be constant and hence dielectric dispersion is not allowed to occur in the frequency range used. From preliminary measurements on polystyrene latices we found that the frequency range should be chosen below 1 kHz to apply the frequency variation method, because relaxation occurs above 1 kHz. Below 1 kHz unfavourably large tg δ-values are encountered and, consequently, large capacitance errors are met. Therefore we did not apply the frequency variation method.

c) Substitution method.

This method · is based on the subtraction of capacitive increments observed at a simple electrolyte solution from the corresponding increment of the unknown solution (Schwan, 1963). Both solutions must have the same conductance. The measurements have to be made under the same experimental conditions (in particular, the current

20

density must be equal and the same pair of electrodes must be used). Furthermore, it has to be assumed that the polarization contribution is the same in both cases. However, some investigators (Moser, Squire and O'Konski, 1966; Wisse, 1970) observed differences in behaviour of the electrode polarization and magnitude of polarization errors between the solutions to be tested and the electrolyte solutions.

d) Method in which a variable electrode distance is involved.

Fricke and Curtis (see section 1.2) proposed this method, whereas Mandel (1956,1965), Rosen (1966,1969), Young and Grant (1968) and Van der Touw (1971a,b , 1975c) further considered and applied this technique. The method starts from the assumption that the electrode polarization capacitance C_e is independent of the distance d. This was proven to be correct experimentally by Mandel (1956). Furthermore, it appeared to be a reasonable assumption that C_e remains constant during the time needed to perform measurements at a restricted number of electrode separations. The time during which C_e remains constant depends on the solution under investigation (see section 2.7.2). A disadvantage of this method is that it is very time-consuming because all measurements have to be repeated at various d-values.

From the investigations described above, where use has been made of the variable electrode distance method, it is established that this method is the most promising one. Therefore, in our investigations the method involving a variable electrode distance was chosen in combination with the use of sandblasted platinum electrodes.

2.2.3. *Instrumentation used*

For the frequency range from 70 Hz to 100 kHz, a General Radio 1621 Precision Capacitance Measurement System was applied (see section 2.3). In the frequency range from 100 Hz to 5 MHz a Wayne Kerr B201

bridge in conjunction with a Wayne Kerr SR268L source and detector was used (see section 2.5). Both bridges directly measure the parameters C_m and G_m in parallel configuration. The applied frequency was measured with a Venner digital counter TSA6634A/2. With the help of a Tektronix 5103N oscilloscope system the voltage across the electrodes of the cell was controlled and kept below 100 mV (r.m.s. value) to avoid electrolysis in the aqueous solutions.

A three-terminal cell was developed for measurements of protein solutions in the frequency range above 100 kHz (Rosen et al., 1969; Wisse et al, 1969). We used this cell[*] as a test cell in establishing the demands for a more appropriate cell. Hence all final measurements were performed using a three-terminal cell designed in cooperation with Blom (see section 2.6). In all the measurements, the cell was thermostatted with a Calora Ultra thermostat NB-33 (accuracy $\pm 0.05\,^{o}$C). The measurements were performed with the solution in the cell kept under a nitrogen atmosphere.

During the measurements, preliminary computations were made with a Hewlett Packard HP97 programmable printing calculator to judge the significance of the results. Final results were obtained by calculations with a DEC-10 computer.

2.3. The General Radio 1621 Precision Capacitance Measurement System

2.3.1. *General features*

The 1621 is an assembly of three integrated instruments. Both the very sensitive GR1238 detector and the GR1316 highly stable oscillator are developed especially for use in combination with the GR1616 bridge, resulting in a measuring system with high sensitivity and allowing easy manipulation.

Eight of the twelve internal capacitance standards of the bridge

---

[*] This cell was constructed by Mr. G. Selier and Mr. T.A.C. van Vliet, Mechanical Workshop, Department of Chemistry, University of Leiden.

22

are enclosed in a thermally insulated compartment with a thermal time constant of six hours to reduce the effects of ambient temperature changes. Metal film resistors in T-networks with small phase angles are used to balance the conductance. Standards not in use are disconnected to reduce shunt capacitances across the detector input. The detector has a 130 dB gain and contains three meters to increase the rate of balancing: one displays the magnitude of the voltage, and the two others show a simultaneous display of the in-phase and quadrature component of the voltage. The effect of input-signal irregularities can be reduced by means of a tunable filter, line-rejection filter (band width 3%) and selectable time constants in the phase-sensitive detector circuits. The 1316 contains a Wien-bridge oscillator and two reference outputs, for use in precise balances of conductance and capacitance.

With this system it is in principle possible to resolve unbalances as small as 0.1 aF and 0.1 fS. Detection of such small unbalances is aided by ratio-transformer voltage capabilities up to 160 Volts at 1 kHz. However, because a voltage of only 100 mV was applied to the cell to avoid electrolysis, the detection was not as sharp as possible but was still satisfactory for our purposes (see section 2.3.2). Furthermore, at high tg δ, only the predominant admittance can be measured accurately (see section 2.2.1). The high accuracy of C is lost when a high G has to be balanced, because G standards always contain some stray capacitance.

It was considered worthwhile to pay much attention to the General Radio system used. As the application of this General Radio system to aqueous solutions has not yet been given in the literature, we decided to analyse the performance under these conditions in some detail.

Fig. (2-2) gives the fundamental bridge network.

2.3.2. *Sensitivity of the system*

The unknowns C_x and G_x can be determined with an accuracy which
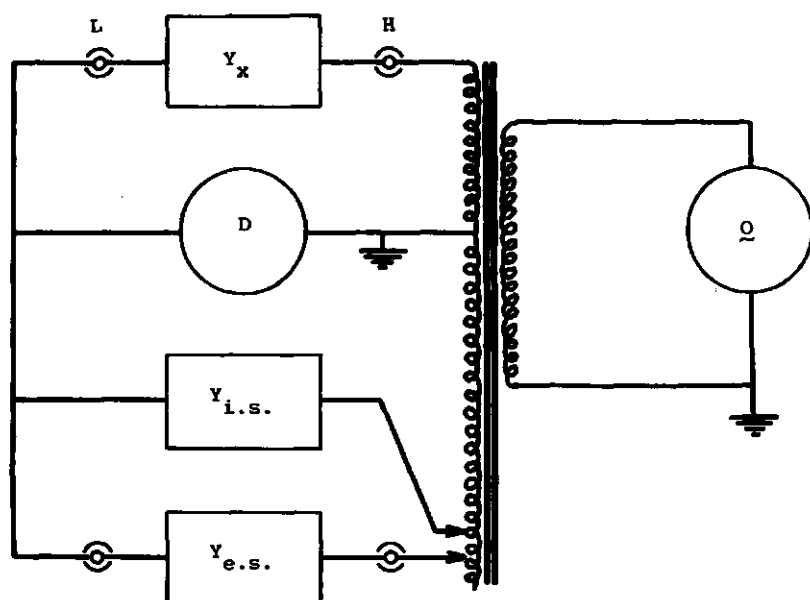
Figure (2-2): Simplified circuit diagram of the GR1621 measuring system. D = GR1328 detector. H = high terminal. L = low terminal O = GR1316 oscillator. $Y_{e.s.}$ = external standards. $Y_{i.s.}$ = internal standards. Y_x = unknown admittance.

depends on the sensitivity of the detector. In our special case the bridge has to measure extremely large capacitances and conductances. The accuracy, as calculated by the General Radio Company (1974a,b), based on the detector sensitivity, does not apply to the conditions of our studies, because of the high tg δ values involved. Therefore, it was found necessary to determine the attainable detector sensitivity independently.

When the bridge is balanced:

$$Y_x = Y_{st} \tag{2-3}$$

Y_x is the unknown admittance and Y_{st} is the sum of the internal and external standards (see fig. 2-3). The amplitude of the minimum de-

24
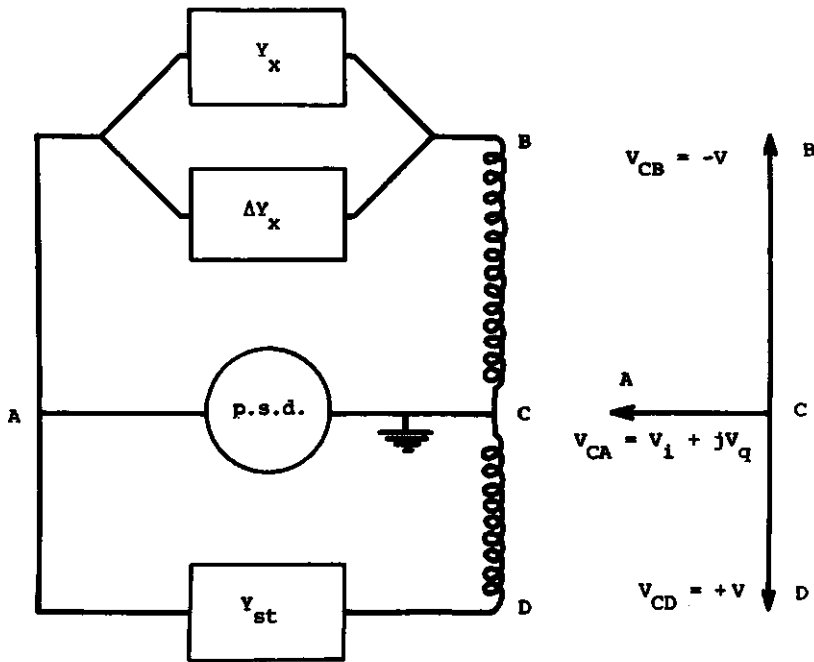
Figure (2-3): Elementary diagram of the balanced bridge.
p.s.d. = the two phase sensitive detectors of the GR1238. Y_{st} =
sum of the internal and external standard admittances. Y_x = un-
known admittance. ΔY_x = minimum detectable change of Y_x.

tectible voltage V_d across the two phase sensitive detectors of the
GR1238 is equal to:

$$V_d = V_{CA} = V_i + jV_q \tag{2-4}$$

Application of Kirchhoff's laws gives:

$$I_{BA} = (Y_x + \Delta Y_x)V_{BA} = (Y_x + \Delta Y_x)(V + V_i + jV_q) \tag{2-5}$$

and

$$I_{AD} = I_{BA} - I_{AC} = Y_{st}V_{AD} = Y_{st}(V - V_i - jV_q) \tag{2-6}$$

25

in which ΔY_x is the minimum detectable change of Y_x. Let Y_d be the total admittance of the phase sensitive detectors, then

$$I_{AC} = Y_d V_{AC} = -Y_d (V_i + j V_q) \qquad (2\text{-}7)$$

Combining equations (2-5), (2-6) and (2-7) results into:

$$\Delta Y_x = Y_{st} \frac{V - V_i - j V_q}{V + V_i + j V_q} - Y_d \frac{V_i + j V_q}{V + V_i + j V_q} - Y_x \qquad (2\text{-}8)$$

V_i and V_q decrease gradually from about 130 nV at 10 Hz to 40 nV at 500 Hz ($V_i = V_q = 70$ nV at 120 Hz; $V_i = V_q = 55$ nV at 220 Hz) and $V_i = V_q = 40$ nV for frequencies above 500 Hz (General Radio Company, 1974b). The applied voltage is 100 mV. Therefore,

$$V \gg V_i \quad \text{and} \quad V \gg V_q \qquad (2\text{-}9)$$

Combining equations (2-3), (2-8) and (2-9) gives:

$$\Delta Y_x \stackrel{\sim}{\sim} -Y_x \frac{V_q^2 + 2 j V V_q}{V^2} - Y_d \frac{V_i + j V_q}{V} \qquad (2\text{-}10)$$

With $Y_x = G_x + j\omega C_x$, $\Delta Y_x = G_x + j\omega \Delta C_x$ and $Y_d = G_d + j\omega C_d$ equation (2-10) can be written as:

$$\Delta G_x \stackrel{\sim}{\sim} G_x \frac{V_q^2}{V^2} - \omega V_q \frac{2 C_x + C_d}{V} + G_d \frac{V_i}{V} \qquad (2\text{-}11)$$

and

$$\Delta C_x \stackrel{\sim}{\sim} C_x \frac{V_q^2}{V^2} + V_q \frac{2 G_x + G_d}{\omega V} + C_d \frac{V_i}{V} \qquad (2\text{-}12)$$

Using the detector specifications $C_d = 20$ pF and $G_d \approx 1$ nS (General Radio Company, 1974b) ΔG_x and ΔC_x have been calculated for some representative experimental conditions (see table 2-1).

As may be deduced from the experimental data, both ΔG_x and ΔC_x are always mainly determined by the second term in the equations (2-11) and (2-12) respectively. Therefore, ΔG_x increases with increasing ωC_x, whereas ΔC_x decreases with increasing ω, because in the

26

TABLE (2-1). ΔG_x and ΔC_x calculated with equations (2-11) and (2-12).

cell content	ν (Hz)	d (mm)	G_x (μS)	C_x (pF)	$|\Delta G_x|$ (pS)	$|\Delta C_x|$ (pF)
H_2O	120	5	17.947	114.50	0.13	0.03
	120	10	8.865	47.28	0.06	0.02
	993	5	18.439	79.49	0.78	0.002
	993	10	9.079	38.64	0.42	0.001
	69850	5	18.584	76.03	53	0.00004
	69850	10	9.219	37.38	29	0.00002
1.000 mol/m^3 KCl in H_2O	706	4	2056.89	11102.4	69	0.37
	706	10	809.09	1761.1	11	0.15
	993	4	2064.78	7253.8	63	0.26
	993	10	810.78	1153.0	10	0.10
	7019	4	2085.26	439.16	28	0.04
	7019	10	813.49	89.88	6.2	0.02
	69850	4	2090.13	106.60	72	0.004
	69850	10	813.74	38.35	30	0.002
polysty-rene latex with 0.5 mol/m^3 KCl	221	4	2648.18	86835	169	2.10
	221	10	1050.25	13919.2	27	0.83
	705	4	2668.93	14296.5	89	0.49
	705	10	1051.74	2405.2	15	0.19
	993	4	2693.51	8408.8	73	0.34
	993	10	1055.49	1502.6	13	0.14
	7019	4	2720.11	981.54	61	0.05
	7019	10	1062.37	306.76	20	0.02
	69860	4	2797.60	221.14	142	0.005
	69860	10	1085.05	84.98	58	0.002

frequency range covered G_x is independent of ω to within 1%. The possible increase or decrease of ωC_x with increasing ω depends on the amount of electrolyte present in the solution and on the extent of electrode polarization. This becomes clear when $\Delta G_x(\omega)$ for H_2O and 1.000 mol/m^3 KCl or the polystyrene latex are compared. The dependences of ΔG_x and ΔC_x on ω, as predicted by the equations (2-11) and (2-12), are always experimentally obeyed in transformer bridge measurements on pure water or poorly conducting solutions.

Only at frequencies below 1 kHz and at d-values below about 7 mm, ΔC_x becomes insufficient if polystyrene latices with about 1.5 mol/m^3 of a simple electrolyte are measured. However, as will be seen in chapter 4, measurements below 700 Hz are less interesting with our equipment, due to the occurrence of an other relaxation mechanism below 1 kHz.

The lowest decade which is needed in the conductance measurements is 1 – 10 nS. Therefore, the minimally detectable ΔG_x is sufficiently low for our measurements.

Based on preliminary measurements, similar to those described here, the sensitivity of the GR1621 system was found to be sufficient to perform measurements on polystyrene dispersions with a maximum of about 1.5 mol/m^3 simple electrolyte present.

2.3.3. *Accuracy*

The most important reason for the limitation of the accuracy at frequencies above 10 kHz is the presence of a leakage reactance in the ratio transformer. The difficulty in determining the residual parameters of the numerous switch combinations renders impracticable the detailed calculation of errors for correction of most measurements. The uncertainties are given by (Homan, 1968):

$$C_{error} = - \omega^2 C_{hs} C_{ls} L_{sg} \qquad (2-13)$$

and

$$G_{error} = -\omega^2 C_{hs} C_{ls} R_{sg} \qquad\qquad (2\text{-}14)$$

with C_{hs} = shunt capacitance from the high terminal side to ground;
C_{ls} = shunt capacitance from the low terminal side to ground. Patch
cord contributions have to be included in C_{hs} and C_{ls}. L_{sg} and R_{sg}
are, respectively, the resistance and inductance of the path from a
virtual common point in the shield surrounding the unknown admittance
to the ground point in the heart of the bridge. Equations (2-13) and
(2-14) do not contain d. Therefore, the permittivity ε and conducti-
vity σ of the measured solutions are independent of C_{error} and G_{error}
(see section 2.7).

In addition, the elimination of Z_e will introduce errors. As may
be seen from table (2-1), values up to about 90 nF for the capaci-
tance of polystyrene solutions may be found. The calculated permitti-
vities at the frequencies mentioned are about ten times the permitti-
vity of water. The corresponding capacitances amount only 0.9 nF, be-
ing only 1% of C_x. Several measurements have to be performed at one
frequency to eliminate Z_e. Advantage was taken of this necessity by
using the same measurements to calculate standard deviations of ε
and σ.

Although the resistors for the external conductance box (see
section 2.4) were carefully selected, systematic errors will be in-
evitably present. The accuracy of the resistors is better than 0.1 %.
The accuracy in σ will be influenced also by the extent to which it
will be possible to correct for the time drift in σ (see section 2.7.2).

In combination with the results given in section 2.3.2 it is
clear that:
1) the final accuracy of ε in the frequency range of the GR1621 sys-
   tem will depend more on C_e than on the quality of the measuring
   system;
2) the final accuracy in σ does not depend on the quality of the meas-
   uring system, but on the quality of the conductance box and on the

time drift in σ;

3) in addition to errors always present (e.g. due to the non-ideality of the cell) the standard deviations are a measure of the reproducibility.

2.4. The conductance box[*]

The GR1616 has the disadvantage of a conductance range which is too limited for our purposes. Therefore an extra conductance box was constructed, to be used in conjunction with the bridge. This box, with a conductance G_b, ranging from 10 μS to 9 mS, is connected to the external standard terminals of the bridge (see fig. 2-2).

The 100 kΩ standard of the bridge, in combination with the terminal selector and the external multiplier, has been used to select by comparison sets of low inductance metal film resistors of 100 kΩ, 10 kΩ and 1 kΩ (Draloric Electronic GmbH, SMA 0207). This type of resistor is very stable (temperature coefficient: 50 ppm/K; constant conductance value and almost constant reactance value up to 100 kHz). The selected resistors were placed parallel in the box. The resistors were connected to the terminals of the box by three sets of push-button switches (Oreor CTN 1008). The same switches were used to earth the resistors not in use.

A problem in the construction is the occurrence of lead inductances L_b, leading to changes in C_x by an amount $L_b G_b^2$. To reduce this effect L_b was kept low by applying short coaxial cables and by placing the decade with the highest G_b closest to the terminals. Although the products $L_b G_b^2$ were kept as low as possible, it was found necessary to calibrate the deviations C_b in the capacitance readings of the bridge. This was performed by comparing the various settings of the

---

[*] Developed in cooperation with J. Blom, A.J. Korteweg and R.A.J. Wegh, Laboratory for Physical and Colloid Chemistry, Agricultural University, Wageningen, The Netherlands.

conductance box, connected to the external standard terminals of the bridge, with additional selected resistors of the same type and values connected to the unknown terminals of the bridge. To obtain reproducible results, the additional resistors were soldered on two parallel brass plates, fixed in a small shielded box. The capacitance of the empty small box was measured directly with the bridge. The obtained corrections ΔC on C_x, including the residual capacitance of the conductance box, are used for all the calculations. ΔC values are listen in appendix A. The values appeared to be independent of the frequency up to at least 80 kHz.

2.5. The Wayne kerr B201 and SR268L measuring system

The B201 is meant to be used for the frequency range 100 kHz to 5 MHz. Calvert (Wayne Kerr monograph no. 1) described the principles of this bridge. Bordewijk (1968) used a B201 to investigate the dielectric behaviour of alcohols. South and Grant (1970,1972) and Williams and James (1973,1976) used this type of bridge for measurements on aqueous solutions.

A simplified circuit diagram of the measuring system is shown in fig.(2-4). Tappings on the two bridge transformers are connected to decade controls. Thereby it is possible to perform measurements with an accuracy of 0.1% for capacitances from 1 pF to 1 nF and an accuracy of 0.5% for conductances from 1 μS to 0.1 S. The accuracy for both C and G decreases above 1 MHz proportionally to the square of the frequency. Therefore almost all measurements were performed below 1 MHz.

The source level and gain control of the bridge were preset to their maximum values, because the attenuators on the SR268L generator and detector were used to reduce the time required for balancing. The balance point is displayed on a magnitude null-meter.

Because only a small contribution of C_e exists for $\nu>100$ kHz, $C_x<0.2$ nF for the measurements with the B201. Therefore this bridge is used for measurements of usual C_x values. Already much attention
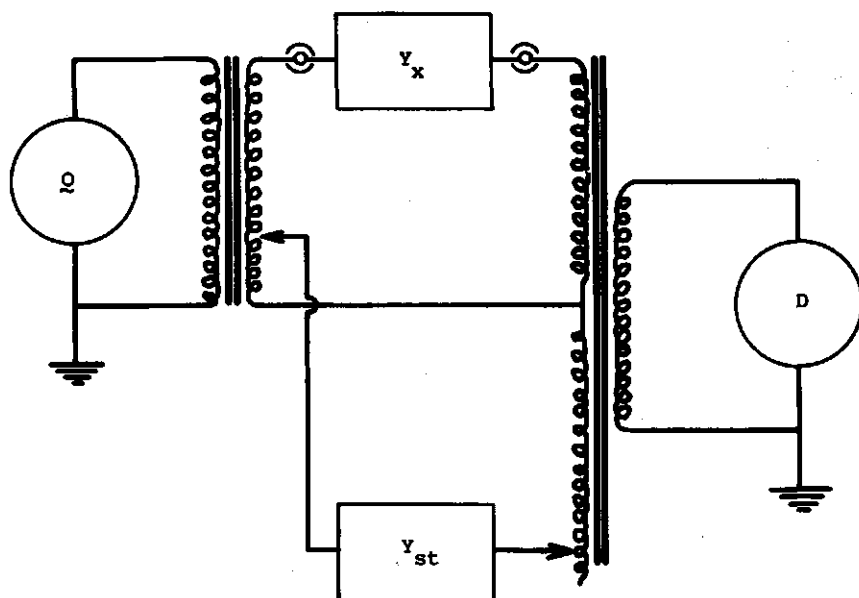
Fig. (2-4). Simplified diagram of the Wayne Kerr measuring system. D = SR268L detector. O = SR268L generator. Y_{st} = standard admittance. Y_x = unknown admittance.

has been paid in literature to the B201 (see section 2.1). Hence it was not considered necessary to repeat the analysis of the merits and demerits of this bridge.

As with the GR1621 system, the standard deviations of ϵ and σ are calculated from the different measurements at one frequency.

2.6. The measuring cell[*]

2.6.1. General description

An important prerequisite in the construction of the cell is the

---

necessity of a variable distance d between the two plane parallel electrodes (see section 2.2.2). Cells with this option have been described by Mandel and Jenard (1958), Schwan and Maczuk (1960), Broadhurst and Bur (1965), Young and Grant (1967,1968), Rosen et al. (1969) and Van der Touw, Selier and Mandel (1975c).

The essential features of the cell are given in fig.(2-5). The electrodes have a diameter of 25 mm and are made of platinum to ensure ideal polarization as well as possible (Grahame, 1946,1947,1954). The total surface area of the electrodes was increased by sandblasting. Accordingly, the influence of Z_e is reduced as described by Schwan (1963,1966,1968). In a theoretical analysis, Scheider (1975) associated the frequency dependence of Z_e with surface roughness. The fixed bottom electrode (32) is connected to the high terminal of the bridge. The upper electrode (31) and the shield (15) are connected to the low terminal. The other metal parts, including the guardring (27) are earthed. The upper electrode, the glass tube (9) containing the coaxial cable (5) and the plateau (8) can move together upwards and downwards. This plateau is moved manually. The fine setting is achieved by a set-screw (2). The associated displacement is registered by a Compaq 523 GL 10 micrometer gauge (1). The inner diameter of the cylindric sample holder (18) is 26 mm. In the top plate (12) of the sample compartment there are three openings: two (11) for the inlet and outlet of nitrogen gas and one (10) for the introduction of electrolyte with an Agla syringe micrometer.

For d > 10 mm stray fields have been found to play a part. Currents from the lower electrode passing through the solution and the teflon cell wall (14) to the shield are purely capacitive. The potential drop in the solution is almost completely determined by G_x and d, because in our measurements usually $G_x > \omega C_x$. This was verified by Blom (1979), performing measurements on a 1.000 mol/m^3 KCl solution. During these measurements the upper electrode was connected to earth, the shield to the low terminal and the bottom electrode to
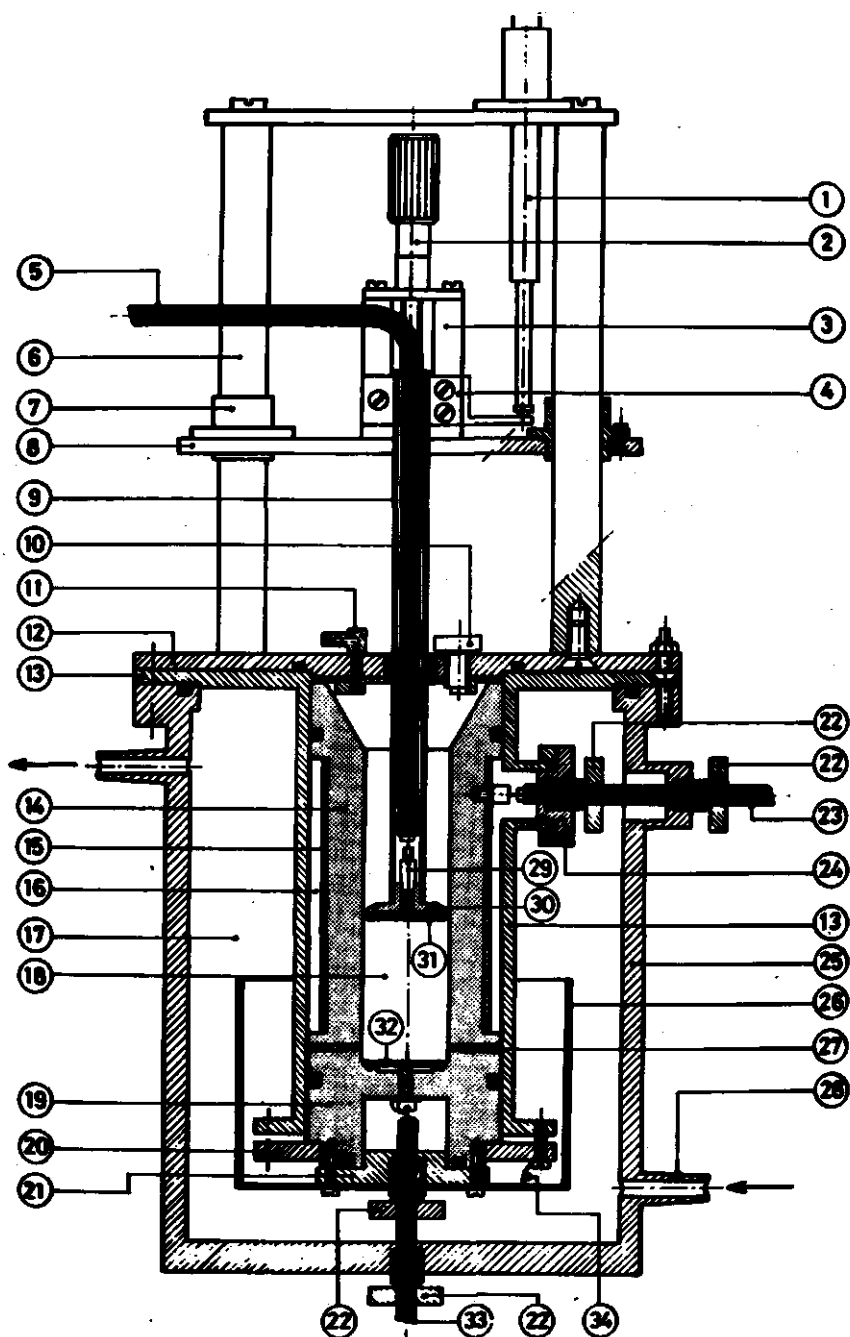
Figure (2-5). The cell construction.
For legends to this figure see the next page.

Materials used:

Brass = A. Copper = B. Stainless steel = C. Polyvinyl chloride = D.
PTFE (teflon) = E. Perspex = F. Glass = G. Aluminum = Al. Platinum
= Pt. Butyl rubber washer = ▣ .

Description:

 1: micrometer gauge
 2: set-screw (Al)
 3: mounting of the set-screw (A and steel)
 4: fastening block upper electrode tube (F)
 5: coaxial cable (GR874)
 6: guiding slide (C)
 7: bearing slide (C)
 8: plateau (C)
 9: tube (G)
10: plug (D) with O-ring
11: N_2-inlet or N_2-outlet opening (D)
12: top plate (C)
13: thermostat mantle (A)
14: cell wall (E)
15: shield (A)
16: inert isolating liquid (3M company, FC 75)
17: thermostat liquid (water)
18: sample
19: mounting bottom electrode (E)
20: end ring (D)
21: packing plate (D)
22: tightening plug (D)
23: coaxial cable (GR874)
24: tightening plate (D)
25: outer wall (D)
26: guarding case (A,B)
27: guard ring (A)
28: inlet thermostat liquid (D)
29: conical bolt to fix the electrode (A)
30: mounting upper electrode (E)
31: upper electrode (Pt)
32: bottom electrode (Pt)
33: coaxial cable (GR874)
34: wire.

the high terminal of the bridge. With this method the stray capacitance was obtained from the bridge readings, because the potentials of the electrodes and the shield are the same as in the normal measurements. It appears that the stray capacitance is independent of the frequency with our cell.

2.6.2. *Equivalent circuit of the cell*

It is generally accepted that the total impedance of connecting leads and the cell filled with a conducting liquid may be represented by the equivalent circuit as shown in fig.(2-6) (e.g. Mandel, 1965; Young and Grant, 1968; Van der Touw et al., 1971a). It is convenient to write the impedance Z of the circuit without C_r:

$$Z = \frac{1}{G_s + j\omega C_s} + \frac{1}{G_e + j\omega C_e} + R_c + j\omega L_c \qquad (2-15)$$

Y_x is the admittance of the completed circuit:

$$Y_x = \frac{1}{Z} + j\omega C_r \qquad (2-16)$$

In electrode kinetic studies it has been argued that the position of C_s is somewhat different, i.e. parallel with the combination C_e, G_e^{-1}. However, it has been shown that for measurements in the frequency range below 10 MHz this is of no importance (Van Leeuwen, 1978).

2.7. Calculation of the permittivity and conductivity

In this part the techniques involved in obtaining the permittivity ε and the conductivity σ of the solution under investigation will be described.

2.7.1. *Mathematical formulation*

Y_x is measured with both bridges as a parallel capacitance C_x and conductance G_x. Due to the use of the conductance box as an external standard, C_x must be corrected with ΔC (see section 2.4). We define:

36
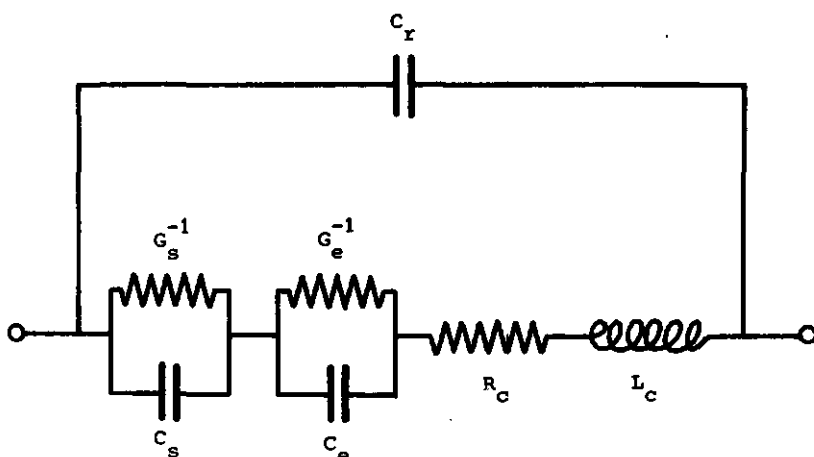
Figure (2-6). Equivalent circuit of the cell.
C_e = electrode polarization capacitance. G_e = electrode polariza-
tion conductance. C_s = capacitance of the bulk of the solution in
the cell. C_r = residual capacitance, depending on the construc-
tion of the cell. L_c and R_c : inductance, respectively resistance
due to the part of the cell not localized between the electrodes
and due to the coaxial cables connecting the cell with the ter-
minals of the bridge. G_s = conductance of the bulk of the solu-
tion in the cell.

$$C_y \equiv C_x - \Delta C \tag{2-17}$$

With (2-16) the relation between the measured quantities and the com-
ponents of the equivalent circuit becomes:

$$G_x + j\omega C_y = \frac{1}{Z} + j\omega C_r \tag{2-18}$$

Combining (2-15) and (2-18):

$$G_x + j\omega C_y - j\omega C_r = \frac{1}{G_s + j\omega C_s} + \frac{1}{G_e + j\omega C_e} + R_c + j\omega L_c \tag{2-19}$$

After separation of the real and imaginary parts of (2-19):

$$\frac{G_x}{G_x^2 + \omega^2 (C_y - C_r)^2} = \frac{G_s}{G_s^2 + \omega^2 C_s^2} + \frac{G_e}{G_e^2 + \omega^2 C_e^2} + R_c \tag{2-20}$$

37

and: (2-21)

$$\frac{C_y}{G_x^2 + \omega^2(C_y - C_r)^2} = \frac{C_s}{G_s^2 + \omega^2 C_s^2} + \frac{C_e}{G_e^2 + \omega^2 C_e^2} + L_c + \frac{C_r}{G^2 + \omega^2(C_y - C_r)^2}$$

For aqueous solutions at frequencies below a few MHz,

$$R_c \ll \frac{G_s}{G_s^2 + \omega^2 C_s^2} \tag{2-22}$$

Therefore, under these conditions, R_c may be neglected.

C_r depends on the nature of the solution in the cell and on d, which makes it impossible to determine C_r exactly in advance. Furthermore, ωC_r has to be compared with ωC_s and G_s to decide whether it is allowed to neglect C_r in equation (2-21). For d < 25 mm it was shown by measurements on a 1.00 mol/m³ KCl solution that C_r < 0.4 pF (see also Blom, 1979). The smallest value of C_s is about 17 pF. Particularly for large values of $G_s/\omega C_s = \mathrm{tg}\, \delta_s$, found at low frequencies, the influence of C_r is negligible in the left hand term of the equations (2-20) and (2-21). As a first approximation, the equations (2-20) and (2-21) can then be simplified to:

$$\frac{G_x}{G_x^2 + \omega^2 C_y^2} = \frac{G_s}{G_s^2 + \omega^2 C_s^2} + \frac{G_e}{G_e^2 + \omega^2 C_e^2} \tag{2-23}$$

and

$$\frac{C_y}{G_x^2 + \omega^2 C_y^2} = \frac{C_s}{G_s^2 + \omega^2 C_s^2} + \frac{C_e}{G_e^2 + \omega^2 C_e^2} + \frac{C_r}{G_x^2 + \omega^2 C_y^2} + L_c \tag{2-24}$$

Use will be made of the well-known expressions for an ideal condensor:

$$C_s = \frac{\varepsilon A}{d} \tag{2-25}$$

and an ideal conductance:

$$G_s = \frac{\sigma A}{d} \tag{2-26}$$

with:

$$\varepsilon = \varepsilon_0 \varepsilon_r \tag{2-27}$$

38

ε_0 = absolute permittivity of free space, ε_r = relative permittivity, and σ = electrical conductivity. A is the area of a cross-section of the cell, parallel to the electrode surfaces (A = 543 mm^2). After introduction of the equations (2-25) and (2-26) in (2-23) and (2-24):

$$\frac{G_x}{G_x^2 + \omega^2 C_y^2} = \frac{\sigma}{\sigma^2 + \omega^2 \varepsilon^2} \cdot \frac{d}{A} + \frac{G_e}{G_e^2 + \omega^2 C_e^2} + O(d^2) \qquad (2-28)$$

and

$$\frac{C_y}{G_x^2 + \omega^2 C_y^2} = \frac{\varepsilon}{\sigma^2 + \omega^2 \varepsilon^2} \cdot \frac{d}{A} + \frac{C_e}{G_e^2 + \omega^2 C_e^2} + L_c + O(d^2) \qquad (2-29)$$

The left hand side terms of equations (2-28) and (2-29) are plotted against d/A. From the intercepts σ, $\Delta\sigma$, ε and $\Delta\varepsilon$ are calculated, using a linear regression procedure. The terms $O(d^2)$ indicate quantities on the order of d^2 and are due to the non-ideality of the cell (Rosen et al., 1969). The term $C_r/(G_x^2 + \omega^2 C_y^2)$, depending on d^2, is the main part of $O(d^2)$ in equation (2-29). Deviations in the geometry of the cell and deviations in the determination of d also lead to terms incorporated in $O(d^2)$. As C_r increases with increasing d, d was kept as small as possible for each frequency in the calculation of ε, to minimize the influence of $O(d^2)$. Especially for the measurements with the B201 bridge the number of d values and the range of d values may be restricted. The frequency at which C_e becomes negligible depends on the nature of the solution in the cell (Schwan, 1963); e.g. for 1.000 mol/m^3 KCl solution it was calculated that measurements with $4 \leqslant d \leqslant 12.5$ mm were sufficient to obtain reliable results for ε at $\nu > 70$ kHz. In the calculation of σ for the same solution measurements with $4 \leqslant d \leqslant 22.5$ were used, because C_r is absent in equation (2-27).

In determining the range of d values to be taken, use was made of the correlation factors from the linear regression calculations.

2.7.2. *Drifts of the conductivity and capacitance with time*

The time dependence of the conductivity, $d\sigma/dt$, is a difficulty

in the dielectric measurements of aqueous solutions. Takashima (1963) reported a time drift for measurements on protein solutions, and Pethybridge and Spiers (1975) made a similar observation in their study of aqueous solutions in Pyrex glass cells.

In our measurements, about eight hours are needed to obtain the data for a complete description of the dielectric behaviour at a particular electrolyte concentration. Therefore the conductivity drift is a complication in our study as well. It was necessary to repeat a chosen frequency a few times during a measuring cycle to establish $d\sigma/dt$. These values were subsequently used to correct σ for this drift.

In section 2.2.2 it was indicated that C_e is independent of d. Therefore it was assumed that C_e, in particular, was constant during the time needed to measure G_x and C_x at the different d values. However, it appears that some drift in C_x occurs usually within a few hours. This drift is probably connected with a change in C_e, due to the adsorption of particles from the solution on the electrodes (Tamamuchi and Takahashi, 1974). Therefore it is not surprising that dC_x/dt is somewhat larger for latices than for simple electrolyte solutions.

2.8. Measuring procedure

The influence of dC_x/dt was kept negligible as compared with the overall accuracy by:
1) observing a waiting time of at least 24 hours, after a new solution was introduced into the cell;
2) measuring C_x and G_x at one frequency at all selected d values before a new frequency was taken;
3) mixing of the solution in the cell was performed by moving the upper electrode up and down. In the case of a new solution this was done thirty times before measurements were started. In addition, this mixing procedure was carried out five times every half

40

hour as a further prevention of drift in C_x;

4) the measurements at one frequency were performed without interruption.

dC_x/dt was checked by repeating after each d-variation cycle the measurement at the first d value.

2.9. Experimental verification of the procedure

2.9.1. *Introduction*

To check the experimental set-up and the basic equations used to calculate σ and ε, test measurements were performed. To measure a system with varying σ and constant ε, pure water and KCl solutions were used for these measurements. In the frequency range of the bridges used, ε of aqueous solutions with less than 10 mol/m^3 KCl is negligibly different from ε of pure water (Rosen, Bignall, Wisse and Van der Drift, 1969).

It is generally accepted in the literature that bridge measurements on aqueous solutions have reached an acceptable degree of reliability (for references, see section 2.1). Therefore only a limited number of test measurements have been performed.

The dielectric loss ε'' is calculated as:

$$\varepsilon'' = \frac{\sigma - \sigma_{dc}}{\varepsilon_o \, \omega} \qquad (2\text{-}30)$$

σ_{dc}, the d.c. value of the conductivity, is subtracted from σ. Therefore σ is a less critical parameter and hence it was found unnecessary to prepare water and KCl solutions of extremely high purity.

2.9.2. *Representative results*

The results collected in tables (2-2), (2-3) and (2-4) are calculated with the use of equations given in section 2.7, in particular with the equations (2-28) and (2-29).

The expected value for ε is 78.4 at 25.0 $^\circ$C (Handbook of Chemist-

41

TABLE (2-2). The dielectric permittivity and conductivity of H_2O, measured at 25.0 °C.

ν (kHz)	r^2_C	ε_r	d-range (mm)	$\Delta\varepsilon_r$	r^2_G	σ (µS/m)	d-range (mm)	$\Delta\sigma$ (µS/m)	$tg\delta_s$
0.120	0.99998	79.0	5 – 22.5	0.6	0.99997	161.81	5 – 22.5	0.36	307
0.222	0.99997	78.8	5 – 22.5	0.5	0.99997	161.80	5 – 22.5	0.34	166
0.993	0.99997	78.5	5 – 22.5	0.5	0.99998	161.95	5 – 22.5	0.32	37.4
9.973	0.99999	78.3	5 – 20	0.4	0.99997	161.31	5 – 22.5	0.41	3.7
69.85	0.99996	76.7	5 – 20	1.0	0.99954	162.65	5 – 22.5	6.15	0.6
150.01	0.99992	75.2	5 – 12.5	1.5	0.99939	154	5 – 22.5	24.7	0.3
400.07	0.99994	75.3	5 – 12.5	0.9	0.99967	152	5 – 22.5	16.9	0.1

TABLE (2-3). The dielectric permittivity and conductivity of 0.500 mol/m³ KCl in H_2O, 25.0 °C.

ν (kHz)	r^2_C	ε_r	d-range (mm)	$\Delta\varepsilon_r$	r^2_G	σ (mS/m)	d-range (mm)	$\Delta\sigma$ (mS/m)	$tg\delta_s$
0.423	0.9974	93.2	7.5 – 20	2.8	0.99998	7.551	5 – 22.5	0.014	3443
0.705	0.9977	85.1	7.5 – 20	2.4	0.99998	7.553	5 – 22.5	0.015	2263
0.993	0.9977	82.0	7.5 – 20	2.3	0.99998	7.568	5 – 22.5	0.016	1671
9.972	0.9986	77.5	5 – 20	1.7	0.99998	7.554	5 – 22.5	0.015	176
69.85	0.9997	76.6	5 – 20	1.0	0.99998	7.540	5 – 22.5	0.016	25.3
150.03	0.9998	77.8	5 – 12.5	0.5	0.99997	7.559	5 – 22.5	0.018	11.7
400.11	0.9999	77.5	5 – 12.5	0.3	0.99997	7.555	5 – 22.5	0.019	4.4
800.00	0.9999	77.7	5 – 12.5	0.5	0.99993	7.553	5 – 22.5	0.031	2.2

TABLE (2-4). The dielectric permittivity and conductivity of 1.000 mol/m^3 KCl in H$_2$O, measured at 25.0° C.

ν (kHz)	r^2_C	ε_r	d-range (mm)	$\Delta\varepsilon_r$	r^2_G	σ (mS/m)	d-range (mm)	Δσ (mS/m)	tgδ$_s$
0.706	0.9894	101.9	7.5 - 22.5	5.3	0.99996	14.896	4 - 22.5	0.035	3722
0.993	0.9990	90.0	7.5 - 22.5	1.7	0.99997	14.896	4 - 22.5	0.030	2996
2.001	0.9989	75.1	7.5 - 22.5	1.5	0.99997	14.899	4 - 22.5	0.030	1782
3.001	0.9993	76.2	4 - 20	1.2	0.99997	14.892	4 - 22.5	0.030	1171
4.009	0.9988	75.1	4 - 20	1.4	0.99997	14.895	4 - 22.5	0.029	889
7.019	0.9982	77.4	4 - 20	1.7	0.99997	14.897	4 - 22.5	0.030	493
9.972	0.9999	76.4	4 - 20	0.7	0.99997	14.900	4 - 22.5	0.030	351
69.85	0.9958	80.5	4 - 20	2.5	0.99997	14.866	4 - 22.5	0.030	47.5
150.01	0.9999	77.8	4 - 12.5	0.5	0.99995	14.764	4 - 12.5	0.014	22.7
400.13	0.9999	77.4	4 - 12.5	0.6	0.99999	14.759	4 - 12.5	0.021	8.6
800.14	0.9999	77.4	4 - 12.5	0.4	0.99999	14.734	4 - 12.5	0.014	4.3

ry and Physics, 1976-1977). In the three tables r^2 is the coefficient
of determination (correlation factor) indicating the quality of the
fit, achieved by the linear regression. r_G^2 stems from equation (2-28)
and r_C^2 from equation (2-29). Two d-ranges are given in the tables,
one for the calculation of ε and one for the calculation of σ. Final-
ly, use is made of:

$$\text{tg } \delta_s = \frac{\sigma}{\omega \varepsilon_0 \varepsilon_r} \tag{2-31}$$

with $\varepsilon_0 = 8.854$ pF/m.

2.9.3. *Conclusion*

The result on water and the KCl solutions show that reliable re-
sults are obtained especially when tg δ_s > about 5 and when tg δ_s <
about 2000.

From extra measurements, necessary to determine $d\sigma/dt$, it fol-
lowed that the results are reproducible to a high extent; e.g. the
following values for ε are obtained: 76.6 and 76.1 (1.000 mol/m^3 KCl;
9.972 kHz), 82.1 (2×) and 81.9 (0.500 mol/m^3 KCl; 993 Hz) and 87.5
(3×) (H_2O; 993 Hz). This reproducibility is even better than expected
from the data in tables (2-2), (2-3) and (2-4).

Comparing the values of $\Delta\varepsilon$ and $\Delta\sigma$ in the tables of section 2.9.2
with the content of section 2.7 it is clear that other errors must
be present as well. These errors are probably due to the occurrence
of the time drift in σ and the neglection of C_r and $O(d^2)$ terms in
the calculations.

In the case of the polystyrene dispersions used, ε is strongly
dependent on the electrolyte concentrations. A further treatment of
this system will be given in chapter 4. At this point it may be con-
cluded that the accuracy obtained is sufficient to serve the purpose
of the present study as described in section 1.1 .

3. MATERIALS

3.1. Chemicals

All chemicals used were of "pro analyse" quality, except for lithium chloride, being of "purum" quality. The water used was always doubly distilled and saturated with nitrogen.

3.2. Preparation and characterization of the polystyrene latices

The latices were prepared by the method of Furusawa, Norde and Lyklema (1972) to obtain particles with surfaces uncontaminated by emulsifiers. This method is based on a procedure described by Kotera, Furusawa and Takeda (1970). A detailed description of the method of preparation and characterization has been given by Norde (1976). Our only modification in the preparation of latices with high surface charge consisted of a change in the amount of distilled styrene used. Like Bijsterbosch (1978), we reduced the amount of styrene to obtain smaller particles. Instead of the amount of 20 ml (Norde, 1976), we used 8.5 ml distilled styrene to prepare latex A, 6.2 ml to prepare latex B and 4.2 ml to prepare latex C.

All measurements were performed on ion-exchanged latex samples.

3.2.1. *Determination of the particle size of the latices*

A Philips EM 300 electron microscope was used to determine mean values for the particle radius a. At least 150 particles of each sample were measured. The number average radius is:

$$a_{10} = \frac{\sum\limits_{i} n_i a_i}{\sum\limits_{i} n_i} \tag{3-1}$$

where n_i is the number of particles with radius a_i. The uniformity ratio can be written as a_{32}/a_{10}, where

$$a_{32} = \frac{\sum\limits_{i} n_i a_i^3}{\sum\limits_{i} n_i a_i^2} \tag{3-2}$$

The two parameters a_{10} and a_{32} were calculated for the latices used. An example of an electron micrograph is given in figure (3-1).
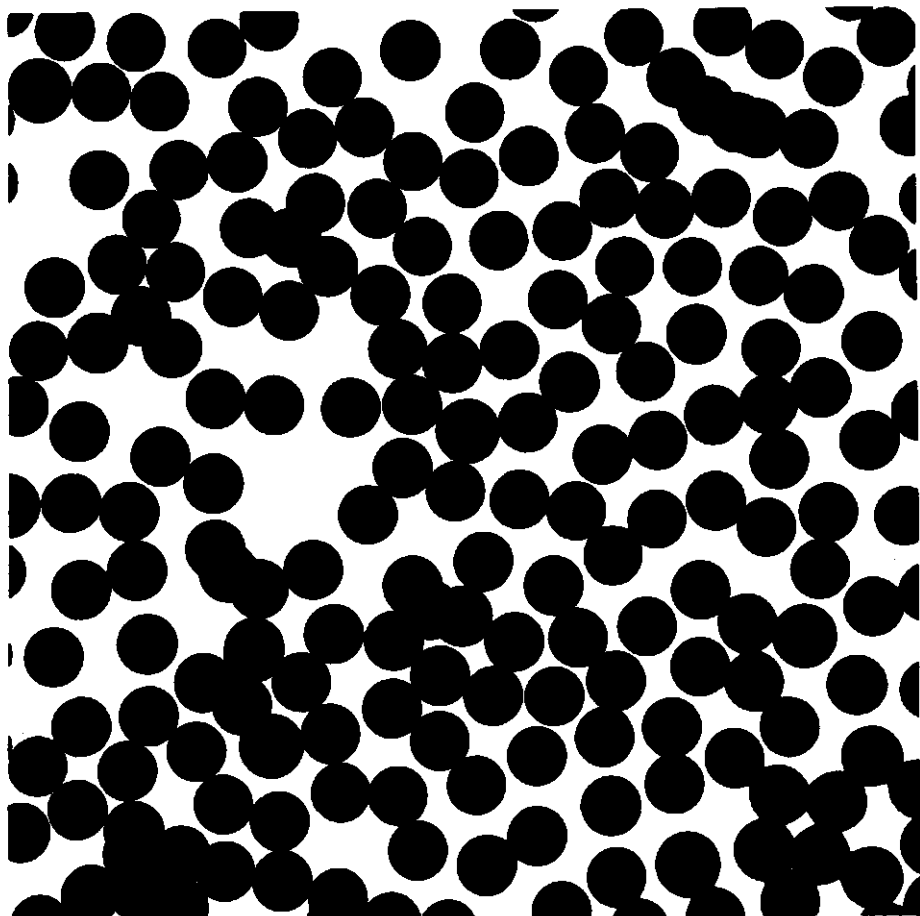
Figure (3-1): Electron micrograph of a latex sample.

3.2.2. *Determination of the surface charge of the latices*

The surface charge density σ_o was determined by conductometric titration. The experimental set-up used was the same as for the dielectric measurements, i.e. the General Radio GR 1621 system and the sample cell described in section 2.6 . The frequency used was 1 kHz. In chapter 5 the results for latex A are used for comparison with theory. Therefore latex A was taken as an example of a titration curve

(see fig. 3-2). The shape of this curve is comparable to the shape
of the curve given in the publication of Furusawa, Norde and Lyklema
(1972): only one distinct kink is present, due to the titratable sul-
phate groups.

All relevant information on the latices used in the dielectric
measurements is collected in table (4-1).
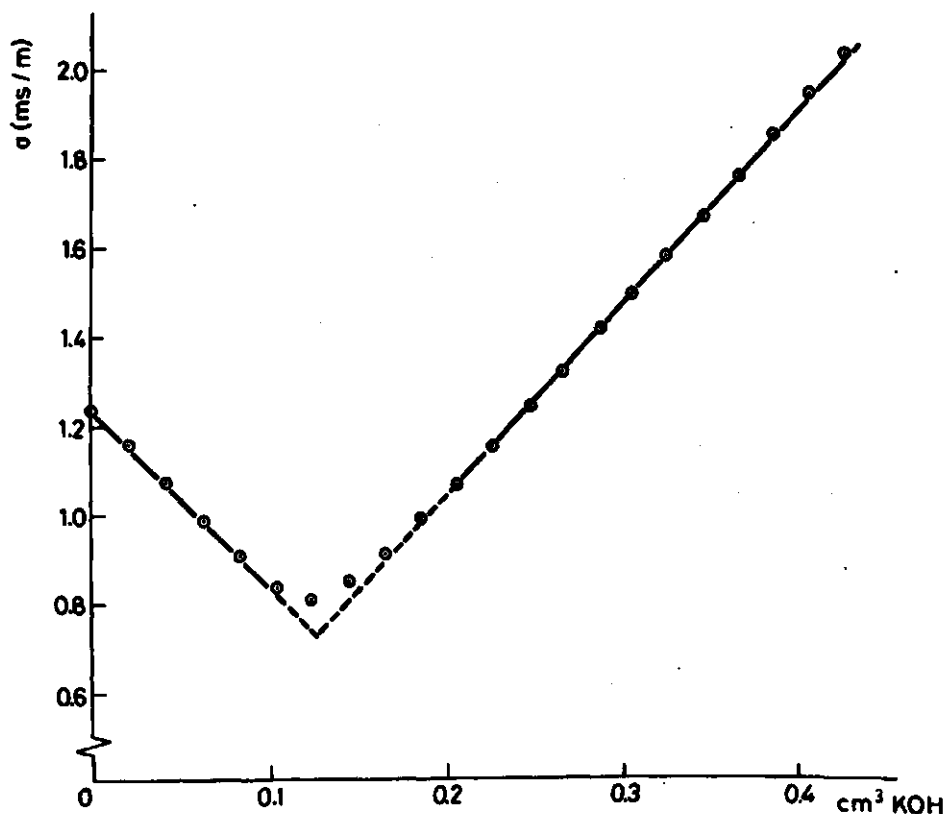
Figure (3-2): Conductivity σ as a function of added volume 22.1
mol/m³ KOH for 55 cm³ of undiluted sample latex A.

4. RESULTS OF THE MEASUREMENTS ON LATICES

4.1. General

To obtain latices with K^+ or Li^+ as the counterions as complete-
ly as possible, the ion exchanged samples were titrated with KOH or
LiOH respectively to the equivalence point of the sulphate groups.
The dielectric investigations were performed with these samples. In
this way the conductivity and permittivity were determined as a func-
tion of added KCl, LiCl or HCl.

In order to describe the dielectric properties of the measured
latices as completely as possible, all the results of the measure-
ments, corrected for drift in conductivity, are given in tables con-
taining ε, $\Delta\varepsilon$, σ and $\Delta\sigma$ (see Appendix B).

TABLE (4-1). Survey of the ion-exchanged latices used in dielectric
investigations.
a_{10} = number average radius; a_{32}/a_{10} = uniformity ratio;
σ_O = surface charge density; ϕ = volume fraction of the
latex sample.

sample	A_1	A_2	A_3	B_1	C_1	C_2	C_3
a_{10} (nm)	222			193	152		
a_{32}/a_{10}	1.001			1.002	1.002		
σ_O (mC/m^2)	16.1	18.6	18.6	21.0	15.4	17.6	17.6
ϕ	0.022	0.021	0.022	0.033	0.016	0.016	0.016
electrolyte	KCl	HCl	LiCl	KCl	KCl	HCl	LiCl

4.2. Graphical representations used

In view of the use of the experimental results in chapter 5, the
data will be presented in three types of figures: ε' versus log ω

graphs, ε'' versus ε' graphs (so-called Cole-Cole plots; Cole and Cole, 1941) and $\Delta\varepsilon_{st}$ versus c_b graphs. Here c_b is the concentration of electrolyte added to the latex samples and $\Delta\varepsilon_{st}$ is the static dielectric increment. To obtain values for $\Delta\varepsilon_{st}$ both the ε' versus log ω graphs and the Cole-Cole plots were used. Cole and Cole (1941) introduced a parameter α in the original Debye equation (Debye, 1929) to account for a distribution of relaxation times. The modified equation is written as follows:

$$\varepsilon' - j\varepsilon'' = \varepsilon_\infty + \frac{\varepsilon_s - \varepsilon_\infty}{1 + (j\omega\tau)^{1-\alpha}} \qquad (4-1)$$

with ε_s = permittivity at low frequencies, ε_∞ = permittivity at high frequencies, α = Cole-Cole distribution parameter $(0 < \alpha < 1)$, and τ = most probable relaxation time. Further,

$$\Delta\varepsilon_{st} = \varepsilon_s - \varepsilon_\infty \qquad (4-2)$$

The diagram of the imaginary part ε'' of the complex permittivity plotted against its real part ε' gives a circular arc. The intersections of the arc with the ε'-axis correspond to ε_s and ε_∞. Dielectric behaviour conforms to the circular arc rule (equation 4-1) if the system obeys a certain distribution of relaxation times around the most probable relaxation time τ, corresponding to the frequency where $\varepsilon'' = \varepsilon''_{max}$. This distribution of relaxation times is characterized by the empirical constant α.

To obtain the best estimates of dispersion parameters, a computer analysis has to be carried out. However, as will be shown in chapter 5, a large discrepancy between theories of dielectric dispersion and experiments is found for dilute latex dispersions. Therefore, it was not considered opportune to perform a detailed statistical analysis of the experimental data by computer to obtain more accurate results.

The values of $\Delta\varepsilon_{st}$ as a function of c_b are our most important results in the comparison with theories.

4.3.1. *Dielectric measurements on latex A_1*

Latex A_1, with the almost symmetrical electrolyte KCl, was chosen for comparison with theory. Therefore the results are given both as plots of ε' against $\log \nu$ and as Cole-Cole plots for the different KCl concentrations used, and as a plot of $\Delta\varepsilon_{st}$ versus c_b (see fig. 4-1 up to fig. 4-9). In table (4-2) the resulting most probable relaxation times are given, obtained from the Cole-Cole plots.

TABLE (4-2). The relaxation times (latex A_1) as a function of c_b.

c_b (mol/m^3)	0.000	0.204	0.417	0.644	0.878	1.236	1.517
τ (μs)	16.6	26.3	25.9	20.3	23.0	22.9	24.5
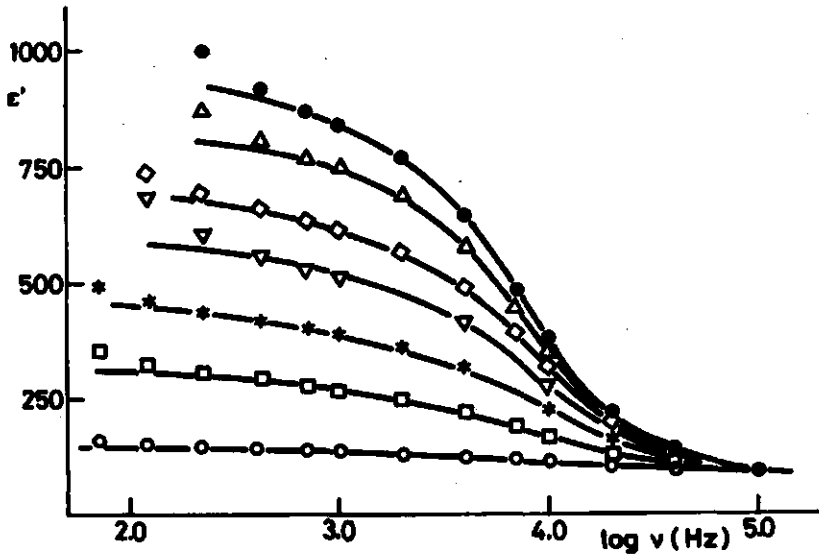
Figure (4-1): Latex A_1: ε' versus $\log \nu$ at different KCl concentrations. $c_b (mol/m^3)$: 0.000 (o); 0.204 (□); 0.417 (*); 0.644 (▽); 0.878 (◇); 1.236 (Δ); 1.517 (●).
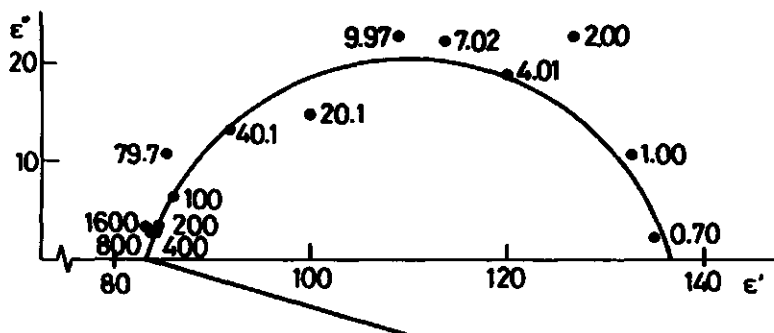
Figure (4-2): Cole-Cole plot for latex A_1 ($c_b = 0.000$ mol/m^3). The numbers refer to frequencies in kHz.
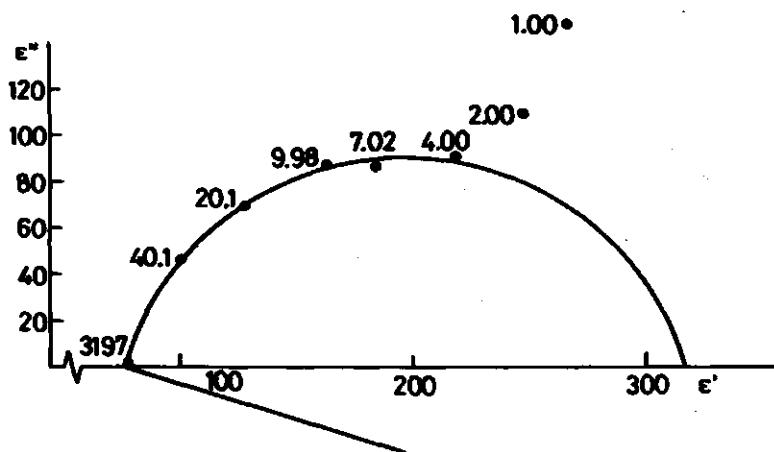
Figure (4-3): Cole-Cole plot for latex A_1 ($c_b = 0.204$ mol/m^3). The numbers refer to frequencies in kHz.
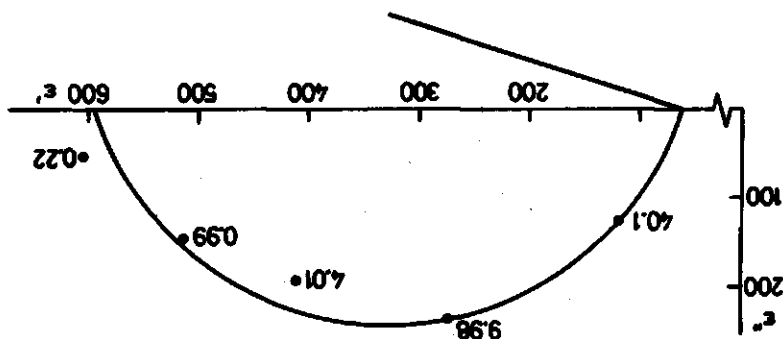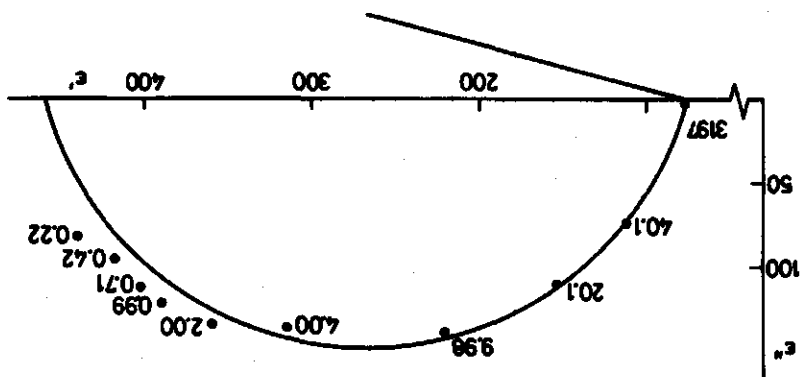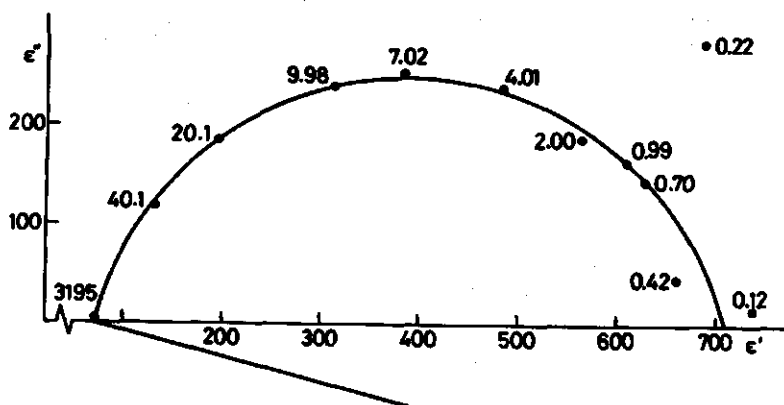
Figure (4-6): Cole-Cole plot for latex A_1 ($c_b = 0.878$ mol/m^3).
The numbers refer to frequencies in kHz.
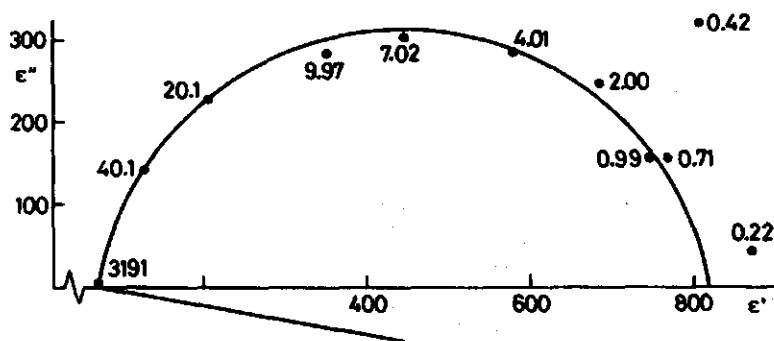
Figure (4-7): Cole-Cole plot for latex A_1 ($c_b = 1.236$ mol/m^3).
The numbers refer to frequencies in kHz.
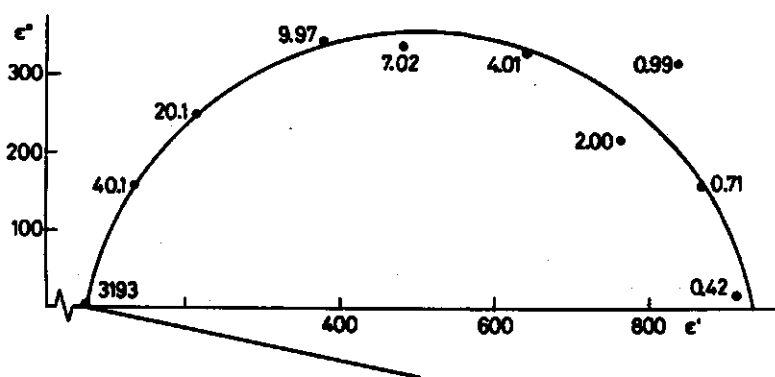
Figure (4-8): Cole-Cole plot for latex A_1 ($c_b = 1.517$ mol/m^3). The numbers refer to frequencies in kHz.
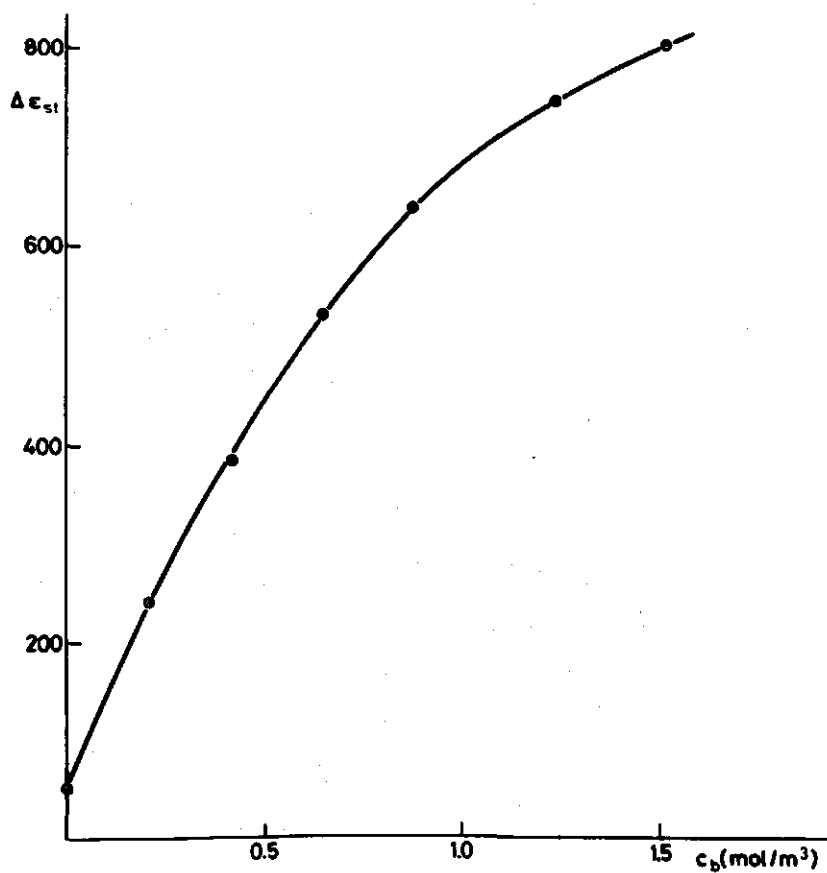
Figure (4-9): Latex A_1: $\Delta\varepsilon_{st}$ versus the KCl concentration c_b.

4.3.2. *Dielectric measurements on latices* B_1 *and* C_1

These experimental results with KCl as added electrolyte are also given to indicate that comparable results are obtained for latices with another surface charge density and another particle radius (figures 4-10 to 4-17). In order to restrict the amount of figures, only a few Cole-Cole plots are given (figures 4-12 to 4-15). In figures (4-16) and (4-17) the results for $\Delta\varepsilon_{st}$ are given.
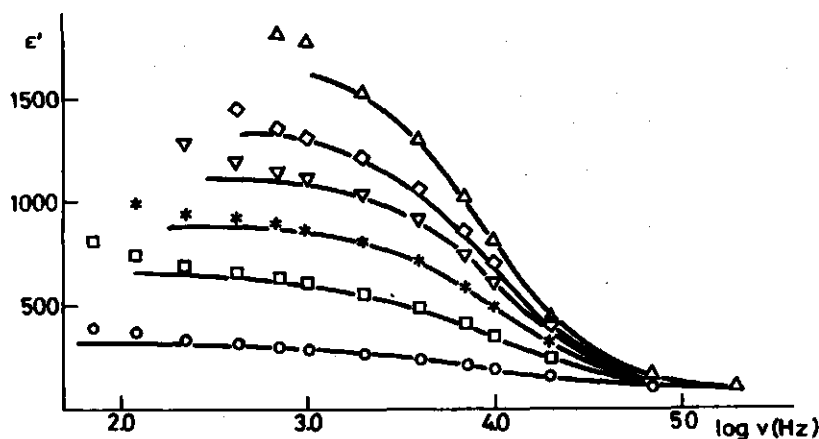
Figure (4-10): Latex B_1: ε' versus log ν at different KCl concentrations c_b (mol/m^3): 0.000 (o); 0.226 ($\square$); 0.457 (*); 0.729 (∇); 0.984 ($\Diamond$); 1.502 (Δ).
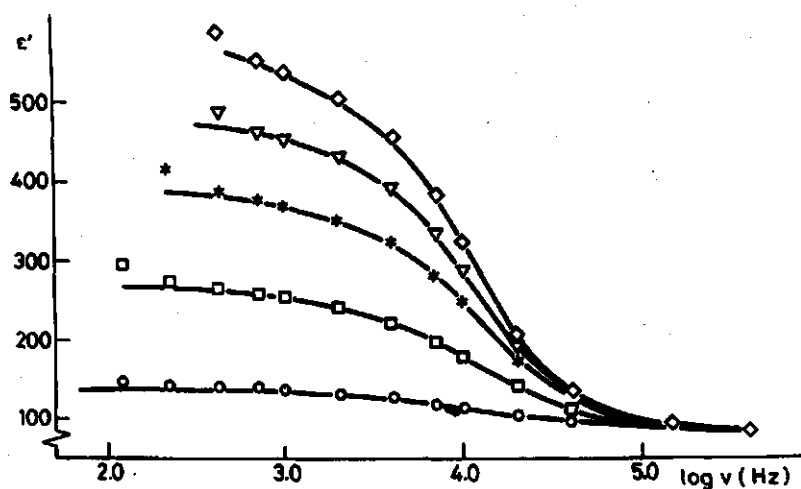
Figure (4-11): Latex C_1: ε' versus log ν at different KCl concentrations c_b (mol/m³): 0.000 (o); 0.331 (□); 0.679 (*); 1.034 (∇); 1.410 (◇).
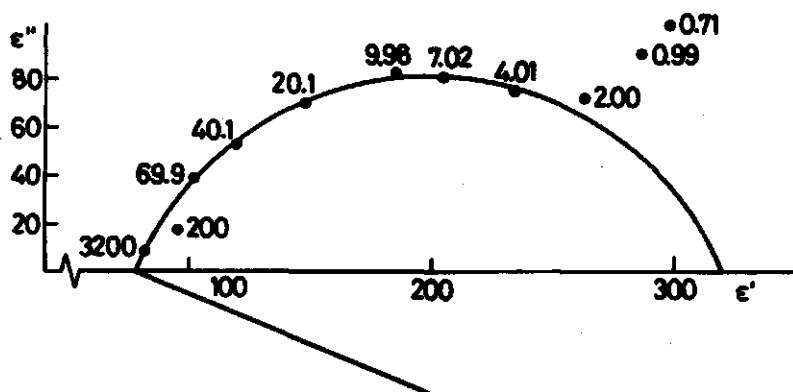
Figure (4-12): Cole-Cole plot for latex B_1 (c_b = 0.000 mol/m³). The numbers refer to fequencies in kHz.

57

ε"
600
9.97
7.02
4.01
20.1
200
40.1
400
69.9
200
200
2200
500   1000   1500   ε'
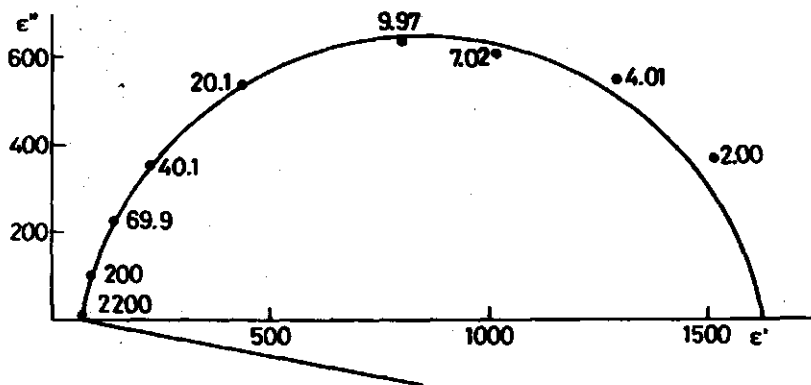
Figure (4-13): Cole-Cole plot for latex B_1 (c_b = 1.502 mol/m^3). The numbers refer to frequencies in kHz.

ε"
2.00
100
9.98   7.02
80
20.1
60
4.01
40.1
40
69.9
150
20
800 400
100   200   300   ε'
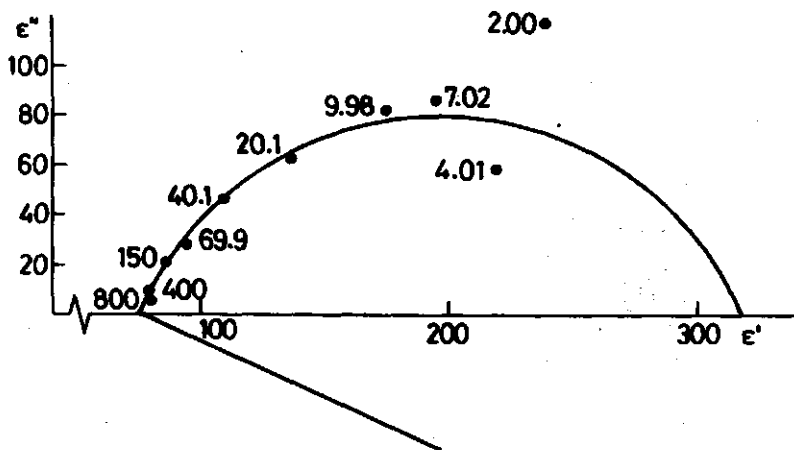
Figure (4-14): Cole-Cole plot for latex C_1 (c_b = 0.331 mol/m^3). The numbers refer to frequencies in kHz.
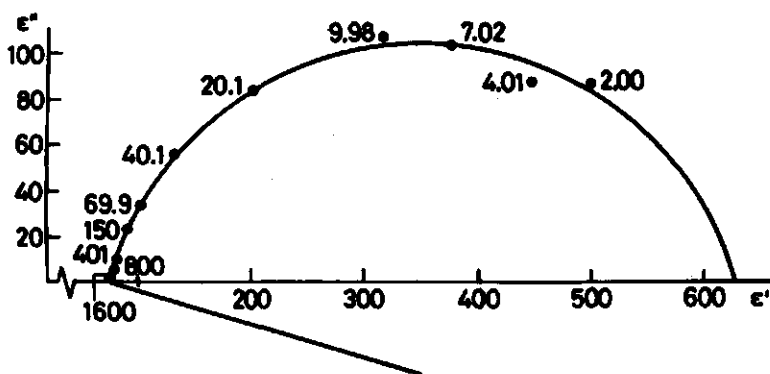
Figure (4-15): Cole-Cole plot for latex C_1 ($c_b = 1.410$ mol/m³). The numbers refer to frequencies in kHz.
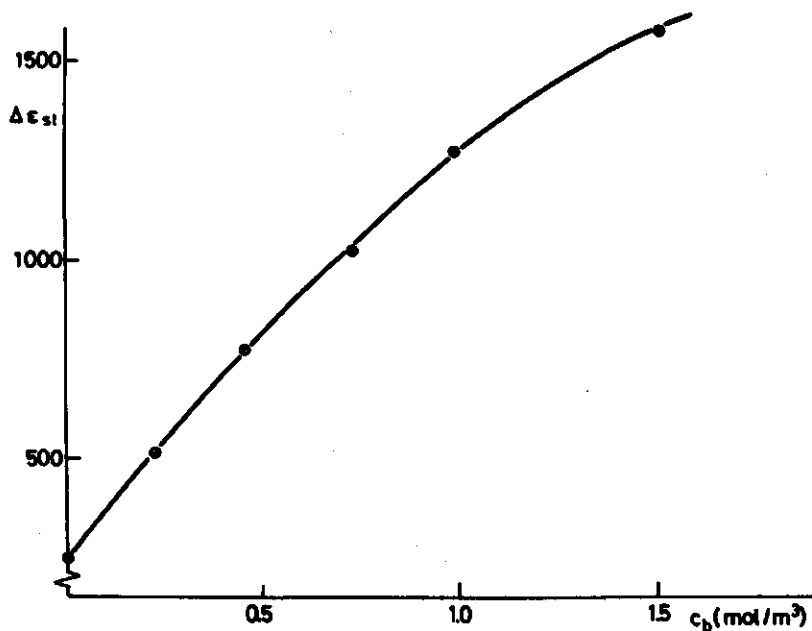
Figure (4-16): Latex B_1: $\Delta\varepsilon_{st}$ versus the KCl concentration c_b.
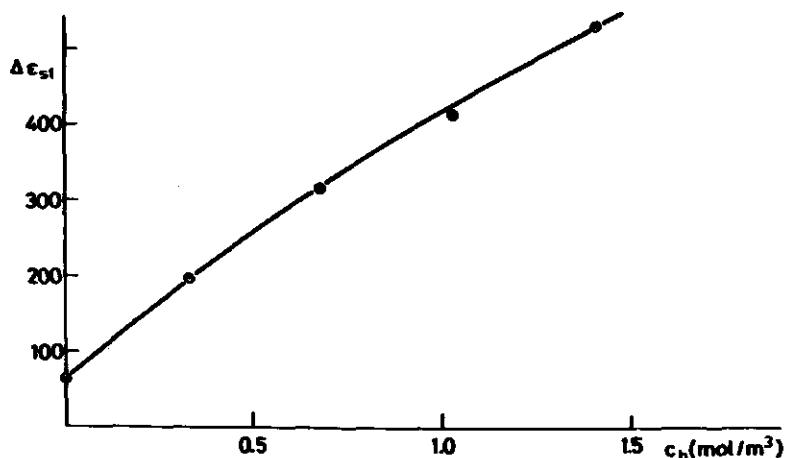
Figure (4-17): Latex C_1: $\Delta\varepsilon_{st}$ versus the KCl concentration c_b.

4.3.3. *Dielectric measurements on the remaining latices*

As will be shown in chapter 5, up to now no satisfactory theory exists to explain the results for experiments on colloidal systems to which a symmetrical electrolyte is added. Therefore, experiments on latices with electrolytes having different diffusion coefficients for anion and cation cannot be explained at the current stage of development of the theory. For possible use in the future, the remaining results are also listed in appendix B. In order to give an overall impression of the experiments with HCl and LiCl as the added electrolyte, plots of ε' against log ν are given for the latices A_2, A_3, C_2 and C_3 in the figures (4-18) to (4-21).
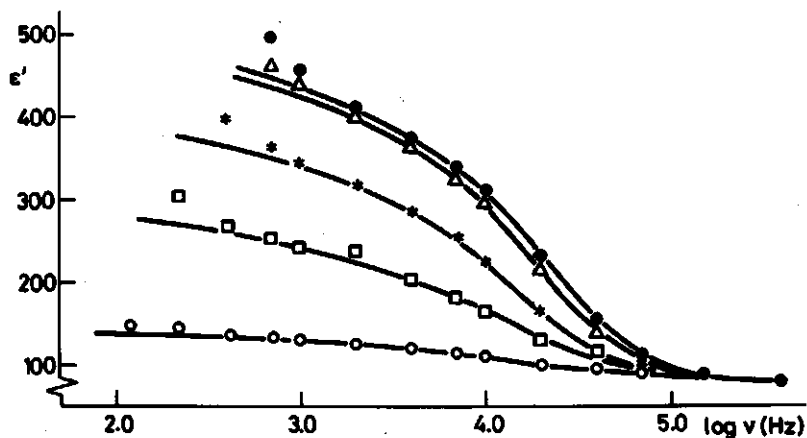
Figure (4-18): Latex A_2: ε' versus log ν at different HCl concentrations c_b (mol/m^3): 0.000 (o); 0.137 ($\square$); 0.272 (*); 0.412 (Δ); 0.493 ($\bullet$).
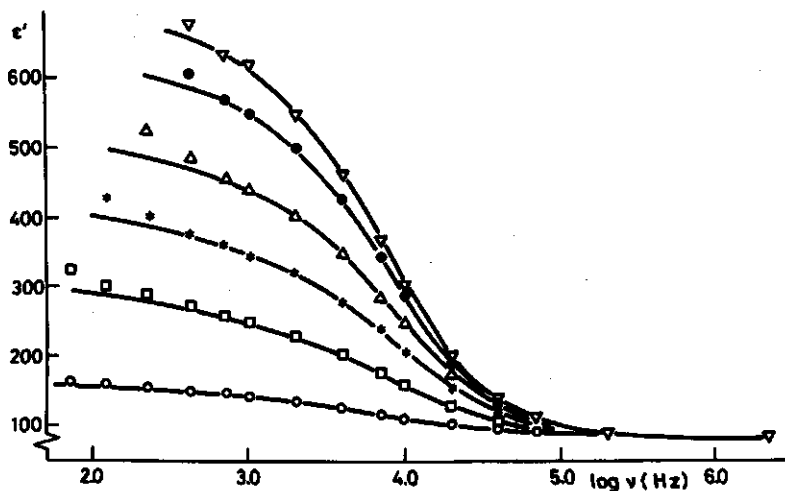
Figure (4-19): Latex A_3: ε' versus log ν at different LiCL concentrations c_b (mol/m^3): 0.000 (o); 0.241 ($\square$); 0.465 (*); 0.737 (Δ); 1.039 ($\bullet$); 1.206 (∇).
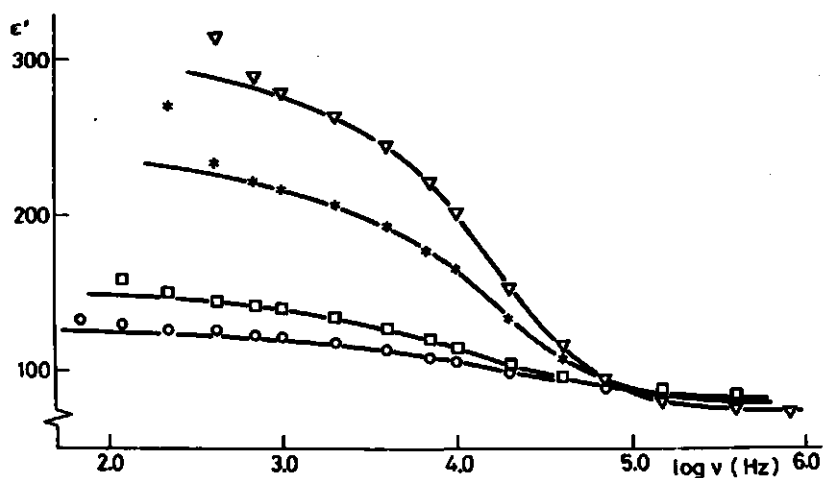
Figure (4-20): Latex C_2: ϵ' versus log ν at different HCl concentrations c_b (mol/m^3): 0.000 (o); 0.057 (□); 0.256 (*); 0.416 (∇).
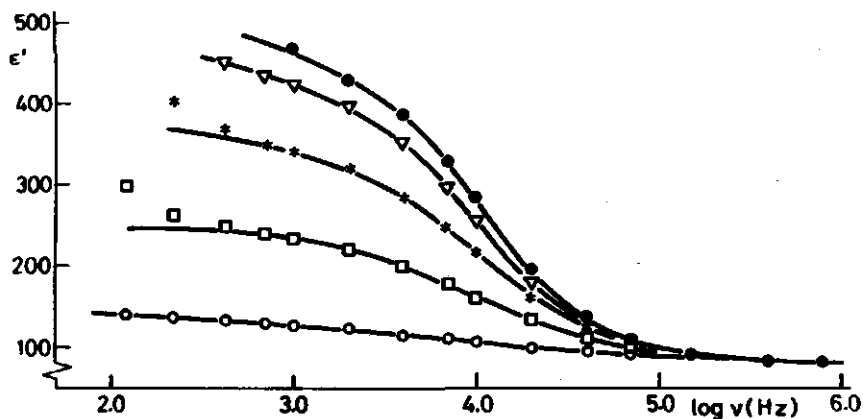
Figure (4-21): Latex C_3: ϵ' versus log ν at different LiCl concentrations c_b (mol/m^3): 0.000 (o); 0.440 (□); 0.931 (*); 1.416 (∇); 1.660 (•).

5. COMPARISON OF EXPERIMENTAL RESULTS AND THEORIES [*]

5.1. Introduction

In this chapter the experimental results are compared with some existing theories. It must be noted that the latter are based on Maxwell's theory (1873). Part of his article 314 states: "In order that the action of the spherical particles may not produce effects depending on their interference, their radii must be small compared with their distances, and therefore ϕ must be a small fraction". Therefore ϕ has to be small to avoid interaction between the particles.

The theory of dielectric dispersion must at least explain the values found for two important parameters, $\Delta\varepsilon_{st}$ and τ. In sections 5.2 and 5.3 $\Delta\varepsilon_{st}$ is considered. The most important fact to be explained here is the strong increase of $\Delta\varepsilon_{st}$ with electrolyte concentration c_b (see figures 4-9, 4-16 and 4-17). In section 5.4 the relaxation time is considered.

For comparison of the various theoretical calculations the experimental data from measurements on latex A_1 are used. The pertinent data are given in table (5-1). As may be seen from figure (4-5), at a KCl concentration $c_b = 0.644$ mol/m^3, a static dielectric increment $\Delta\varepsilon_{st} = 530$ is found experimentally. At this particular KCl concentration calculations with the different theories are performed.

5.2. Comparison with the existing theories on $\Delta\varepsilon_{st}$

5.2.1. *Theory of De Backer*

De Backer (1966) applies a three-phase heterogeneous Maxwell-Wagner approach to the problem of double layer relaxation (Maxwell, 1873; Wagner, 1914). De Backer considers the particle and its double

---

[*] This chapter has been written in cooperation with Mr. P.J.A.M. Mertens, Laboratory for Physical and Colloid Chemistry, Agricultural University, Wageningen, The Netherlands.

TABLE (5-1). Data used in the calculations

relative permittivity of polystyrene (25.0 $^{\circ}$C)	: ε_1 = 2.55
conductivity of polystyrene	: σ_1 = 0.00 mS/m
volume fraction of latex A_1	: ϕ = 0.022
mean particle radius of latex A_1	: a = 222 nm
surface charge density of particles of latex A_1:	σ_0 = 16.1 mC/m^2
relative permittivity of water (25.0 $^{\circ}$C)	: ε_w = 78.36
viscosity of water (25.0 $^{\circ}$C)	η_w = 0.890 mNs/m^2
temperature at which measurements are performed:	298.2 K
molar conductivity of K$^+$ ion (25.0 $^{\circ}$C)	: Λ_+ = 7.45 mS m^2/mol
molar conductivity of Cl$^-$ ion (25.0 $^{\circ}$C)	: Λ_- = 7.55 mS m^2/mol
diffusion coefficient of K$^+$ ion (25.0 $^{\circ}$C)	: D_+ = 1984 μm^2/s
diffusion coefficient of Cl$^-$ ion (25.0 $^{\circ}$C)	: D_- = 2011 μm^2/s

layer as two separate phases having different permittivities and conductivities. A first Maxwell-Wagner treatment leads to the formulation of the permittivity and the conductivity of an equivalent spherical particle having homogenous dielectric properties. Next, this particle is thought of as embedded in the bulk electrolyte. To the resulting two-phase heterogeneous system the Maxwell-Wagner treatment is applied again. The final expression contains three sets of dielectric properties: those from the particle, from its double layer and from the bulk electrolyte. According to De Backer the static dielectric increment is given by:

$$\Delta\varepsilon_{st} = \frac{9\phi(1 - \phi)(\varepsilon_w\sigma_h - \varepsilon_h\sigma_b)^2}{\{\varepsilon_h + 2\varepsilon_w - \phi(\varepsilon_h - \varepsilon_w)\}\{\sigma_h + 2\sigma_b - \phi(\sigma_h - \sigma_b)\}^2} \tag{5-1}$$

with:

$$\varepsilon_h = \varepsilon_1 + \frac{2\varepsilon_d}{\kappa a} \tag{5-2}$$

and

64

$$\sigma_h = \sigma_1 + \frac{2\sigma_d}{\kappa a} \tag{5-3}$$

ε_1 = relative permittivity of the dispersed medium

σ_1 = conductivity of the dispersed medium

ε_d = relative permittivity of the diffuse double layer

σ_d = conductivity of the diffuse double layer

κ^{-1} = thickness of the diffuse double layer

σ_b = conductivity of the bulk electrolyte

σ_d depends on the surface conductivity κ_1^σ of the latex particles:

$$\sigma_d = \sigma_b + \kappa\kappa_1^\sigma \tag{5-4}$$

κ_1^σ is calculated with the use of the equation:

$$\kappa_1^\sigma = \frac{FD_c\sigma_o}{RT} \tag{5-5}$$

with D_c = diffusion coefficient of the counterion.

The equations (5-1), (5-2) and (5-3) are valid for spherical parti-
cles with the assumptions (De Backer, 1966):

$$\sigma_d > \sigma_1 \tag{5-6}$$

$$\kappa a > 1 \tag{5-7}$$

$$\varepsilon_d = \varepsilon_w \tag{5-8}$$

The conductivity σ_b of a 0.644 mol/m^3 KCl solution at 25.0 $^\circ$C is 9.96
mS/m. The calculation is performed with:

$$\sigma_b = \Lambda c_b \tag{5-9}$$

and the Nernst-Einstein equation for a symmetrical electrolyte:

$$\Lambda = \frac{zF^2(D_+ + D_-)}{RT}$$ (5-10)

Λ is the molar conductivity of the electrolyte solution and z is the charge number. κ^{-1} is obtained with equation (1-2): κ^{-1} = 120 nm. From the data given it follows that the assumption (5-6) is correct. Because κa = 18, the assumption (5-7) is also obeyed. Using data given in a publication by Lyklema and Overbeek (1961) concerning the permittivity in the double layer, it appears that for the σ_b value used equation (5-8) is realistic. However, substitution of these dat in the above equations leads to $\Delta\epsilon_{st}$ = 0.81 which is far below our experimental value $\Delta\epsilon_{st}$ = 530.

5.2.2. *Theory of Schwarz*

Schwarz (1962) examined the low frequency dielectric behaviour of colloid dispersions with the aid of a model employing a frequency dependent surface conductivity. With this model the particle polarization from tangential electromigration and diffusion fluxes of what he terms "bound ions" was calculated. This approach leads to a Debye-like relaxation process with a static dielectric increment:

$$\Delta\epsilon_{st} = \frac{9\phi a \sigma_o F}{4(1 + 0.5\phi)^2 \epsilon_o RT}$$ (5-11)

Substitution of the appropriate values leads to $\Delta\epsilon_{st}$ = 761 for the experimental conditions as given in table (5-1).

Apart from the fact that this increment is too high, the main drawback of the Schwarz approach is that the dielectric increment is independent of the electrolyte concentration, whereas a strong increase with the electrolyte concentration is found experimentally (see figure 4-9).

According to Dukhin and Shilov (1974) equation (5-11) has to be

66

corrected for the occurrence of radial fluxes partly compensating the tangential electromigration fluxes. The corrected formula reads for $z_+ = z_- = 1$:

$$\Delta\varepsilon_{st} = \frac{9\phi a \sigma_o F}{4(1 + 0.5\phi)^2 \varepsilon_o RT(1 + 2\kappa\sigma_o c_b^{-1} F^{-1})} \qquad (5-12)$$

Substitution of $\kappa = 83.3 \ \mu m^{-1}$ and $c_b = 0.644 \ mol/m^3$ gives $\Delta\varepsilon_{st} = 17.6$ which again is far below the actual value. The alleged importance of radial fluxes is precisely the argument used by Dukhin and Shilov to reject Schwarz's approach and hence design a better theory.

5.2.3. *Theory of Schurr*

Schurr (1964) introduces the concept of two different values of the surface conductivity: κ_1^σ and κ_2^σ. A distinction is made between a bound charge current, leading to κ_2^σ, and a true or d.c. current, which persists in accordance with Ohm's law in the steady state. The true current leads to the surface conductivity κ_1^σ, as given in equation (5-5). In this treatment, Schurr makes use of both the theory of O'Konski (1955, 1960) and that of Schwarz (1962). Schurr gives an expression for the complex conductivity of the colloid particle. This expression has to be used to calculated $\Delta\varepsilon_{st}$, performed by us through substitution of the expression of Schurr into the formulae of the Maxwell-Wagner theory for the complex dielectric increment (Maxwell, 1873; Wagner, 1914). With $\kappa a > 1$:

$$\Delta\varepsilon_{st} = \frac{9\phi a \sigma_o F\sigma_b^2}{\varepsilon_o RT\{\sigma_b(2+\phi) + 2\kappa_2^\sigma a^{-1}(1-\phi)\}^2} \qquad (5-13)$$

We calculated κ_2^σ with the Bikerman formula for a symmetrical electrolyte (Bikerman, 1935):

$$\kappa_2^\sigma = \frac{2F^2 c_b D(1 + 3m)}{RT\kappa} \{\exp(\tfrac{1}{2} F \psi_d/(RT)) + \exp(-\tfrac{1}{2}F \psi_d/RT) - 2\} \qquad (5-14)$$

with $D = D_+ = D_-$, and: $\quad\quad\quad\quad\quad\quad\quad\quad\quad\quad\quad\quad$ (5-15)

$$m = \frac{2\varepsilon_o \varepsilon_w R^2 T^2}{3F^2 D\eta_w} \quad\quad\quad\quad\quad\quad\quad\quad (5\text{-}16)$$

Assuming that specific adsorption is absent, ψ_d is calculated from the surface charge density with the formula:

$$\sinh\left(\frac{F\psi_d}{2RT}\right) = \frac{\sigma_o}{2(2\varepsilon_o \varepsilon_w c_b RT)^{\frac{1}{2}}} \quad\quad\quad (5\text{-}17)$$

which stems from Gouy-Chapman theory (Kruyt, 1952). κ is calculated with equation (1-2). Substitution of the data given in table (5-1) leads to: $\kappa = 83.3 \ \mu m^{-1}$

$\quad\quad\quad\quad m = 0.172$

$\quad\quad\quad\quad \psi_d = 123 \ mV$

$\quad\quad\quad\quad \kappa_2^\sigma = 1.59 \ nS$

With equation (5-13) $\Delta\varepsilon_{st} = 265$ is calculated. However, compared with the experimental $\Delta\varepsilon_{st} = 530$, this value is too low.

$\quad\quad$ This theory predicts $\Delta\varepsilon_{st}$ to depend on c_b (see equations (5-9) and (5-13)). Hence, for $\phi \ll 1$, equation (5-13) may be written as:

$$\Delta\varepsilon_{st} = \text{constant} \times f(c_b, \psi_d) \quad\quad\quad\quad (5\text{-}18)$$

with:

$$\text{constant} = \frac{9\phi a \sigma_o F}{\varepsilon_o RT} \quad\quad\quad\quad\quad\quad (5\text{-}19)$$

and:

$$f(c_b, \psi_d) = \frac{\sigma_b^2}{(2\sigma_b + 2\kappa_2^\sigma a^{-1})^2} \quad\quad\quad (5\text{-}20)$$

We calculated the dependence of $\Delta\varepsilon_{st}$ on c_b with these equations. The results are given in table (5-2) and figure (5-2). For the data used the constant given in equation (5-19) is equal to 3111. This is the

68

maximum for $\Delta\varepsilon_{st}$, reached when $\kappa_2^\sigma a^{-1}$ is negligibly small compared with σ_b. In the experimentally accessible range of c_b given in table (5-2), the influence of κ_2^σ remains considerable. This influence is

TABLE (5-2). Dependence of $\Delta\varepsilon_{st}$ on c_b, calculated with equation (5-18)

c_b (mol/m^3)	σ_b (mS/m)	ψ_d (mV)	κ_2^σ (nS)	$\Delta\varepsilon_{st}$	$f(c_b, \psi_d)$	$\kappa_2^\sigma a^{-1}$ (mS/m)	$J(\kappa_2^\sigma)$ (%)
0.20	3.00	153	1.73	62	0.019	7.78	72
0.30	4.50	142	1.67	111	0.035	7.50	62
0.40	6.00	135	1.65	160	0.050	7.41	55
0.60	9.00	125	1.60	241	0.077	7.23	45
0.80	12.00	117	1.53	314	0.101	6.91	37
1.00	15.00	112	1.52	366	0.118	6.85	31
1.50	22.50	102	1.45	464	0.150	6.53	22
2.00	30.00	95	1.39	526	0.171	6.28	17

given in the table as the ratio

$$J(\kappa_2^\sigma) = \frac{\kappa_2^\sigma a^{-1}}{(\sigma_b + \kappa_2^\sigma a^{-1})} \tag{5-21}$$

To compare the theories of Schwarz and Schurr with each other, equation (5-13) is rewritten as:

$$\Delta\varepsilon_{st} = \frac{9\phi a \sigma_o F \sigma_b^2}{4\sigma_b^2 (1 + 0.5\phi)^2 (1+x)^2 \varepsilon_o RT} \tag{5-22}$$

indicating that for $x \ll 1$ equations (5-11) and (5-13) become identical. The magnitude of $(1+x)$ follows from the equations (5-13), (5-22):

$$(1+x) = \left[1 + \frac{\kappa_2^\sigma (1-\phi)}{a\sigma_b (1 + 0.5\phi)}\right] \tag{5-23}$$

69

x << 1 corresponds with:

$$\sigma_b \gg \frac{\kappa_2^\sigma (1-\phi)}{a(1 + 0.5\phi)} \tag{5.24}$$

For $\phi \ll 1$ formula (5-24) reduces to:

$$\sigma_b \gg \kappa_2^\sigma / a \tag{5.25}$$

The theoretical calculations by Schwarz are based on experimental re-
sults (polystyrene latices; electrolyte: KCl) of Schwan, Schwarz,
Maczuk and Pauly (1962) : $\phi = 0.22$; $a = 585$ nm; $\sigma_b = 0.07$ S/m and
$\sigma_o = 32$ mC/m^2. In addition, we calculated κ_2^σ by use of the equations
(1-2), (5-9), (5-10), (5-14) and (5-17): $\kappa_2^\sigma = 1.38$ nS. Using these
values, it is concluded that the condition given as formula (5-24) is
very well satisfied. From this it is understood that the theory of
Schwarz is in rather good agreement with the experimental results of
Schwan et al., although in this theory $\Delta\varepsilon_{st}$ is independent of c_b.
However, our experiments are not comparable with the experiments of
Schwan et al., because ϕ and σ_b are lower in our case. Therefore, in
our experiments condition (5-24) is not satisfied and hence it is
not surprising that Schwarz's theory does not apply to our data.

5.2.4. *Theory of Einolf and Carstensen*

Einolf and Carstensen (1971) apply the Schurr model to porous
particles containing both the "surface charge" and the counterions.
Therefore, the counterions are also present inside the particles.
Assuming that the polystyrene particles are porous in this sense, the
calculation has to be performed now with N_o charges per m^3:

$$N_o = \frac{3\sigma_o}{ea} \tag{5-26}$$

If, in addition to the theory of Einolf and Carstensen, the approxi-
mations $\kappa a > 1$ and $\varepsilon_1 < \Delta\varepsilon_1$ are used, the following expression is ob-

70

tained:

$$\Delta\varepsilon_{st} = \frac{9}{4} \phi \, \Delta\varepsilon_1 \qquad (5-27)$$

with $\Delta\varepsilon_1$ = static dielectric increment of the permittivity of the colloid particle due to the double layer polarization. In the theory of Schwarz (1962), $\Delta\varepsilon_1$ depends on σ_o. In the treatment of Einolf and Carstensen $\Delta\varepsilon_1$ depends on δ_o, being essentially a function of $N_o^{\frac{1}{2}}$, leading to $\Delta\varepsilon_1 = 1878$ and $\Delta\varepsilon_{st} = 93$. Compared with the low value of 265, calculated with the theory of Schurr (1964), the supposed porosity of the polystyrene particles leads to a further decrease of $\Delta\varepsilon_{st}$. This could be expected because in the case of porosity an extra depolarizing mechanism exists, namely the diffusion of the counterions through the colloid particles.

5.2.5. *Theory of Ballario, Bonincontro and Cametti*

Ballario, Bonincontro and Cametti (1976) follow the approach of Schurr but their theory specifically applies to systems of low electrolyte concentrations. Their treatment results in an expression for $\Delta\varepsilon_{st}$ consisting of two contributions; one from double layer polarization and one from the Maxwell-Wagner effect:

$$\Delta\varepsilon_{st} = \frac{9\phi\{\sigma_b^2(2+\phi)2\tau\kappa_1^\sigma a^{-1}\varepsilon_o^{-1} + (1-\phi)\varepsilon_w(2\kappa_1^\sigma a^{-1})^2\}}{(2+\phi)\{\sigma_b(2+\phi) + 2(1-\phi)\kappa_2^\sigma a^{-1})\}^2} +$$

$$+ \frac{9\phi(1-\phi)\{2\varepsilon_w a^{-1}(\kappa_1^\sigma + \kappa_2^\sigma)\}^2}{\varepsilon_w(2+\phi)\{\sigma_b(2+\phi) + 2a^{-1}(\kappa_1^\sigma + \kappa_2^\sigma)(1-\phi)\}^2} \qquad (5-28)$$

with κ_1^σ = d.c. surface conductivity, κ_2^σ = surface conductivity of bound ions, as before, and:

$$\tau = \frac{a^2 F\sigma_o}{2RT\kappa_1^\sigma} \qquad (5-29)$$

On the right hand side of equation (5-28) the first term is the double layer polarization contribution and the second term is due to

the Maxwell-Wagner effect. We calculated κ_1^σ with equation (5-5) and κ_2^σ with the Bikerman formula (eq. 5-14). Substitution of the given data and $c_b = 0.644$ mol/m^3 leads to:

$\kappa_1^\sigma = 1.25$ nS

$\tau = 12.4$ µs

m = 0.172

$\psi_d = 123$ mV

$\kappa_2^\sigma = 1.59$ nS

Because $\phi << 1$ in our experiments, equation (5-28) can be approximated by:

$$\Delta\epsilon_{st} = \frac{9\phi\sigma_b^2\tau\kappa_1^\sigma}{2a\epsilon_o(\sigma_b + \kappa_2^\sigma a^{-1})^2} + \frac{9\phi\epsilon_w(\kappa_1^\sigma)^2}{2(a\sigma_b + \kappa_2^\sigma)^2} + \frac{9\phi\epsilon_w(\kappa_1^\sigma + \kappa_2^\sigma)^2}{2(a\sigma_b + \kappa_1^\sigma + \kappa_2^\sigma)^2} \quad (5-30)$$

In this equation the third term of the right hand side is again the Maxwell-Wagner contribution. The second and third terms on the right hand side of equation (5-30) contribute only 1.2% to $\Delta\epsilon_{st}$. With the use of equation (5-29) τ may be eliminated from equation (5-22). Thereby, for $\phi << 1$ the first term on the right hand side of equation (5-30) becomes equal to equation (5-13). Therefore, it is not surprising that, compared with the result of section 5.2.3, the theory of Ballario et al. gives almost the same $\Delta\epsilon_{st}$, viz. 266. It must be concluded that this theory is no improvement compared with the theory of Schurr.

5.2.6. *Theory of Shilov and Dukhin*

A major difference from Schwarz's approach (1962) occurs in the theory proposed by Shilov and Dukhin (1970a,1970b) and Dukhin and Shilov (1974). This theory includes diffusion phenomena, which take place between the bulk and the diffuse double layer as secondary effects following the primary effect of electromigration due to the applied field. Tangential electromigration is compensated for by radial diffusion. The application of an alternating electric field leads to

the establishment of three kinds of ion fluxes:

a. electromigration fluxes due to the applied field

b. diffusion fluxes due to the polarization field

c. convection fluxes due to electroosmosis.

Using flux equations from irreversible thermodynamics, the authors proceeded to calculate the stationary state of the "perturbed" double layer which can be expressed as an asymmetric potential distribution or, alternatively, as an asymmetric concentration distribution. Shilov and Dukhin obtained mathematical expressions by which the perturbed potential distribution can be expressed in terms of the original Poisson-Boltzmann distribution, characterized by the parameters ψ_d and κa. In dielectric measurements an alternating polarization field is obtained which lags in phase behind the applied field (see also section 1.1). The imaginary part of the complex conductance can formally be related to the real part of the complex permittivity. The latter quantity decreases with increasing frequency. The static dielectric increment is found by extrapolating to zero frequency and depends on the double layer parameters ψ_d and κa and on the diffusion constants of anion and cation.

Since the effect of dielectric dispersion amplification is associated with the imaginary part of the dipole moment of the particle, the theory of strong low-frequency dielectric dispersion should be based on the theory of double layer polarization in an alternating field. However, Overbeek (1941) calculated the dielectric increment by solving the problem of polarization in a constant electric field. Although correct allowance is made for all the factors affecting the static polarization of the diffuse double layer, the theory of Overbeek does not yield the effect of strong low-frequency dispersion, because the system described is conducting. Relaxation has to be considered as an increase of the conductivity with increasing frequency, which formally can be related to a decrease of the permittivity with increasing frequency.

The perturbation of the double layer lags in phase behind the applied alternating field. The result is a perturbed double layer, the composition of which is a function of time, described as a polarization field $\phi(r, \vartheta, \omega)$. This field is equivalent to the field of an alternating dipole moment μ, located in the centre of the spherical particle. Because the polarization field can be expressed in terms of the original Poisson-Boltzmann distribution, as stated before, the dipole moment depends on the double layer parameters ψ_d and κa. Moreover, μ is complex due to the phase difference with the applied alternating field. Working with this model, Shilov and Dukhin had to introduce some approximations into the double layer concept. This is necessary because it is impossible to give analytical solutions for the spherically symmetrical Poisson-Boltzmann differential equation. The double layer polarization theory needs such an explicit solution for the potential distribution $\psi(r)$ in order to solve the flux equations. Dukhin and Shilov applied the solution for a flat surface to any angle ϑ. This of course means that the result can only be valid for $\kappa a \gg 1$ (see section 1.2). The final result of this theory is given as equations III.103,104 and 108 in the work of Dukhin and Shilov (1974). In these equations the parameter ζ occurs, due to the theoretical accommodation of the electroosmosis phenomenon. ζ is the electrokinetic potential, an important parameter in colloid chemistry (see e.g. Kruyt, 1952). The picture is that behind the shear plane no convective liquid movement occurs, whereas electromigration and diffusion are taking place from the distance $r = a$ onward.

A very remarkable feature of these dispersion equations is that double layer polarization does not exhibit a Debye-like relaxation behaviour. Double layer polarization according to Dukhin and Shilov can formally be described as the behaviour of a circuit consisting of a resistance R, a Warburg impedance Z_w and a capacitance C in series (see figure 5-1).
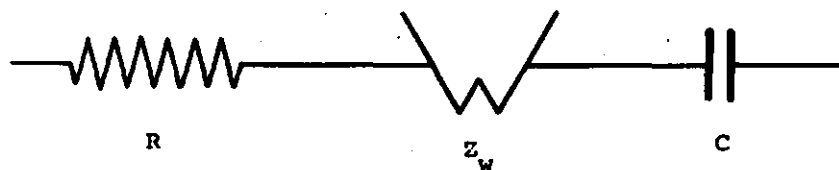
Figure (5-1): The electrical equivalent circuit for the model of Dukhin and Shilov for double layer polarization.

Z_w is given by (Vetter, 1961)[*] :

$$Z_w = (1-j)\sigma_w\omega^{-\frac{1}{2}} \tag{5-31}$$

The parallel capacitance C_p of the equivalent circuit shown in figure (5-1) is given by:

$$C_p(\omega) = C\frac{1+W}{(1+W)^2 + W^2(1+\beta W)^2} \tag{5-32}$$

with:

$$W = \sigma_w C\omega^{\frac{1}{2}} \tag{5-33}$$

and

$$\beta = \frac{R}{C\sigma_w^2} \tag{5-34}$$

Equation (III,103) from Dukhin and Shilov (1974) can be represented by analogy with equation (5-32) as:

$$\Delta\varepsilon'(\omega) = \Delta\varepsilon_{st}\frac{1+W}{(1+W)^2 + W^2(1+\beta W)^2} \tag{5-35}$$

---

[*] In electrochemistry Z_w is used in the representation of the diffusional impedance of an electrochemical cell. Then, σ_w is inversely proportional to the square root of the diffusion coefficients and the concentrations of the electro-active species.

with:

$$w^2 = \frac{\omega a^2}{2D_e}$$ (5-36)

$$\beta = A_2 A_1^{-1}$$ (5-37)

$$D_e = \frac{2D_+ D_-}{D_+ + D_-} \qquad \text{for } z_+ = z_-$$ (5-38)

A_1 and A_2 are complicated factors, depending on ψ_d, κa, D_e and the quantity m, given in equation (5-16). Using the formulas (5-33) and (5-36), it is found that σ_w depends on $D_e^{-\frac{1}{2}}$ (see footnote on page 75). Using the set of about twenty equations needed to calculate A_1 and A_2 (see Dukhin and Shilov, 1974) and the data from the preceding sections of this chapter, we find $\Delta\varepsilon_{st} = 154$ for this theory. It is shown that the theory of Dukhin and Shilov is also unable to explain the experimental results. Furthermore, we calculated that even at infinitely high surface charge $\Delta\varepsilon_{st}$ attains a maximum value of 377 at 0.644 mol/m^3 KCl.

Moreover, another prediction of the theory of Dukhin and Shilov, i.e. the occurrence of a maximum in the static dielectric increment as a function of the electrolyte concentration (or κa) is not corroborated by experimental results. Table (5-3) shows results calculated with the known set of data and equation III,104 (Dukhin and Shilov, 1974), reading:

$$\Delta\varepsilon_{st} = \frac{9}{4} \phi\varepsilon_r (\kappa a)^2 (A_1 a_2 - A_2 a_1) A_1^{-2}$$ (5-39)

a_1 and a_2 are again complicated factors, depending on ψ_d, κa, D_e and m. The experimental and theoretical results are compared in figure (5-2). Thereby, κ is calculated with equation (1-2) and ψ_d with equation (5-17). In the theoretical calculations the maximum value of $\Delta\varepsilon_{st}$ is caused by an increase of κa with increasing c_b, resulting in an increase of $\Delta\varepsilon_{st}$ together with a decrease of ψ_d at constant σ_o and increasing c_b, resulting in a decrease in $\Delta\varepsilon_{st}$.

76
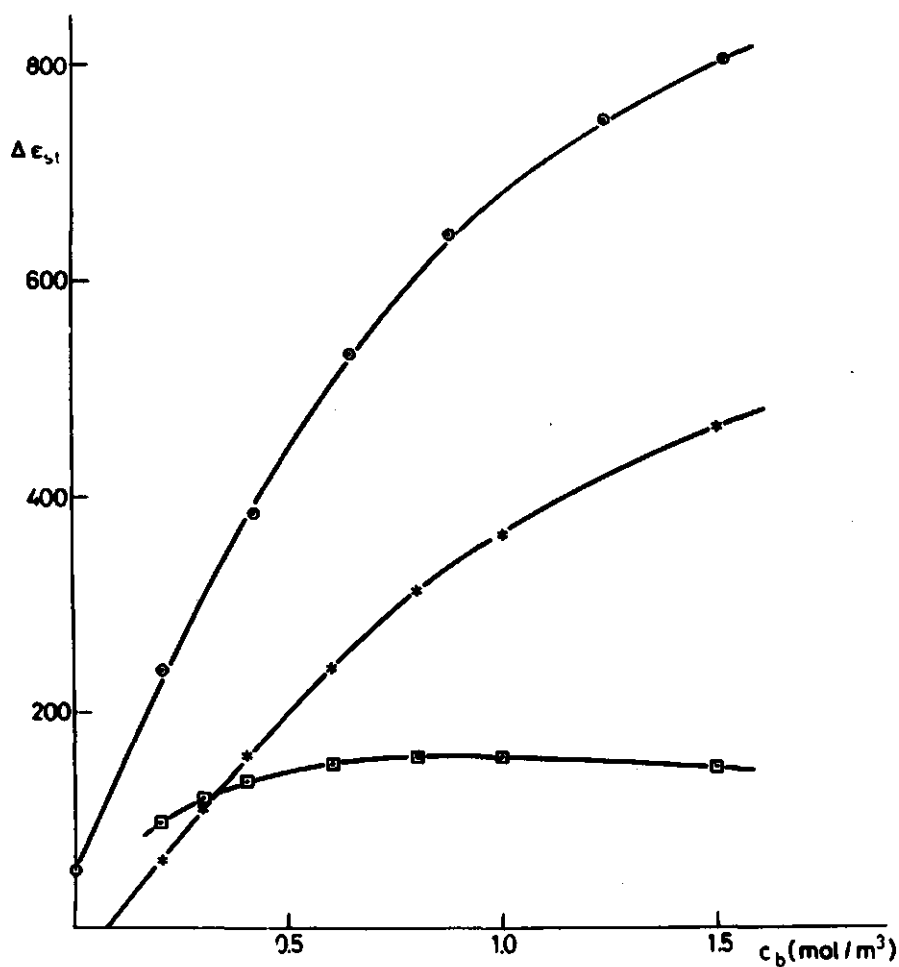
Figure (5-2): Dependence of $\Delta\varepsilon_{st}$ on c_b, with: O: experimental results on latex A_1 (from fig.4-9); *: results according to the theory of Schurr; □: results according to the theory of Dukhin and Shilov.

TABLE (5-3). Theoretical values of $\Delta\epsilon_{st}$, calculated with eq. (5-39)

c_b (mol/m^3)	κa	ψ_d (mV)	$\Delta\epsilon_{st}$
0.20	10.3	153	97
0.30	12.6	142	119
0.40	14.6	135	135
0.60	17.9	125	151
0.80	20.6	118	157
1.00	23.1	112	157
1.50	28.3	102	147
2.00	32.6	95	133

TABLE (5-4). Comparison of the results for $\Delta\epsilon_{st}$

Theory	Section	$\Delta\epsilon_{st}$
De Backer	5.2.1.	0.81
Schwarz	5.2.2.	761
Schwarz, corrected	5.2.2.	17.2
Schurr	5.2.3.	265
Einolf and Carstensen	5.2.4.	93
Ballario, Bonincontro and Cametti	5.2.5.	266
Dukhin and Shilov	5.2.6.	154
Calculated from our experiments (latex A_1, $\sigma_b = 0.644$ mol/m^3)		530

5.2.7. *Survey of results*

In Table (5-4) the results for $\Delta \varepsilon_{st}$ by various workers are shown together for convenience.

It must be concluded that there is no theory as yet which can explain the increment $\Delta \varepsilon_{st}$ obtained from our experiments. Moreover, the increase of $\Delta \varepsilon_{st}$ with increasing electrolyte concentration, c_b, for our experiments on polystyrene latices with low volume fraction ϕ (see fig.5-2) is not explained theoretically. The Dukhin-Shilov approach is, up to now, the most elaborate and comprehensive treatment of the double layer polarization problem. However, it must be noted that the diffusion-determined frequency dependence of the permittivity in this theory is not corroborated by the experimental, almost Debye-like, Cole-Cole plots. Considering a homodispersed colloid system and taking $\beta = 1$ the maximum value of the dielectric loss $\varepsilon"_{max}$ only amounts to 0.277 $\Delta \varepsilon_{st}$. The expression for $\varepsilon"_{max}$ is obtained by substituting equation (5-39) and $\beta = 1$ in equation III.108 (Dukhin and Shilov, 1974), resulting in

$$\varepsilon"(\omega) = \Delta \varepsilon_{st} \frac{W}{(1+W) + W^2 (1+W)} \tag{5-40}$$

The maximum value of $\varepsilon"(\omega)$, $\varepsilon"_{max}$, is calculated with equation (5-40) and is found to occur at $W = 0.66$. Experimentally an $\varepsilon"_{max}$ value of nearly 0.5 $\Delta \varepsilon_{st}$ is found for our nearly homodispersed latices. For a single Debye relaxation process $\varepsilon"_{max} = 0.5 \Delta \varepsilon_{st}$ (see e.g. Böttcher and Bordewijk, 1978). Therefore, the experimentally determined frequency dependence exhibits an almost normal Debye-like function instead of the diffusion-like function of Dukhin and Shilov.

From the criticism of Dukhin and Shilov (1974) of the theories of O'Konski (1955, 1960) and Schwarz (1962) in particular, it appears that it is necessary to introduce in the theoretical treatment the diffusion processes of ion exchange between the bulk and the diffuse double layer. Although the model of Schurr (1964) is an improvement,

the diffusion fluxes of ions in the diffuse double layer are disregarded by Schurr. The diffusion processes have to be considered as a consequence of the electromigration due to the applied electric field. Therefore, the tangential electromigration along the colloid particles results in a radial diffusion process. As a consequence, it is artificial to consider the two surface conductivities κ_1^σ and κ_2^σ as two independent quantities as Schurr and Ballario et al. (1976) have done. The treatment of Dukhin and Shilov is based on the above considerations. The concept of diffusion processes of ions in the double layer is best elaborated in the theory of Schurr and the theory of Dukhin and Shilov.

Comparison of our experimental results on latex A_1 with our results on other latices (see chapter 4) shows that the chosen results on latex A_1 are characteristic of the dielectric behaviour of polystyrene latices at low volume fractions ϕ. Therefore it may be taken as a general conclusion that Schurr's theory leads to a better agreement with experiment than that proposed by Dukhin and Shilov as is shown by:

1. $\Delta\epsilon_{st}$ (experimental) > $\Delta\epsilon_{st}$ (Schurr) > $\Delta\epsilon_{st}$ (Dukhin and Shilov);
2. the theory of Schurr does not predict a maximum for $\Delta\epsilon_{st}$ against c_b;
3. experimentally a Debye-like behaviour is found. This is more in
   concordance with Schurr's theory than with that of Dukhin and Shilov

However, theoretically the theory of Dukhin and Shilov must be considered as the best one up to now, because Schurr disregards the diffusion fluxes of ions in the diffuse part of the double layer. Unfortunately, Dukhin and Shilov's theory is very complicated, and our comparison of experiment and theory has shown that at least for our results a discrepancy exists between experiment and theory. It was therefore thought appropriate to attempt to obtain a better agreement between experiment and theory. The approach is described in section 5.3 .

5.3. Comparison with a theory based on the parameter M_e

5.3.1. *Introduction of the parameter M_e*

None of the theories conforms with the demands that the dielectric increment should increase strongly with the electrolyte concentration c_b. Bearing the experimental results in mind, we postulated a Debye-like complex dipole moment, characterized by a dimensionless parameter M_e. Instead of the very complicated expression for the complex dipole moment μ (Dukhin and Shilov, 1974, equation III.101), which is a function of both σ_o (via ψ_d) and c_b (via κa), the following simple expression is assumed:

$$\mu = - \frac{6\pi\epsilon_o Ea^3 M_e}{(1 + j\omega\tau)} \qquad (5\text{-}41)$$

in which E is the applied electric field strength. In this equation, M_e determines the value of μ through the influence of the properties of the double layer. The particular advantages of this parameter M_e is that the unwieldy factors A_1 and A_2 used by Dukhin and Shilov are not longer needed. As has already been mentioned in section 5.2.6 A_1 and A_2 are calculated through a set of about twenty equations. The appearance of all these equations makes it difficult to trace the influence of the colloid-chemical parameters ψ_d and κa on $\Delta\epsilon_{st}$. Therefore, we are not able to determine why the expression for $\Delta\epsilon_{st}$ given as equation (5-39) is not in accordance with our experimental results.

Equation (5-41) will now be used to obtain an expression for $\Delta\epsilon_{st}$ in which M_e occurs. Equation (5-41) is substituted next in equation II.38 (Dukhin and Shilov, 1974), giving the complex dielectric increment as:

$$\Delta(\epsilon'-j\epsilon") = \frac{j3\pi Na^3(\kappa a)^2\epsilon_w A(D_+,D_-)M_e(1-j\omega\tau)}{W^2(1+\omega^2\tau^2)} \qquad (5\text{-}42)$$

with N = number of colloid particles per m^3, and for $z_+ = z_- = 1$:

$$A(D_+,D_-) = \frac{D_+ + D_-}{2 D_e} \qquad (5\text{-}43)$$

To obtain equation (5-42) we have assumed, like Dukhin and Shilov, that $\kappa a \gg 1$, implying that

$$\frac{\omega \tau A(D_+, D_-)(\kappa a)^2}{4 D_e W^2} \gg 1 \tag{5-44}$$

With equations (1-2), (5-36) and (5-43), this is transformed as:

$$\frac{\tau \sigma_b}{\epsilon_o \epsilon_w} \gg 1 \tag{5-45}$$

Because $\omega_{cr} \tau = 1$ (see e.g. Böttcher and Bordewijk, 1978), using equation (2-31), formula (5-45) is expressed as:

$$(tg \, \delta_s)_{\omega = \omega_{cr}} \gg 1 \tag{5-46}$$

In practice this means that the continuous medium should possess an appreciable conductance over the whole frequency range in which relaxation occurs. This condition is fulfilled with our experiments (see also section 2.2.1). More generally, formula (5-46) is expressed as $tg \, \delta \gg 1$ (compare with section 1.2).

Introducing equations (1-2), (5-36),(5-43) and

$$\phi = \frac{4}{3} \pi N a^3 \tag{5-47}$$

the real part of the dielectric increment from equation (5-42) is given as

$$\Delta \epsilon' = \frac{9 \phi F^2 c_b M_e (D_+ + D_-) \tau}{2 \epsilon_o RT (1 + \omega^2 \tau^2)} \tag{5-48}$$

Using the Nernst-Einstein equation (5-10) with $z = 1$ and the definition of $\Delta \epsilon_{st}$, already given as equation (4-2), the static dielectric increment is given by:

$$\Delta \epsilon_{st} = \frac{9 \phi \Lambda \tau M_e c_b}{2 \epsilon_o} \tag{5-49}$$

If the factor M_e is independent of the electrolyte concentration c_b, equation (5-49) predicts an increment varying linearly with c_b. Furthermore, according to equation (5-49), the slope of the straight line

82

$\Delta\varepsilon_{st}$ against c_b depends on the molar conductivity Λ of the electrolyte used.

From the experimental results on latex A_1 (see figure 4-9), a slope of about 620 m^3/mol is calculated. From table (4-2) $\tau = 23$ μs is taken as a mean value. With additional data given in table (5-1), M_e is calculated as 0.31 from experiment.

In the sections 5.3.2. and 5.3.3., two theories on the static dipole moment μ_o of spherical particles surrounded by a diffuse double layer are used to derive an expression for M_e. The expression for μ_o follows from equation (5-41):

$$\mu_o = -6\pi\varepsilon_o Ea^3 M_e . \tag{5-50}$$

5.3.2. *Theory of Dukhin and Shilov*

The expression for μ_o (Dukhin and Shilov, 1974, eq. III.71), disregarding electroosmotic effects, reads:

$$\mu_o = -\frac{24\pi\varepsilon_o Ea^3 \sinh^2\{F\psi_d/(4\,RT)\}}{\kappa a + 8\sinh^2\{F\psi_d/(4\,RT)\}} \tag{5-51}$$

The disregard of electroosmotic effects leads only to a correction of about 3% in equation (5-51). ψ_d is 150-100 mV (see table 5-6). Therefore, the next approximation may be applied:

$$\sinh\left(\frac{F\psi_d}{2\,RT}\right) = 2\sinh^2\left(\frac{F\psi_d}{4\,RT}\right) \tag{5-52}$$

Combining equations (1-2), (5-17), (5-50), (5-51) and (5-52), the following expression for M_e can be derived:

$$M_e = \frac{\sigma_o}{2\sigma_o + 2aFc_b} \tag{5-53}$$

With data from table (5-1) M_e and $\Delta\varepsilon_{st}$ are calculated for the concentration series 0.2 - 2.0 mol/m^3 (see table 5-5). Use is made of equations (5-53), (5-49), table (5-1), and of $\tau = 23$ μs (from table (4-2)).

TABLE (5-5). Calculated values for M_e and $\Delta\epsilon_{st}$ with equations (5-53)
and (5-49)

c_b (mol/m^3)	M_e	$\Delta\epsilon_{st}$
0.2	0.39	301
0.4	0.33	497
0.6	0.28	635
0.8	0.24	738
1.0	0.21	817
1.5	0.17	953
2.0	0.14	1040

5.3.3. *Theory of Overbeek*

The expression of Overbeek (1941) for the static dipole moment reads:

$$\mu_o = - \frac{4\pi\epsilon_o EB}{\kappa^3}$$ (5-54)

where B is a very complicated function of ψ_d and κa (see Overbeek, 1941, eq.84'). However, this expression for B can be approximated for $\kappa a \gg 1$, $\psi_d = \zeta$, $z_+ = z_-$ and $D_+ = D_-$ by:

$$2B = (\kappa a)^3 \frac{1 - \dfrac{(1+3m)(F\psi_d)^2}{2\kappa a(RT)^2}}{1 + \dfrac{(1+3m)(F\psi_d)^2}{4\kappa a(RT)^2}}$$ (5-55)

In the range of c_b values under consideration this expression is correct within 5 - 10%. The expression for m is given by eq. (5-16). Now the following expression for M_e can be obtained by using the equations (5-50), (5-54) and (5-55):

84

TABLE (5-6). Calculated values for M_e and $\Delta\varepsilon_{st}$ with equations (5-56) and (5-49)

c_b (mol/m^3)	κa	ψ_d (mV)	M_e	$\Delta\varepsilon_{st}$
0.20	10.3	153	− 0.23	− 177
0.30	12.6	142	− 0.15	− 166
0.40	14.6	135	− 0.08	− 128
0.60	17.9	125	− 0.0003	− 1
0.80	20.6	117	+ 0.05	+ 164
1.00	23.1	112	+ 0.10	+ 365
1.50	28.3	102	+ 0.16	+ 909
2.00	32.7	95	+ 0.20	+1495

$$M_e = \frac{1}{3}\ \frac{1 - \dfrac{(1+3m)\,(F\psi_d)^2}{2\kappa a(RT)^2}}{1 + \dfrac{(1+3m)\,(F\psi_d)^2}{4\kappa a(RT)^2}} \qquad (5-56)$$

In an analogous way as in section 5.3.2., M_e and $\Delta\varepsilon_{st}$ are calculated (see table 5-6).

5.3.4. *Concluding remarks*

It is clear that the treatments of sections 5.3.2. and 5.3.3. predict values for M_e which are dependent on the electrolyte concentration. Furthermore, in section 5.3.3. negative results for $\Delta\varepsilon_{st}$ are obtained at low c_b. This may only partly be due to the approdimations used. However, let us reason the other way around, i.e. accept the theory and accept $M_e = 0.31$ as obtained from the experiments (fig. 4-9). It is then possible to calculate the consequences for the surface charge, as shown in table (5-7). Thereby ψ_d (Dukhin) is calcu-

TABLE (5-7). Calculated values for ψ_d and σ_o for the case that M_e is independent from c_b ($M_e = 0.31$)

c_b (mol/m^3)	κa	ψ_d(Dukhin) (mV)	ψ_d(Overbeek) (mV)	σ_o(Dukhin) (mC/m^2)	σ_o(Overbeek) (mC/m^2)
0.20	10.3	110	21	3.1	0.31
0.30	12.6	120	23	5.7	0.52
0.40	14.6	128	25	8.9	0.75
0.60	17.9	138	27	16	1.2
0.80	20.6	145	29	25	1.8
1.00	23.1	151	31	35	2.4
1.50	28.3	161	34	64	4.0
2.00	32.7	169	37	100	5.8

lated by use of equations (5-50), (5-51) and (5-52), whereas ψ_d (Overbeek) is obtained from equation (5-56). Next, the ψ_d values in combination with equation (5-17) are used to calculate σ_o (Dukhin) and σ_o (Overbeek).

Accepting equation (5-49), the theory of Dukhin and Shilov and the theory of Overbeek means that the potential ψ_d would increase with increasing electrolyte concentration. However, from equation (5-17) it must be concluded that ψ_d decreases with increasing electrolyte concentration at constant σ_o. Not only the application of the theory based on the parameter M_e, but also the use of the theories treated in section 5.2 leads to a discrepancy between theory and experiment. This discrepancy gives rise to doubt as to the quality of the model system used for our investigations, i.e. the monodispersed polystyrene latices.

Therefore, as a next step in testing the theories it may be worthwhile to perform measurements on another type of colloid sys-

tems, e.g. chromium hydroxide sols. Matijević et al. (1971) describe the preparation and characterization of this colloid. According to Matijević et al., it is possible to obtain spherical particles of narrow size distribution. Furthermore the same order of magnitude for the particle radius may be obtained compared with the latices used in our investigations.

5.4. Some remarks on the relaxation time

From the table (4-2) it follows that the characteristic relaxation time τ for a distribution of relaxation times is independent of c_b within the experimental accuracy.

To compare theory and experiment again use is made of the measurements with latex A_1 with c_b = 0.644 mol/m^3 and the theoretical considerations of the authors as treated in section 5.2 .

De Backer (1966) gives an expression for the relaxation time obtained by applying the procedure as described in section 5.2.1.:

$$\tau = \varepsilon_o \frac{\varepsilon_h + 2\varepsilon_w - \phi(\varepsilon_h - \varepsilon_w)}{\sigma_h + 2\sigma_b - \phi(\sigma_h - \sigma_b)} \tag{5-57}$$

where ε_h and σ_h are given by the equations (5-2) and (5-3).

Schwarz (1962), Schurr (1964), Einolf and Carstensen (1971) all use the following expression for the relaxation time:

$$\tau = a^2/(2D_c) \tag{5-58}$$

The expression for the relaxation time in the theory of Ballario et al. (1976) has already been given as equation (5-29), which may be transformed into equation (5-58) by use of equation (5-5).

The relaxation time occurring in the theory of Dukhin and Shilov (1974) may be obtained when use is made of the definition that the relaxation time relates to the frequency at which

$$\Delta\varepsilon'(\omega) = \frac{1}{2} \Delta\varepsilon_{st} \tag{5-59}$$

This particular frequency is called the critical frequency ω_{cr}, with

$$\omega_{cr} = \frac{1}{\tau} \qquad (5\text{-}60)$$

With equation (5-36) the following expression for τ is obtained:

$$\tau = \frac{a^2}{2D_e W^2} \qquad (5\text{-}61)$$

Combining the equations (5-35) and (5-59), W may be obtained when a value for β, given in equation (5-37), is calculated from the data of our measurements ($\beta = 0.705$).

Finally, the relaxation time relating to the correction of the theory of Schwarz by Dukhin and Shilov (1974) reads, for $z_+ = z_- = 1$:

$$\tau = \frac{a^2}{2D_c(1 + 2\kappa\sigma_o c_b^{-1} F^{-1})} \qquad (5\text{-}62)$$

In table (5-8) results are shown for relaxation time calculations with the relevant formulas.

TABLE (5-8). Comparison of the results for τ.

Theory	Equation used	τ (μs)
De Backer	(5-57)	0.047
Schwarz	(5-58)	12.4
Schwarz, corrected	(5-62)	0.28
Schurr	(5-58)	12.4
Einolf and Carstensen	(5-58)	12.4
Ballario, Bonincontro and Cametti	(5-58)	12.4
Dukhin and Shilov	(5-61)	37.0
Calculated from our experiments (latex A_1, $c_b = 0.644$ mol/m^3)		20.3

From table (5-8) it is observed that the relaxation times calculated with the equations (5-58) and (5-61) are of the right order of magnitude. As with the results for $\Delta\varepsilon_{st}$ given in table (5-4), the theory of De Backer and the correction of Dukhin and Shilov on the theory of Schwarz lead to a discrepancy between theory and experiment which is far beyond the accuracy of our experiments. Based on the results for $\Delta\varepsilon_{st}$, we concluded in section 5.2.7. that the theory of Schurr leads to a better agreement with experiment than the theory of Dukhin and Shilov. This is not contradicted by the results for τ. Schwan et al.(1962) concluded from their experiments that τ is proportional to a^2. Both equation (5-58) and equation (5-61) show this proportionality.

In the calculations use is made of the values for the diffusion coefficients of ions in the bulk. However, in Schurr's theory the unknown diffusion coefficients of the ions in the double layer occur, whereas in the theory of Dukhin and Shilov the diffusion coefficients of ions in the bulk occur. It is reasonable to suppose that the diffusion coefficient of a certain counterion in the double layer is smaller than the diffusion coefficient of the same ion in the bulk. This would increase the calculated value for τ in the theory of Schurr. As a consequence, based on the results for the relaxation time, it is impossible to discriminate between Schurr's theory and that of Dukhin and Shilov. However, in both theories τ is in good agreement with the experimental value.

With respect to $\Delta\varepsilon_{st}$, we demonstrated in this thesis that a better agreement with experiment is obtained with the theory of Schurr than with the theory of Dukhin and Shilov. This may be caused by an overestimation of the radial fluxes by Dukhin and Shilov. However, because their theory is very complicated, it is difficult to estimate the influence of this eventual overestimation. Therefore, further consideration of the theory is desired.

APPENDIX A. <u>Capacitance corrections on the conductance box</u> (see section 2.4)

In the first three columns the values of the three decades are given. In the last column the calculated correction factors ΔC are listed. From the measurements it became clear that the influences of the resistors of the lowest conductance decade on the two other decades is negligibly small. Therefore, the corrections of the different settings of the box are obtained by adding the value x for a particular setting of the lowest conductance decade to the listed value of the highest decades. Conductances above 4.0 mS were not calibrated, because they were not needed in our measurements of polystyrene latices.

$$x = 0,1,2, \ldots ,9.$$

(cont.d)

setting G-box (S)			ΔC
10^{-3}	10^{-4}	10^{-5}	(pF)
0	0	0	+ 0.29
0	0	1	− 0.44
0	0	2	− 0.54
0	0	3	− 0.43
0	0	4	− 0.50
0	0	5	− 0.60
0	0	6	− 0.48
0	0	7	− 0.24
0	0	8	− 0.45
0	0	9	− 1.03
0	1	x	− 0.34
0	2	x	− 0.14
0	3	x	+ 0.02
0	4	x	+ 0.22
0	5	x	+ 0.21
0	6	x	+ 0.36
0	7	x	+ 0.81
0	8	x	+ 1.55
0	9	x	+ 1.38
1	0	x	+ 1.75
1	1	x	+ 1.88
1	2	x	+ 2.35
1	3	x	+ 2.81
1	4	x	+ 3.17
1	5	x	+ 3.38

setting G-box (S)			ΔC
10^{-3}	10^{-4}	10^{-5}	(pF)
1	6	x	+ 3.80
1	7	x	+ 4.40
1	8	x	+ 5.38
1	9	x	+ 5.44
2	0	x	+ 6.62
2	1	x	+ 6.98
2	2	x	+ 7.74
2	3	x	+ 8.36
2	4	x	+ 9.02
2	5	x	+ 9.39
2	6	x	+ 9.85
2	7	x	+10.64
2	8	x	+11.83
2	9	x	+12.06
3	0	x	+13.84
3	1	x	+14.45
3	2	x	+15.45
3	3	x	+16.20
3	4	x	+17.10
3	5	x	+17.76
3	6	x	+18.54
3	7	x	+19.64
3	8	x	+20.89
3	9	x	+21.42
4	0	x	+23.76

APPENDIX B. <u>Results of the dielectric measurements</u> (see chapter 4)

The results are obtained by using the formulae given in section 2.7 .

Latex: A_1 c_b(KCl) = 0.000 mol/m^3

ν (kHz)	ε	$\Delta\varepsilon$	σ (mS/m)	$\Delta\sigma$ (mS/m)
0.075	158.1	1.2	1.180	0.001
0.126	150.6	1.0	1.184	0.001
0.217	145.0	1.0	1.181	0.001
0.413	139.1	0.9	1.174	0.001
0.705	135.1	0.6	1.175	0.001
0.993	132.8	0.8	1.176	0.001
2.001	127.0	0.7	1.177	0.001
4.009	120.3	0.8	1.179	0.001
7.019	113.6	0.8	1.184	0.001
9.974	108.9	0.7	1.188	0.001
20.083	99.7	0.7	1.191	0.001
40.093	91.6	0.7	1.204	0.002
79.684	85.1	1.2	1.222	0.004
100.228	85.9	0.3	1.211	0.003
200.330	84.4	0.6	1.213	0.005
400.400	84.2	0.9	1.235	0.011
799.670	83.7	1.3	1.298	0.027
1600.300	83.1	1.4	1.457	0.263
3195.700	82.6	3.6	1.913	1.490

Latex: A_1 $c_b(KCl) = 0.204$ mol/m^3

ν (kHz)	ε	$\Delta\varepsilon$	σ (mS/m)	$\Delta\sigma$ (mS/m)
0.070	351.4	2.2	3.741	0.004
0.120	323.8	3.8	3.744	0.004
0.221	304.0	3.4	3.747	0.004
0.423	289.4	2.9	3.745	0.004
0.705	276.8	2.8	3.747	0.004
0.993	267.9	2.7	3.748	0.004
2.001	247.2	2.7	3.752	0.004
4.009	219.7	2.6	3.761	0.004
7.019	186.0	2.3	3.773	0.004
9.975	164.5	1.8	3.786	0.004
20.085	128.0	1.8	3.814	0.004
40.097	103.6	1.7	3.843	0.003
3196.600	80.0	3.2	4.105	0.637

Latex: A_1 $c_b(KCl) = 0.417$ mol/m^3

ν (kHz)	ε	$\Delta\varepsilon$	σ (mS/m)	$\Delta\sigma$ (mS/m)
0.070	497.3	10.0	6.975	0.007
0.120	461.3	6.1	6.976	0.007
0.221	439.1	4.2	6.975	0.007
0.423	418.7	3.8	6.976	0.007
0.705	402.8	3.6	6.978	0.007
0.993	390.8	3.6	6.981	0.007
2.001	360.4	3.5	6.989	0.008
4.008	315.0	3.4	7.004	0.007
9.976	221.1	1.6	7.051	0.007
20.085	153.9	3.5	7.097	0.007
40.099	112.7	3.3	7.138	0.007
3197.700	77.5	1.5	7.594	0.361

Latex: A_1 c_b(KCl) = 0.644 mol/m^3

ν (kHz)	ϵ	$\Delta\epsilon$	σ (mS/m)	$\Delta\sigma$ (mS/m)
0.070	833.2	26.1	10.634	0.010
0.120	682.5	9.1	10.616	0.011
0.221	604.8	5.7	10.615	0.010
0.403	560.6	4.5	10.613	0.012
0.705	526.6	2.1	10.647	0.012
0.994	515.0	1.6	10.621	0.010
4.009	412.8	1.3	10.649	0.010
9.979	275.5	1.2	10.719	0.010
40.105	119.9	2.8	10.837	0.010

Latex: A_1 c_b(KCl) = 0.878 mol/m^3

ν (kHz)	ϵ	$\Delta\epsilon$	σ (mS/m)	$\Delta\sigma$ (mS/m)
0.070	817.0	12.3	13.980	0.015
0.120	738.6	10.9	13.959	0.016
0.221	691.5	5.4	13.963	0.015
0.423	660.1	4.4	13.960	0.017
0.705	630.4	3.8	13.965	0.015
0.993	612.2	4.1	13.968	0.014
2.001	565.5	4.1	13.980	0.015
4.008	486.3	4.1	14.013	0.016
7.019	385.0	4.1	14.058	0.016
9.974	313.4	3.2	14.092	0.015
20.080	195.9	1.1	14.167	0.016
40.090	131.3	1.6	14.222	0.016
3194.700	71.1	2.9	14.508	0.347

Latex: A_1 $c_b(KCl)$ = 1.236 mol/m^3

ν (kHz)	ϵ	$\Delta\epsilon$	σ (mS/m)	$\Delta\sigma$ (mS/m)
0.120	933.9	55.8	19.296	0.019
0.221	869.1	9.3	19.297	0.019
0.423	805.2	6.5	19.304	0.021
0.705	768.3	3.3	19.302	0.020
0.993	746.4	2.5	19.305	0.021
2.001	685.2	4.4	19.324	0.021
4.009	579.2	4.6	19.360	0.021
7.019	443.0	4.1	19.414	0.020
9.973	349.9	4.2	19.454	0.021
20.080	204.6	4.2	19.551	0.020
40.090	128.0	4.1	19.606	0.020
3191.400	73.2	1.9	19.836	0.162

Latex: A_1 $c_b(KCl)$ = 1.517 mol/m^3

ν (kHz)	ϵ	$\Delta\epsilon$	σ (mS/m)	$\Delta\sigma$ (mS/m)
0.221	997.2	20.7	23.462	0.026
0.423	914.5	7.5	23.458	0.026
0.705	868.2	5.5	23.464	0.026
0.993	837.7	5.4	23.475	0.024
2.001	765.6	4.8	23.482	0.025
4.008	640.8	4.4	23.531	0.025
7.019	480.7	1.8	23.589	0.024
9.973	374.5	3.1	23.649	0.023
20.080	213.6	2.8	23.737	0.024
40.090	132.0	2.6	23.807	0.023
3193.300	70.7	2.3	24.010	0.347

Latex: A_2 $c_b(HCl) = 0.000$ mol/m^3

ν (kHz)	ε	$\Delta\varepsilon$	σ (mS/m)	$\Delta\sigma$ (mS/m)
0.120	145.9	1.1	0.976	0.002
0.221	144.5	1.2	0.978	0.002
0.423	135.5	0.8	0.980	0.002
0.705	129.3	0.9	0.981	0.002
0.994	129.8	0.9	0.981	0.002
2.001	124.3	0.9	0.982	0.002
4.009	117.9	0.8	0.984	0.002
7.019	111.8	0.9	0.987	0.002
9.980	107.6	0.8	0.989	0.002
20.088	98.2	0.7	0.993	0.002
40.103	93.0	0.8	0.999	0.003
69.871	88.8	0.9	0.991	0.004
150.055	85.3	0.4	1.020	0.003

Latex: A_2 $c_b(HCl) = 0.137$ mol/m^3

ν (kHz)	ε	$\Delta\varepsilon$	σ (mS/m)	$\Delta\sigma$ (mS/m)
0.120	369.8	8.5	6.571	0.012
0.221	303.0	4.6	6.573	0.012
0.423	268.3	3.2	6.672	0.012
0.705	250.3	2.7	6.575	0.012
0.994	240.7	2.5	6.576	0.012
2.001	237.7	2.5	6.579	0.012
4.009	202.4	2.2	6.584	0.012
7.019	180.6	2.1	6.600	0.013
9.979	163.7	2.0	6.611	0.013
20.087	128.6	1.7	6.640	0.013
40.100	101.8	0.9	6.660	0.011
69.868	88.8	0.9	6.665	0.011
150.050	83.3	0.7	6.713	0.014
400.080	80.1	0.6	6.730	0.020

Latex: A_2 $c_b(HCl) = 0.272$ mol/m^3

ν (kHz)	ϵ	$\Delta\epsilon$	σ (mS/m)	$\Delta\sigma$ (mS/m)
0.221	481.2	9.1	12.313	0.024
0.423	398.4	2.5	12.311	0.022
0.705	414.8	3.4	12.312	0.024
0.994	344.3	3.0	12.313	0.024
2.001	316.4	1.6	12.316	0.023
4.009	286.4	1.8	12.328	0.023
7.019	252.4	1.7	12.351	0.024
9.978	224.6	3.8	12.493	0.019
20.087	161.0	1.4	12.424	0.024
40.096	112.1	1.4	12.474	0.024
69.865	89.9	1.3	12.481	0.023
150.000	84.7	2.3	12.541	0.005
400.070	80.4	2.1	12.567	0.027

Latex: A_2 $c_b(HCl) = 0.412$ mol/m^3

ν (kHz)	ϵ	$\Delta\epsilon$	σ (mS/m)	$\Delta\sigma$ (mS/m)
0.221	685.4	14.5	18.055	0.034
0.423	523.7	7.6	18.021	0.035
0.705	464.6	3.6	18.049	0.034
0.994	437.7	3.0	18.065	0.034
2.001	398.3	3.3	18.080	0.036
4.009	360.7	3.1	18.021	0.034
7.019	322.9	2.9	18.056	0.035
9.977	291.4	2.9	18.059	0.035
20.086	210.7	2.6	18.151	0.035
40.097	136.8	2.5	18.284	0.031
69.861	102.3	2.1	18.282	0.035
150.040	78.8	2.2	18.371	0.034
400.010	72.2	1.5	18.416	0.026

Latex: A_2 c_b(HCl) = 0.493 mol/m^3

ν (kHz)	ε	$\Delta\varepsilon$	σ (mS/m)	$\Delta\sigma$ (mS/m)
0·221	757·0	20·0	20·814	0·038
0·423	577·1	8·4	20·770	0·039
0·705	495·0	6·4	20·738	0·040
0·994	456·4	5·0	20·719	0·038
2·001	409·9	4·3	20·722	0·040
4·009	372·3	3·9	20·757	0·040
7·019	336·5	3·6	20·761	0·040
9·977	307·4	3·6	20·787	0·032
20·086	229·0	3·1	20·912	0·041
40·097	152·1	2·5	21·032	0·040
69·861	109·4	2·2	21·028	0·040
150·050	80·9	1·0	21·221	0·051
400·057	74·6	2·5	21·162	0·047

Latex: A_3 c_b(LiCl) = 0.000 mol/m³)

ν (kHz)	ε	Δε	σ (mS/m)	Δσ (mS/m)
0.070	165.2	1.3	0.598	0.001
0.120	160.4	1.1	0.597	0.001
0.221	155.5	0.9	0.601	0.001
0.423	149.4	0.9	0.596	0.001
0.705	144.6	0.9	0.595	0.001
0.994	141.0	0.7	0.593	0.001
2.001	132.6	0.9	0.594	0.001
4.009	123.7	0.8	0.596	0.001
7.019	115.3	0.8	0.598	0.001
9.976	110.3	0.8	0.601	0.001
20.085	100.8	0.7	0.609	0.001
40.098	93.3	0.8	0.619	0.002
69.866	88.1	0.9	0.629	0.003
199.990	83.2	1.0	0.631	0.008
2199.800	80.3	2.3	1.131	0.803

Latex: A_3 c_b(LiCl) = 0.241 mol/m³

ν (kHz)	ε	Δε	σ (mS/m)	Δσ (mS/m)
0.070	324.5	6.3	3.157	0.004
0.120	300.2	12.6	3.158	0.004
0.221	287.5	4.9	3.161	0.004
0.423	271.8	3.8	3.155	0.004
0.705	256.3	4.4	3.150	0.004
0.993	248.1	3.4	3.159	0.004
2.001	226.9	3.2	3.162	0.004
4.009	200.6	2.2	3.168	0.004
7.019	174.4	2.2	3.181	0.004
9.975	157.0	2.0	3.192	0.004
20.084	126.2	2.0	3.217	0.004
40.096	103.4	1.9	3.245	0.005
69.862	91.3	1.9	3.273	0.006
199.972	84.1	0.9	3.319	0.012
2221.800	77.2	4.8	3.592	0.816

Latex: A_3 c_b(LiCl) = 0.465 mol/m^3

ν (kHz)	ε	Δε	σ (mS/m)	Δσ (mS/m)
0.070	449.3	9.0	5.490	0.007
0.120	431.7	6.9	5.485	0.007
0.221	404.2	4.9	5.489	0.006
0.423	378.6	4.6	5.486	0.007
0.705	360.1	4.1	5.492	0.007
0.993	347.8	3.5	5.495	0.007
2.001	317.8	3.3	5.498	0.007
4.009	277.8	1.3	5.510	0.007
7.019	233.9	1.2	5.529	0.007
9.975	204.9	0.8	5.550	0.007
20.084	154.2	3.3	5.588	0.007
40.095	117.7	3.2	5.633	0.008
69.860	99.3	2.5	5.664	0.006
199.960	86.1	0.7	5.738	0.010
2200.700	76.9	4.5	5.952	0.357

Latex: A_3 c_b(LiCl) = 0.737 mol/m^3

ν (kHz)	ε	Δε	σ (mS/m)	Δσ (mS/m)
0.070	440.6	17.1	8.360	0.011
0.120	558.1	13.3	8.341	0.011
0.221	523.7	12.4	8.346	0.011
0.423	486.7	7.6	8.357	0.008
0.705	455.2	8.3	8.353	0.011
0.993	440.7	7.0	8.345	0.010
2.001	401.9	6.3	8.353	0.011
4.009	346.5	4.0	8.373	0.011
7.019	283.0	5.3	8.398	0.011
9.976	246.5	2.4	8.416	0.011
20.085	173.3	2.0	8.474	0.010
40.095	127.5	1.3	8.524	0.011
69.859	103.6	1.2	8.561	0.012
200.060	69.4	6.0	7.382	0.009
2199.900	76.9	2.0	8.888	0.138

Latex: A_3 $c_b(\text{LiCl}) = 1.039 \text{ mol/m}^3$

ν (kHz)	ϵ	$\Delta\epsilon$	σ (mS/m)	$\Delta\sigma$ (mS/m)
0.070	571.2	34.7	11.467	0.016
0.120	594.4	6.7	11.477	0.013
0.221	666.8	8.1	11.467	0.015
0.423	604.0	5.8	11.469	0.016
0.705	567.6	5.4	11.463	0.015
0.993	548.1	5.3	11.469	0.014
2.001	498.2	4.7	11.472	0.014
4.009	427.8	2.5	11.503	0.014
7.019	343.2	1.8	11.539	0.017
9.974	285.1	3.9	11.567	0.016
20.083	189.1	2.9	11.627	0.015
40.083	131.5	2.8	11.683	0.016
69.857	103.4	2.8	11.707	0.014
200.010	81.4	0.8	11.796	0.013
2200.000	72.7	2.6	11.892	0.231

Latex: A_3 $c_b(\text{LiCl}) = 1.206 \text{ mol/m}^3$

ν (kHz)	ϵ	$\Delta\epsilon$	σ (mS/m)	$\Delta\sigma$ (mS/m)
0.120	662.0	18.8	13.179	0.014
0.221	752.5	13.5	13.152	0.018
0.423	673.1	8.7	13.152	0.017
0.705	630.4	3.8	13.150	0.018
0.993	613.8	3.7	13.123	0.019
2.001	545.1	6.1	13.168	0.020
4.009	460.4	4.9	13.192	0.017
7.019	366.6	3.3	13.233	0.018
9.975	302.4	2.3	13.266	0.018
20.084	199.1	3.4	13.339	0.017
40.095	136.0	3.0	13.406	0.018
69.859	106.6	2.9	13.442	0.020
200.081	82.2	1.9	13.550	0.010
2200.170	73.6	0.6	13.633	0.084

Latex: B_1 c_b(KCl) = 0.000 mol/m^3

ν (kHz)	ε	$\Delta\varepsilon$	σ (mS/m)	$\Delta\sigma$ (mS/m)
0·070	388·5	2·6	1·726	0·001
0·120	361·9	2·2	1·726	0·002
0·221	335·6	2·1	1·727	0·002
0·423	314·9	1·9	1·730	0·002
0·705	298·4	1·8	1·729	0·002
0·993	287·3	1·8	1·730	0·002
2·001	262·7	1·7	1·733	0·002
4·008	234·4	1·7	1·742	0·002
7·019	205·8	1·7	1·757	0·002
9·975	185·9	1·8	1·771	0·002
20·084	148·2	1·5	1·803	0·002
40·096	119·7	1·6	1·845	0·004
69·863	101·6	1·3	1·879	0·004
200·000	95·8	5·6	1·916	0·007
3200·000	81·8	5·3	3·197	1·550

Latex: B_1 c_b(KCl) = 0.226 mol/m^3

ν (kHz)	ε	$\Delta\varepsilon$	σ (mS/m)	$\Delta\sigma$ (mS/m)
0·070	811·3	7·2	5·305	0·005
0·120	739·5	4·8	5·300	0·006
0·221	692·0	3·8	5·311	0·005
0·423	653·9	3·5	5·302	0·006
0·705	623·8	3·4	5·300	0·006
0·993	601·2	3·1	5·297	0·005
2·001	551·3	3·2	5·308	0·006
4·008	483·4	3·0	5·331	0·006
7·019	402·9	3·5	5·370	0·006
9·975	342·9	3·5	5·405	0·006
20·084	232·0	0·8	5·485	0·006
40·095	159·7	3·3	5·565	0·007
69·862	121·4	2·6	5·628	0·010
196·688	94·3	0·2	5·755	0·009
2200·400	77·2	3·4	6·273	0·249

Latex: B_1 c_b(KCl) = 0.457 mol/m^3

ν (kHz)	ε	$\Delta\varepsilon$	σ (mS/m)	$\Delta\sigma$ (mS/m)
0.070	989.6	13.3	8.928	0.010
0.120	987.9	8.3	8.924	0.010
0.221	946.4	10.4	8.935	0.009
0.423	923.4	3.4	8.928	0.010
0.705	890.7	3.6	8.925	0.011
0.993	865.7	3.3	8.926	0.011
2.001	801.4	3.0	8.936	0.010
4.009	703.9	3.5	8.970	0.010
7.019	580.8	3.3	9.038	0.010
9.976	483.3	2.6	9.088	0.012
20.085	301.3	3.2	9.218	0.011
40.097	185.7	3.2	9.331	0.012
69.865	131.8	2.7	9.418	0.012
200.030	93.0	0.3	9.560	0.007
2199.900	75.5	2.4	9.912	0.181

Latex: B_1 c_b(KCl) = 0.729 mol/m^3

ν (kHz)	ε	$\Delta\varepsilon$	σ (mS/m)	$\Delta\sigma$ (mS/m)
0.120	1254.3	23.7	13.017	0.014
0.221	1277.5	9.3	13.032	0.015
0.423	1198.8	8.8	13.012	0.015
0.705	1145.3	4.9	13.019	0.016
0.993	1112.8	3.8	13.020	0.017
2.001	1029.6	3.6	13.034	0.015
4.009	901.7	5.5	13.085	0.014
7.019	735.9	4.2	13.179	0.019
9.975	603.1	3.2	13.255	0.016
20.084	355.0	3.1	13.425	0.017
40.090	205.0	2.9	13.581	0.018
69.860	139.4	2.7	13.667	0.020
199.960	91.3	0.3	13.828	0.012
2197.000	74.0	0.4	14.065	0.064

Latex: B_1 c_b(KCl) = 0.984 mol/m^3

ν (kHz)	ε	Δε	σ (mS/m)	Δσ (mS/m)
0.221	1641.8	22.6	16.900	0.020
0.423	1447.0	18.3	16.885	0.020
0.705	1358.3	7.4	16.881	0.021
0.993	1308.8	6.6	16.884	0.020
2.001	1209.9	6.3	16.897	0.021
4.009	1057.7	5.4	16.967	0.021
7.019	855.0	2.9	17.061	0.019
9.975	692.2	2.4	17.159	0.019
20.085	392.3	1.6	17.346	0.022
40.096	216.9	1.3	17.539	0.021
69.860	143.3	2.3	17.591	0.022
200.050	87.2	4.0	17.799	0.021
2200.000	71.1	2.5	18.001	0.179

Latex: B_1 c_b(KCl) = 1.502 mol/m^3

ν (kHz)	ε	Δε	σ (mS/m)	Δσ (mS/m)
0.221	2444.6	41.5	24.711	0.029
0.423	1946.1	24.6	24.717	0.032
0.705	1800.3	25.5	24.710	0.036
0.993	1776.8	35.7	24.705	0.030
2.001	1520.0	10.1	24.746	0.029
4.009	1297.5	8.7	24.827	0.033
7.019	1020.2	6.6	24.940	0.030
9.973	805.6	6.3	25.055	0.031
20.082	433.6	4.2	25.305	0.031
40.091	227.2	4.4	25.487	0.032
69.852	143.6	4.3	25.583	0.034
200.000	90.9	1.3	25.821	0.044
2200.000	74.3	0.6	25.955	0.177

Latex: C_1 c_b(KCl) = 0.000 mol/m^3

ν (kHz)	ϵ	$\Delta\epsilon$	σ (mS/m)	$\Delta\sigma$ (mS/m)
0.120	145.8	1.8	1.167	0.003
0.221	141.6	1.6	1.172	0.002
0.423	139.3	1.5	1.169	0.003
0.704	137.2	1.5	1.172	0.003
0.994	134.1	1.4	1.167	0.003
2.001	128.6	1.4	1.168	0.003
4.009	121.9	1.3	1.171	0.003
7.019	115.5	1.3	1.175	0.003
9.977	110.9	1.3	1.179	0.003
20.087	101.3	1.1	1.185	0.003
40.096	93.8	1.1	1.193	0.004
69.860	88.5	0.9	1.191	0.003
149.920	81.7	0.3	1.210	0.005
399.960	80.7	1.0	1.235	0.014
800.000	80.3	0.6	1.173	0.051

Latex: C_1 c_b(KCl) = 0.331 mol/m^3

ν (kHz)	ϵ	$\Delta\epsilon$	σ (mS/m)	$\Delta\sigma$ (mS/m)
0.120	293.4	4.9	6.847	0.014
0.221	271.7	3.9	6.854	0.014
0.423	262.4	3.0	6.847	0.013
0.705	255.1	3.1	6.853	0.013
0.994	250.4	3.1	6.858	0.013
2.001	238.3	3.0	6.860	0.013
4.009	219.3	3.0	6.860	0.014
7.019	195.0	2.8	6.880	0.014
9.979	175.2	2.8	6.892	0.014
20.089	137.1	2.6	6.917	0.014
40.101	109.6	2.5	6.950	0.015
69.868	94.6	2.4	6.958	0.014
150.010	85.9	1.4	7.024	0.015
400.040	79.9	1.8	7.062	0.019
800.050	79.1	0.9	7.088	0.034

Latex: C_1 c_b(KCl) = 0.679 mol/m^3

ν (kHz)	ε	$\Delta\varepsilon$	σ (mS/m)	$\Delta\sigma$ (mS/m)
0.120	470.6	6.2	12.853	0.027
0.221	414.3	5.3	12.872	0.028
0.423	387.0	5.3	12.843	0.026
0.705	373.7	3.5	12.837	0.028
0.994	365.9	3.3	12.829	0.028
2.001	348.3	3.2	12.866	0.030
4.009	321.0	3.1	12.881	0.030
7.019	279.8	2.5	12.902	0.027
9.978	245.6	2.4	12.924	0.026
20.088	172.8	1.7	12.973	0.028
40.099	126.6	1.6	13.012	0.027
69.866	103.3	1.6	13.018	0.027
150.020	85.9	1.1	13.105	0.022
400.050	78.2	1.2	13.126	0.021
799.990	76.4	1.0	13.157	0.016

Latex: C_1 c_b(KCl) = 1.034 mol/m^3

ν (kHz)	ε	$\Delta\varepsilon$	σ (mS/m)	$\Delta\sigma$ (mS/m)
0.120	652.8	16.4	18.199	0.042
0.221	552.5	9.6	18.180	0.037
0.423	484.3	4.9	18.173	0.038
0.705	458.9	2.8	18.166	0.038
0.994	449.7	3.8	18.177	0.036
2.001	426.5	3.7	18.169	0.040
4.009	387.5	3.2	18.188	0.040
7.018	331.6	1.8	18.200	0.027
9.978	284.3	2.0	18.245	0.039
20.087	189.4	2.0	18.318	0.036
40.098	128.1	1.7	18.378	0.036
69.864	100.5	2.3	18.396	0.036
150.030	82.8	3.7	18.483	0.034
400.060	72.9	3.9	18.569	0.041
800.150	71.3	3.7	18.563	0.060

Latex: C_1 $c_b(KCl) = 1.410$ mol/m^3

ν (kHz)	ε	$\Delta\varepsilon$	σ (mS/m)	$\Delta\sigma$ (mS/m)
0.120	770.0	68.8	23.846	0.048
0.221	689.6	15.0	23.802	0.044
0.423	581.6	6.1	23.799	0.045
0.705	547.1	6.5	23.813	0.047
0.994	530.7	4.8	23.817	0.044
2.001	500.8	3.5	23.818	0.045
4.009	451.3	3.9	23.838	0.046
7.019	378.5	3.5	23.879	0.045
9.978	318.7	3.5	23.917	0.049
20.087	203.3	2.9	23.986	0.048
40.097	133.5	2.4	24.049	0.048
69.861	103.4	2.3	24.059	0.048
150.032	91.5	0.7	24.201	0.055
400.797	81.8	0.5	24.220	0.053
800.220	79.0	0.3	24.309	0.059
1600.000	77.2	2.2	24.327	0.070

Latex: C_2 c_b(HCl) = 0.000 mol/m^3

ν (kHz)	ε	$\Delta\varepsilon$	σ (mS/m)	$\Delta\sigma$ (mS/m)
0.070	132.0	1.7	1.272	0.003
0.120	129.0	1.4	1.272	0.003
0.221	126.4	1.2	1.272	0.003
0.423	125.7	1.2	1.271	0.003
0.705	122.2	1.0	1.271	0.003
0.994	120.6	1.0	1.272	0.003
2.001	117.0	1.0	1.271	0.003
4.009	112.3	0.9	1.272	0.003
7.020	107.7	0.9	1.275	0.003
9.978	104.5	0.9	1.277	0.003
20.087	97.7	0.8	1.282	0.002
40.100	91.8	0.8	1.285	0.003
69.868	87.6	0.8	1.270	0.003
150.008	83.3	0.2	1.308	0.004
400.084	82.0	0.8	1.330	0.013

Latex: C_2 c_b(HCl) = 0.057 mol/m^3

ν (kHz)	ε	$\Delta\varepsilon$	σ (mS/m)	$\Delta\sigma$ (mS/m)
0.120	158.5	2.6	3.264	0.007
0.221	150.2	2.1	3.267	0.007
0.423	144.6	1.9	3.269	0.007
0.705	140.9	2.3	3.263	0.006
0.994	139.0	1.9	3.271	0.007
2.001	133.7	1.4	2.272	0.007
4.009	127.0	1.8	3.275	0.007
7.019	119.9	1.3	3.276	0.007
9.977	114.6	1.3	3.279	0.007
20.086	103.5	1.2	3.287	0.006
40.097	93.3	1.6	3.295	0.007
69.863	86.7	1.5	3.287	0.007
150.080	85.9	0.9	3.329	0.010
400.244	81.7	1.4	3.346	0.031

Latex: C_2 c_b(HCl) = 0.256 mol/m^3

ν (kHz)	ε	Δε	σ (mS/m)	Δσ (mS/m)
0.120	344.7	13.4	11.309	0.024
0.221	268.7	7.3	11.309	0.025
0.423	234.7	3.3	11.300	0.023
0.705	219.9	3.2	11.311	0.030
0.994	216.0	2.1	11.304	0.024
2.001	205.0	2.0	11.293	0.024
4.009	192.1	1.9	11.314	0.023
7.019	175.4	1.7	11.320	0.023
9.977	163.1	2.1	11.331	0.023
20.086	132.1	1.4	11.365	0.025
40.095	106.3	1.2	11.389	0.023
69.860	92.1	0.9	11.392	0.023
150.033	82.7	0.6	11.448	0.025
400.060	78.5	0.7	11.458	0.026

Latex: C_2 c_b(HCl) = 0.416 mol/m^3

ν (kHz)	ε	Δε	σ (mS/m)	Δσ (mS/m)
0.221	383.9	11.1	18.030	0.039
0.423	312.7	5.7	18.056	0.038
0.705	287.7	3.5	18.050	0.036
0.994	277.0	3.2	18.042	0.039
2.001	261.7	2.8	18.058	0.038
4.009	243.7	2.8	18.064	0.036
7.019	220.5	2.7	18.075	0.036
9.976	199.9	2.6	18.081	0.037
20.085	152.1	2.5	18.134	0.036
40.094	113.1	2.4	18.162	0.036
69.857	94.1	2.5	18.178	0.038
150.000	78.5	2.3	18.244	0.031
400.219	73.4	1.8	18.290	0.038

Latex: C_3 c_b(LiCl) = 0.000 mol/m^3

ν (kHz)	ε	$\Delta\varepsilon$	σ (mS/m)	$\Delta\sigma$ (mS/m)
0.120	137.9	1.2	0.829	0.002
0.221	135.8	0.9	0.830	0.002
0.423	132.7	0.8	0.830	0.002
0.705	127.9	0.8	0.835	0.002
0.994	125.9	0.7	0.834	0.002
2.001	121.1	0.6	0.833	0.002
4.009	114.8	0.6	0.834	0.002
7.019	109.5	0.5	0.838	0.002
9.977	105.7	0.7	0.841	0.002
20.087	98.4	0.6	0.848	0.002
40.097	92.3	0.6	0.852	0.002
69.862	87.6	0.6	0.846	0.002
150.030	82.9	0.3	0.869	0.003
400.070	81.8	0.9	0.887	0.011
800.170	81.6	0.7	0.936	0.046

Latex: C_3 c_b(LiCl) = 0.439 mol/m^3

ν (kHz)	ε	$\Delta\varepsilon$	σ (mS/m)	$\Delta\sigma$ (mS/m)
0.120	296.8	3.0	5.892	0.012
0.221	261.7	4.2	5.892	0.012
0.423	247.9	3.2	5.887	0.011
0.705	239.6	3.1	5.886	0.011
0.994	233.6	2.8	5.887	0.011
2.001	219.5	2.8	5.890	0.012
4.009	199.1	2.7	5 897	0.011
7.019	176.1	2.6	5.906	0.011
9.978	160.2	2.6	5.915	0.013
20.088	131.3	2.6	5.939	0.012
40.100	109.7	2.4	5.960	0.012
69.868	96.5	2.4	5.975	0.011
150.040	86.7	1.3	6.041	0.014
400.060	81.1	1.8	6.087	0.021
800.010	79.8	1.4	6.122	0.048

Latex: C_3 c_b(LiCl) = 0.931 mol/m^3

ν (kHz)	ε	$\Delta\varepsilon$	σ (mS/m)	$\Delta\sigma$ (mS/m)
0.120	498.1	12.6	11.187	0.023
0.221	401.5	7.4	11.192	0.024
0.423	367.1	5.6	11.187	0.024
0.705	348.2	3.9	11.176	0.021
0.994	338.9	3.6	11.167	0.023
2.001	317.0	3.3	11.182	0.022
4.009	284.1	2.1	11.193	0.023
7.019	243.0	2.0	11.213	0.022
9.980	213.1	2.5	11.233	0.022
20.089	158.7	1.6	11.270	0.021
40.102	123.6	0.7	11.304	0.021
69.868	103.0	1.1	11.326	0.021
400.060	77.8	0.6	11.456	0.027

Latex: C_3 c_b(LiCl) = 1.416 mol/m^3

ν (kHz)	ε	$\Delta\varepsilon$	σ (mS/m)	$\Delta\sigma$ (mS/m)
0.120	538.5	14.1	16.372	0.034
0.221	506.3	21.3	16.404	0.032
0.423	450.9	9.6	16.402	0.037
0.705	433.9	5.8	16.376	0.033
0.994	422.4	5.4	16.381	0.032
2.001	394.6	3.7	16.378	0.034
4.009	351.3	2.0	16.396	0.034
7.019	294.0	2.9	16.419	0.031
9.978	251.2	2.7	16.442	0.033
20.086	175.9	1.7	16.500	0.033
40.097	126.3	1.6	16.561	0.035
69.862	106.9	1.6	16.573	0.032
150.006	89.5	2.5	16.271	0.036
400.150	79.9	0.9	16.773	0.026

Latex: C_3 $c_b(LiCl) = 1.660$ mol/m^3

ν (kHz)	ε	$\Delta\varepsilon$	σ (mS/m)	$\Delta\sigma$ (mS/m)
0.221	500.6	13.0	19.129	0.035
0.423	478.6	6.4	19.155	0.040
0.705	451.5	2.8	19.123	0.034
0.994	465.7	6.1	19.121	0.035
2.001	426.3	4.4	19.122	0.037
4.009	385.0	4.0	19.138	0.039
7.019	328.5	3.7	19.171	0.038
9.977	282.8	3.7	19.208	0.038
20.086	193.9	3.2	19.284	0.036
40.096	133.6	3.3	19.333	0.038
69.861	104.2	3.3	19.354	0.037
150.000	87.8	2.4	19.487	0.040
400.120	78.1	1.7	19.549	0.040

Summary

The main aim of the investigations, described in this thesis
is to provide data which can be used to test theories of dielectic
phenomena in dilute colloid systems.

The possibility of preparing homodisperse polystyrene latices
with surfaces uncontaminated by emulsifiers, means that dielectric
methods can be applied to these colloid dispersions. The equipment
used and the latices which where prepared are described in chapters
two and three respectively.

The experimental results for latex A_1, with KCl as the added
electrolyte, are particularly relevant. These results, which are
characteristic of the dielectric behaviour of dilute polystyrene
latices, are used in chapter five for calculations with different
theories. Based on the dependence of the static dielectric increment
$\Delta\varepsilon_{st}$ on c_b, the concentration of added electrolyte, it appears that
until now no theory exists, by which the experimental results ob-
tained are explained conclusively. The best agreement between theory
and experiment is obtained both with the theory of Dukhin and Shilov
and with that of Schurr. Using the calculated relaxation times, it
is impossible to discriminate between these two theories, because
in both cases a relaxation time is calculated which is of the right
order of magnitude compared with the experimental value.

Figure (5-2) demonstrates that Schurr's theory is the best in
accordance with the experimental results. However, in Schurr's theory
the diffusion fluxes of the ions in the diffuse part of the double
layer are not taken into account. In view of their theoretical star-
ting points the theory of Dukhin and Shilov must be considered as
the best one. The larger discrepancy between the theory of Dukhin
and Shilov and the experimental results for $\Delta\varepsilon_{st}$ as a function of
c_b may be caused by an overestimation of the influence of radial
fluxes in their theory.

In conclusion, based on the established discrepancies between theory and experiment it is thought to be pertinent to perform further dielectric measurements on other colloid model systems such as chromium hydroxide sols. Probably, a part of these discrepancies is due to irregularities in the polystyrene latices used. On the other hand, it is necessary to develop the theory further. In this case special attention must be paid to the role played by the diffusion coefficients and diffusion fluxes around the colloid particles.

Samenvatting

Het hoofddoel van het in dit proefschrift beschreven onderzoek is: het verkrijgen van gegevens uit experimenten om hiermee theoriën over diëlectrische eigenschappen van verdunde kolloïdale systemen te testen.

De mogelijkheid om homodisperse polystyreen latices te bereiden zonder gebruik te maken van emulgatoren maakte het zinvol om diëlectrische onderzoekmethoden op deze kolloïdale systemen toe te passen. De voor dit doel opgebouwde meetopstelling en de gebruikte latices zijn beschreven in respectievelijk hoofdstuk twee en hoofdstuk drie.

Met name de meetresultaten voor latex A_1, waarbij KCl als electrolyt gebruikt is, zijn van belang. Deze resultaten, die karakteristiek blijken te zijn voor het diëlectrisch gedrag van verdunde polystyreen latices, dienen in hoofdstuk vijf als basis voor de berekeningen met verschillende theoriën. Met name op basis van de afhankelijkheid van het statisch diëlectrisch increment $\Delta\varepsilon_{st}$ van c_b, de concentratie aan toegevoegd electrolyt, blijkt dat er nog geen theorie bestaat die in afdoende mate de verkregen meetresultaten kan verklaren. De beste overeenstemming tussen theorie en experiment wordt verkregen met de theorie van Dukhin en Shilov enerzijds en die van Schurr anderzijds. Op grond van de berekende relaxatietijden kan geen onderscheid tussen deze theoriën gemaakt worden, omdat met beide theoriën een relaxatietijd berekend wordt, die van de juiste orde van grootte is in vergelijking met de waarde, die uit de metingen berekend is.

Figuur (5-2) toont aan, dat de theorie van Schurr het beste op de experimentele resultaten aansluit. Hier staat echter tegenover dat in Schurr's theorie de diffusie fluxen van de ionen in het diffuse deel van de dubbellaag niet in beschouwing worden genomen. Op grond van de theoretische uitgangspunten moet geconcludeerd worden dat de theorie van Dukhin en Shilov beter is dan die van Schurr.

117

De grotere discrepantie tussen de theorie van Dukhin en Shilov en de experimentele resultaten voor $\Delta\varepsilon_{st}$ als functie van c_b zou veroorzaakt kunnen worden door een overschatting van de invloed van de radiële fluxen in hun theorie.

Op grond van de geconstateerde verschillen tussen theorie en experiment is het enerzijds gewenst om diëlectrische metingen te gaan verrichten aan andere kolloïdale modelsystemen, zoals chroomhydroxide solen. Wellicht is een deel van de geconstateerde discrepanties toe te schrijven aan onregelmatigheden in het als modelsysteem gebruikte polystyreen latex. Anderzijds is het nodig om de theorie verder te ontwikkelen waarbij met name aandacht besteed zal moeten worden aan de rol die de diffusie coefficiënten en de diffusie fluxen rond de kolloïdale deeltjes spelen.

REFERENCES

Backer, R. de, Thesis, Brussels, (1966).

Backer, R. de, Watillon, A., J. Coll.Interface Sci. 43 (1973), 277.

Ballario, C., Bonincontro, A., Cametti, C., J.Coll.Interface Sci. 54 (1976), 415.

Berberian, J.G., Thesis, Brown University, Providence, (1968).

Berberian, J.G., Cole, R.H., Rev.Sci.Instrum. 40 (1969), 811.

Bijsterbosch, B.H., Colloid & Polymer Sci. 256 (1978), 343.

Bikerman, J.J., Kolloid-Z. 72 (1935), 100.

Blom, J., J.Phys.E, submitted (1979).

Bordewijk, P., Thesis, Leiden, (1968).

Böttcher, C.J.F., Bordewijk, P., "Theory of electric polarization", Vol. II, Elsevier, Amsterdam, (1978).

Broadhurst, M.G., Burr, A.J., J.Res.Nat.Bur.Stand. 690 (1965), 165.

Calvert, R., Wayne Kerr Monograph no.1, The Wayne Kerr Laboratories Ltd., Sycamore Grove, New Malden, Surrey.

Calvert, R., Cornelius, J.A., Griffiths, V.S., Stock, D.J., J.Phys. Chem. 62 (1958), 47.

Calvert, R., Mildwater, J., Electr.Engineering (G.B.), 35 (1963), 782.

Cole, K.S., Cole, R.H., J.Chem.Phys. 9 (1941), 341.

Cole, R.H., Gross, P.M. Jr., Rev.Sci.Instrum. 20 (1949). 252.

Debye, P., "Polar molecules", Dover, New York, (1929).

Derjaguin, B.V., Landau, L., Acta Physico Chim. USSR 10 (1939), 153.

Derjaguin, B.V., Dukhin, S.S., in "Surface and Colloid Science",Vol. 7, Matijević, E. (Ed.), Wiley, New York, (1974), 273

Dukhin, S.S., Shilov, V.N., Coll.J. USSR 31 (1969), 564.

Dukhin, S.S., Special Disc. Faraday Soc. no.1 (1970), 158.

Dukhin, S.S., in "Surface and Colloid Science", Vol. 3, Matijević, E. (Ed.), Wiley, New York, (1971), 83.

Dukhin, S.S., Shilov, V.N., "Dielectric phenomena and the double layer in disperse systems and polyelectrolytes", Wiley, New York, (1974).

Einolf, C.W. Jr., Carstensen, E.L., J.Phys.Chem. 75 (1971), 1091.

Ferris, C.D., Rev.Sci.Instrum. 34 (1963), 109.

Fricke, H., Curtis, H.J., J.Phys.Chem. 41 (1937), 729.

Furusawa, K., Norde, W., Lyklema, J., Kolloid-Z. Z.Polym. 250 (1972), 908.

General Radio instruction manual (GR 1616 Capacitance Bridge), General Radio Company, Concord, Massachusetts, (1974a).

General Radio instruction manual (GR 1238 Detector), General Radio Company, Concord, Massachusetts, (1974b).

Goodwin, J.W., Hearn, J., Ho, C.C., Ottewill, R.H., Br.Polym.J. 5 (1973), 347.

Goodwin, J.W., Hearn, J., Ho, C.C., Ottewill, R.H., Colloid & Polym. Sci. 252 (1974), 464.

Grahame, D.C., J.Am.Chem.Soc. 68 (1946), 301.

Grahame, D.C., Chem.Rev. 41 (1947), 441.

Grahame, D.C., J.Am.Chem.Soc. 76 (1954), 4819.

Hayakawa, R., Kanda, H., Sakamoto, M., Wada, Y., Japan.J.Appl.Phys. 14 (1975), 2039.

Homan, D.N., J.Res.Nat.Bur.Stand. 72C (1968), 161.

Kotera, A., Furusawa, K., Takeda, Y., Kolloid-Z. Z.Polym. 239 (1970), 677.

Kruyt, H.R., "Colloid Science", Vol. 1, Elsevier, Amsterdam, (1952).

Leeuwen, H.P. van, Electrochim.Acta 23 (1978), 207.

Lijklema, J., Thesis, Utrecht, (1957), theorem no. 3.

Lyklema, J., Overbeek, J.Th.G., J.Coll.Sci. 16 (1961), 501.

Mandel, M., Jung, P., Bull.Soc.Chim.Belg. 61 (1952), 533.

Mandel, M., Bull.Soc.Chim.Belg. 65 (1956), 308.

Mandel, M., Jenard, A., Bull.Soc.Chim.Belg. 67 (1958), 575.

Mandel, M., Protides Biol.Fluids 13 (1965), 415.

Matijević, E., J.Coll.Interface Sci. 36 (1971), 273.

Maxwell, J.C., "A treatise on electricity and magnetism", Oxford Un. Press, London, (1873), article 314.

Middelhoek, J., Thesis, Leiden, (1967).

Moser, P., Squire, P.G., O'Konski, C.T., J.Phys.Chem. 70 (1966), 744.

Norde, W., Thesis, Wageningen, (1976).

O'Konski, C.T., J.Chem.Phys. 23 (1955), 1559.

O'Konski, C.T., J.Chem.Phys. 64 (1960), 605.

Oncley, J.L., Chem.Rev. 30 (1942), 433.

Overbeek, J.Th.G., Thesis, Utrecht, (1941).

Pethybridge, A.D., Spiers, D.J., J.Electroanal.Chem. 66 (1975), 231.

Rosen, D., in "A laboratory manual of analytical methods of protein chemistry", Vol. 4, Alexander, P., Lundgren, H.P. (Eds.), Pergamon Press, Oxford, (1966).

Rosen, D., Bignall, R., Wisse, J.D.M., Drift, A.C.M. van der, J.Phys. E. 2 (1969), 22.

Scheider, W., J.Phys.Chem. 79 (1975), 127.

Schurr, J.M., J.Phys.Chem. 68 (1964), 2407.

Schwan, H.P., Sittel, K., Trans.Am.Inst.Elect.Engrs. 72 (1953), 114.

Schwan, H.P., Maczuk, J., Rev.Sci.Instrum. 31 (1960), 59.

Schwan, H.P., Schwarz, G., Maczuk, J., Pauly, H., J.Phys.Chem. 66 (1962), 2626.

Schwan, H.P., in "Physical techniques in biological research", Vol. 6, Part B, Nastuk, W.L. (Ed.), Acad.Press, New York, (1963).

Schwan, H.P., Biophysik 3 (1966), 181.

Schwan, H.P., Ann.New York Acad.Sci. 148 (1968), 191.

Schwarz, G., J.Phys.Chem. 66 (1962), 2636.

Shilov, V.N., Dukhin, S.S., Colloid J. USSR 32 (1970a), 90.

Shilov, V.N., Dukhin, S.S., Colloid J. USSR 32 (1970b), 245.

Small, H., J.Coll.Interface Sci. 48 (1974), 147.

South, G.P., Thesis, London, (1970).

South, G.P., Grant, E.H., Proc.Roy.Soc.London A 328 (1972), 371.

Stone-Masui, J., Watillon, A., J.Coll.Interface Sci. 52 (1975), 479.

Takano, K., Hachisu, S., J.Coll.Interface Sci. 66 (1978), 130.

Takashima, S., J.Molec.Biol. 7 (1963), 445.

Takashima, S., Biochem.Biophys.Acta 79 (1964), 531.

Tamamushi, R., Takahashi, K., Electroanal.Chem.& Interf.Electrochem. 50 (1974), 277.

Touw, F. van der, Mandel, M., Trans.Faraday Soc. 67 (1971a), 1336.

Touw, F. van der, Mandel, M., Honijk, D.D., Verhoog, H.G.F., Trans. Faraday Soc. 67 (1971b), 1343.

Touw, F. van der, Thesis, Leiden, (1975a).

Touw, F. van der, Goede, J. de, Beek, W.M. van, Mandel, M., J.Phys.E 8 (1975b), 840.

Touw, F. van der, Selier, G., Mandel. M., J.Phys.E 8 (1975c), 844.

Verwey, E.J., Overbeek, J.Th.G., "The theory of the stability of lyophobic colloids", Elsevier, Amsterdam, (1948).

Vetter, K.J., "Elektrochemische Kinetik", Springer, Berlin, (1961).

Wagner, K.W., Arch.Electrotechn. 3 (1914), 83.

Weast, R.C. (Ed.), "Handbook of chemistry and physics", 57th edition, C.R.C. Press, West Palm Beach, Florida, (1976-1977).

Williams, I.M., Thesis, London, (1973).

Williams, I.M., James, A.M., J.Chem.Soc. Farad.Trans.I 3 (1976), 803.

Wisse, J.D.M., Drift, A.C.M. van der, Springer, M.M., Internal Report, Dept. Physical Chemistry, University, Leiden, (1968).

Wisse, J.D.M., Drift, A.C.M. van der, Rosen, D., Bignall, R., Protides Biol.Fluids 16 (1969), 87.

Wisse, J.D.M., unpublished results, (1970).

Young, S.E., Thesis, London, (1967).

Young, S.E., Grant, E.H., J.Phys.E 1 (1968), 429.

Zwolle, S., Thesis, Leiden, (1978).

Curriculum Vitae

Op 4 juni 1940 ben ik geboren te Leiderdorp.
Mijn middelbare schoolopleiding kreeg ik aan het Praedinius Gymnasium te Groningen, het Coevorder Lyceum en het Leids Gymnasium.
Aan laatstgenoemde school behaalde ik in juni 1960 het diploma gymnasium-β. Na vervulling van de militaire dienstplicht bij de Koninklijke Luchtmacht van augustus 1960 tot augustus 1962 begon ik in september 1962 de studie scheikunde aan de Rijksuniversiteit te Leiden. Het kandidaatsexamen, studieletter f, werd in juni 1966 afgelegd. De studie werd voortgezet onder leiding van de hoogleraren Dr. C.J.F.Böttcher, Dr. L.J.Oosterhoff, Dr. P.Mazur en Dr. E.Havinga. Het doctoraalexamen scheikunde, omvattende het hoofdvak fysische chemie, het bijvak theoretische natuurkunde en het bijvak organische chemie, werd afgelegd in april 1969.

Van juli 1966 tot april 1969 vervulde ik een student-assistentschap bij de afdeling Fysische Chemie II van de Rijksuniversiteit te Leiden.

Van april 1969 tot augustus 1971 ben ik als wetenschappelijk werker verbonden geweest aan de groep Fysische Chemie van het Unilever Research Laboratorium te Vlaardingen.

Van augustus 1971 tot april 1979 ben ik in dienst geweest van de Landbouwhogeschool te Wageningen, afdeling Fysische en Kolloidchemie, aanvankelijk als wetenschappelijk medewerker in tijdelijke dienst, sinds augustus 1975 als wetenschappelijk medewerker I in vaste dienst. Tijdens dit dienstverband werd, naast onderwijskundige en organisatorische werkzaamheden, het in dit proefschrift beschreven onderzoek verricht.

Van augustus 1977 tot augustus 1978 ben ik docent scheikunde bij de avondopleiding van de STOVA te Wageningen geweest.

Sinds april 1979 vervul ik de funktie van adjunkt-directeur van de Laboratoriumschool Zeeland te Goes.